

THE POTENTIAL INHIBITORY EFFECT OF DIHOMO-GAMMA-LINOLENIC ACID ON
COLON CANCER CELL GROWTH VIA FREE RADICAL METABOLITES IN
CYCLOOXYGENASE-CATALYZED PEROXIDATION

A Dissertation
Submitted to the Graduate Faculty
of the
North Dakota State University
of Agriculture and Applied Science

By

Yan Gu

In Partial Fulfillment of the Requirements
for the Degree of
DOCTOR OF PHILOSOPHY

Major Department:
Pharmaceutical Sciences

August 2012

Fargo, North Dakota

North Dakota State University

Graduate School

Title

THE POTENTIAL INHIBITORY EFFECT OF DIHOMO-GAMMA-LINOLENIC ACID ON COLON CANCER

CELL GROWTH VIA FREE RADICAL METABOLITES IN CYCLOOXYGENASE-CATALYZED PEROXIDATION

By

YAN GU

The Supervisory Committee certifies that this *disquisition* complies with North Dakota State University's regulations and meets the accepted standards for the degree of

DOCTOR OF PHILOSOPHY

SUPERVISORY COMMITTEE:

Dr. Steven Qian

Chair

Dr. Jagdish Singh

Dr. Benedict Law

Dr. Erxi Wu

Dr. Clifford Hall

Approved:

11/06/2012

Date

Jagdish Singh

Department Chair

ABSTRACT

Cyclooxygenase (COX) can metabolize dihomo- γ -linolenic acid (DGLA) and arachidonic acid (AA) through free radical-mediated lipid peroxidation to form the anti-carcinogenic 1-series of prostaglandins and pro-carcinogenic 2-series of prostaglandins, respectively. Our previous studies had demonstrated that in ovine COX-mediated DGLA and AA peroxidation, there are common and exclusive free radicals formed through different free radical reactions. However, it was still unclear whether the differences are associated with the contrasting bioactivity of DGLA *vs.* AA. In order to investigate the possible association between cancer cell growth and the exclusive free radicals generated from COX/DGLA *vs.* COX/AA, we refined our combined spin-trapping/LC/MS method with solid phase extraction to characterize free radicals in their reduced forms in the human colon cancer cell line HCA-7 colony 29, which has a high COX-2 expression. For the first time, we were able to profile free radical formation in the experimental settings in which cell proliferation (*via* MTS assay) and cell cycle distribution (*via* PI staining) could be assessed. Our results showed that DGLA- and AA-derived exclusive free radicals, rather than prostaglandins, were closely associated with the opposing bioactivities of DGLA *vs.* AA.

Due to rapid conversion from DGLA to AA *via* Δ -5 desaturase (D5D), the anti-proliferative effect of DGLA on cancer cell growth was limited. Thus, double doses of DGLA and D5D inhibitor were introduced. Among DGLA, double-dose DGLA, and combined DGLA/D5D inhibitor treatments, the latter exerted the most anti-proliferative effect on cancer cell growth and caused significant cell G₂/M arrest. D5D knockdown cells (*via* siRNA transfection) were used to further investigate the possible mechanism underlying the anti-proliferative effect of DGLA on cancer cell growth. In addition, the combined DGLA/D5D

inhibitor treatment increased the susceptibility of cancer cells to the chemotherapy drug 5-fluorouracil. In D5D knockdown cells, DGLA and 5-fluorouracil exerted greater effects on cell growth inhibition and cytotoxicity due to synergism.

In summary, increasing DGLA and concurrently decreasing AA in cells could be a novel approach to controlling the development of AA-dependent cancer. Our study allowed us to directly study the free radical-associated PUFA bioactivity, thus improving our understanding of COX-catalyzed lipid peroxidation in cancer biology.

ACKNOWLEDGMENTS

It is a pleasure to thank the many people who made this thesis possible.

It is difficult to overstate my gratitude to my Ph.D. supervisor, Dr. Steven Qian. With his enthusiasm, his inspiration, and immense knowledge, he helped to make research fun for me. Throughout my thesis-writing period, he provided encouragement, sound advice, and lots of good ideas. I would have been lost without him.

I would like to thank members of my graduate committee, Dr. Jagdish Singh, Dr. Benedict Law, Dr. Erxi Wu and Dr. Clifford Hall, for their guidance and suggestions.

I am grateful to the secretaries, Janet and Jean, in the pharmaceutical science department, for assisting me in many different ways.

I am indebted to the whole department of pharmaceutical sciences for providing a stimulating and fun environment in which to learn and grow. I am especially grateful to my labmates and people who helped me with my experiments, Qingfeng Yu, Yi Xiao, Yonghua Yang, Susan Zhong, Evan Eide, Preeti Purwaha and Yi Xu.

I wish to thank my friends Jing Zhang, Shuang Zhou, Hui Xu, Fanrong Yao, Chengluan Xuan, Wen Yan and Yue Li at NDSU for helping me get through the difficult times, and for all the emotional support, encouragement, entertainment, and caring they provided.

I wish to thank my entire extended family for providing a loving environment for me, especially my fiancé, Yin Wan, for supporting and encouraging me to pursue this degree. Without his encouragement, I would not have finished the degree.

Lastly, and most importantly, I wish to thank my parents, Qiusong Gu and Lixia Ni. They bore me, raised me, supported me, taught me, and loved me. To them I dedicate this thesis.

TABLE OF CONTENTS

ABSTRACT.....	iii
ACKNOWLEDGMENTS.....	v
LIST OF TABLES.....	xi
LIST OF FIGURES.....	xii
LIST OF SCHEMES.....	xiv
LIST OF ABBREVIATIONS.....	xv
CHAPTER 1. INTRODUCTION.....	1
1.1. Polyunsaturated Fatty Acids, Eicosanoids and Inflammation Related Diseases....	1
1.1.1. Metabolism of dietary polyunsaturated fatty acids.....	1
1.1.2. AA-derived eicosanoids and inflammation related diseases.....	6
1.1.3. DGLA-derived eicosanoids and inflammation related diseases.....	8
1.2. Lipid Peroxidation and Lipid Mediators in Inflammatory Diseases.....	12
1.3. The Catalytic Mechanism of COX.....	16
1.4. PUFA-Derived Free Radical's Detection and Characterization.....	20
1.4.1. Electron spin resonance and spin-trapping.....	20
1.4.2. Development of the combined HPLC/ESR/MS and spin-trapping technique.....	23
1.4.3. Detection of free radical from COX-catalyzed AA and DGLA peroxidation <i>via</i> spin-trapping and LC/ESR/MS.....	26
1.4.4. Refining the approach to ESR spin trapping and LC/MS to detect free radicals under normal biological conditions.....	27
CHAPTER 2. METATERIALS AND METHODS.....	31
2.1. Chemicals and Reagents.....	31
2.2. Cell Culture.....	33

2.3.	Preparation of Reaction Solution.....	34
2.3.1.	Stock solutions.....	34
2.3.2.	Cell lysis buffer.....	34
2.3.3.	Protein assay.....	35
2.3.4.	SDS-polyacrylamide gel electrophoresis (SDS-PAGE).....	36
2.3.5.	Immunoblotting.....	38
2.3.6.	Cell cycle distribution.....	38
2.3.7.	Transfection with siRNA.....	39
2.4.	Spin-Trapping Experiments in Cell-PBS Suspension.....	39
2.5.	Spin-Trapping Experiments under Normal Cell Growth Conditions.....	39
2.6.	Extraction and Analysis of Hydroxylamine.....	40
2.7.	Spin-Trapping of Hydroxyethyl Radical (Test of POBN's Trapping Ability).....	41
2.8.	Extraction and Analysis of PUFAs and PGEs in Cell Culture Medium.....	42
2.9.	Offline ESR.....	42
2.10.	LC/MS and LC/MS ²	43
2.10.1.	LC/MS and LC/MS ² for identification of free radical adducts and hydroxylamines.....	43
2.10.2.	LC/MS for quantification of hydroxylamine.....	44
2.10.3.	LC/MS for PUFAs and PGEs detection and quantification.....	45
2.11.	Transfect HCA-7 Colony 29 Cells with FADS1 siRNA.....	45
2.12.	Western Blot Analysis.....	46
2.13.	Cell Proliferation Assay <i>via</i> MTS.....	48
2.14.	Cell Cycle Distribution Analysis <i>via</i> PI Staining.....	49
2.15.	Statistics.....	50

CHAPTER 3. DETECTION AND IDENTIFICATION OF FREE RADICALS FORMED FROM CELLULAR COX-CATALYZED AA AND DGLA PEROXIDATION.....	51
3.1. Introduction.....	51
3.2. Results and Discussion.....	56
3.2.1. COX-2 expression in HCA-7 colony 29 cells.....	56
3.2.2. Offline ESR detection of free radicals.....	56
3.2.3. LC/ESR/MS identification of free radicals in cell-PBS suspension.....	58
3.2.4. Assessment of POBN's trapping ability.....	61
3.2.5. LC/MS and dual spin-trapping in detection of free radicals as hydroxylamines.....	63
3.2.6. LC/MS, LC/MS ² and dual spin-trapping in characterization of hydroxylamines.....	66
CHAPTER 4. THE ASSOCIATION BETWEEN AA-/DGLA-DERIVED FREE RADICAL METABOLITES AND COLON CANCER CELL GROWTH.....	74
4.1. Introduction.....	74
4.2. Results and Discussion.....	75
4.2.1. Quantification of hydroxylamines as free radicals in a single dose of PUFA treatment.....	75
4.2.2. Profile of PUFAs and PGEs in a single dose of PUFA treatment.....	80
4.2.3. Effect of PUFAs on cell proliferation and cell cycle distribution.....	84
4.2.4. Comparison of effects of free radical metabolites and PGEs on cell growth.....	86
4.2.5. Study of double doses of PUFA treatment.....	91
CHAPTER 5. INHIBITION OF THE CONVERSION FROM DGLA TO AA ATTENUATED CANCER CELL GROWTH AND ENHANCED THE EFFICACY OF A CHEMOTHERAPY DRUG.....	99
5.1. Introduction.....	99

5.2.	Results and Discussion.....	103
5.2.1.	Hydroxylamines, PUFA and PGEs in co-treatment with DGLA and CP-24879.....	103
5.2.2.	Effect of DGLA and CP-24879 on cell proliferation and cell cycle distribution.....	108
5.2.3.	Possible inhibition mechanism of CP-24879.....	110
5.2.4.	Study of other D5D inhibitor.....	111
5.2.5.	DGLA enhanced the efficacy of the chemotherapy drug 5-FU.....	119
5.2.6.	Effect of DGLA in D5D knockdown cells.....	122
CHAPTER 6. CONCLUSION AND FUTURE DIRECTION.....		128
6.1.	Introduction.....	128
6.2.	Summary of Research Data.....	129
6.2.1.	Summary of chapter 3: detection and characterization of free radicals from COX/AA and COX/DGLA in cells.....	129
6.2.2.	Summary of chapter 4: assessment of the association between AA/DGLA-derived free radicals and colon cancer cell growth.....	129
6.2.3.	Summary of chapter 4: double dose of DGLA attenuates colon cancer cell growth.....	130
6.2.4.	Summary of chapter 5: blocking D5D activity inhibits cell proliferation and sensitizes cells to chemotherapy drugs.....	131
6.3.	Discussion.....	132
6.4.	Future Directions.....	137
6.4.1.	Study of the association between the AA-derived exclusive free radical and colon cancer cell growth.....	137
6.4.2.	Study of the roles of AA-and DGLA-derived free radicals' metabolism in signal transduction.....	137
6.4.3.	Study of the inhibitory mechanism of D5D and search for new inhibitors.....	138

6.4.4. Investigation of the effect of normal diet in a D5D knockout mouse
Model.....139

REFERENCES.....140

LIST OF TABLES

<u>Table</u>	<u>Page</u>
1. Scaling up or down transfections.....	46
2. Volume of components required to cast gels.....	47
3. Effect on cell proliferation and cell cycle distribution from PUFAs.....	84
4. The tested free radical derivatives (metabolites).....	89
5. Effect of DGLA and CP-24879 on cell cycle distribution and proliferation.....	108
6. Common and exclusive free radicals in COX/AA vs. COX/DGLA.....	129

LIST OF FIGURES

<u>Figure</u>	<u>Page</u>
1. Typical ESR spectrum of POBN radical adduct.....	23
2. Western blot analysis of COX-2 expression with PUFA treatment.....	56
3. Offline ESR spectra of spin-trapping experiments in cell-PBS suspensions.....	57
4. LC/MS chromatogram (EICs) of POBN adducts formed from cellular COX-catalyzed AA and DGLA peroxidation.....	59
5. POBN's trapping ability and stability in cell culture medium.....	62
6. LC/MS chromatogram (EICs) of hydroxylamines formed from cellular COX-catalyzed PUFA peroxidation.....	65
7. LC/MS chromatogram (EICs) and LC/MS ² analysis of m/z 306 and m/z 297 in dual spin-trapping experiment.....	68
8. LC/MS chromatogram (EICs) and LC/MS ² analysis of m/z 458 and m/z 449 in dual spin-trapping experiment.....	69
9. LC/MS chromatogram (EICs) and LC/MS ² analysis of m/z 334 and m/z 325 in dual spin-trapping experiment.....	71
10. LC/MS chromatogram (EICs) and LC/MS ² analysis of m/z 364 and m/z 355 in dual spin-trapping experiment.....	72
11. Profiles of hydroxylamines with a single dose of AA treatment.....	77
12. Profiles of hydroxylamines with a single dose of DGLA treatment.....	78
13. Profiles of AA and PGE ₂ with a single dose of AA treatment.....	81
14. Profiles of DGLA, AA, PGE ₁ and PGE ₂ with a single dose of DGLA treatment.....	82
15. Effect of PUFAs on cell cycle distribution.....	85
16. Effect of PGEs on colon cancer cell growth.....	87
17. Effect of free radical derivatives on colon cancer cell growth.....	90
18. Profile of hydroxylamines with double doses of DGLA treatment.....	92

19. Profile of hydroxylamines with double doses of AA treatment.....	93
20. Profile of DGLA, AA, PGE ₁ and PGE ₂ with double doses of DGLA treatment.....	95
21. Profile of AA and PGE ₂ with double doses of AA treatment.....	96
22. Effects of single dose vs. double dose treatment of DGLA or AA on cell proliferation.....	97
23. Profiles of hydroxylamines with co-treatment of DGLA and CP-24879.....	104
24. Profiles of DGLA, AA, PGE ₁ and PGE ₂ with co-treatment of DGLA and CP-24879.....	106
25. Effects of co-treatment of DGLA and CP-24879 on cell cycle distribution.....	109
26. Western blot analysis of D5D expression with co-treatment of PUFA and CP-24879.....	111
27. Profiles of hydroxylamines with co-treatment of DGLA and sesamin.....	113
28. Profile of DGLA, AA, PGE ₁ and PGE ₂ with co-treatment of DGLA and sesamin.....	114
29. Profiles of hydroxylamines with co-treatment of DGLA and curcumin.....	116
30. Profiles of DGLA, AA, PGE ₁ and PGE ₂ with co-treatment of DGLA and curcumin.....	117
31. Effect of DGLA with sesamin or curcumin on cell proliferation.....	119
32. Co-treatment of DGLA and CP-24879 enhanced the efficacy of 5-FU.....	120
33. Western blot analysis of D5D knockdown.....	122
34. Profiles of hydroxylamines in D5D knockdown cells with DGLA treatment.....	124
35. Profiles of DGLA, AA, PGE ₁ and PGE ₂ in D5D knockdown cells with DGLA treatment.....	125
36. Cell proliferation assays in D5D knockdown cells.....	126

LIST OF SCHEMES

<u>Scheme</u>	<u>Page</u>
1. The structure and metabolism of ω -6 and ω -3 PUFAs.....	3
2. An overview of eicosanoid biosynthesis pathways.....	5
3. Structure of tested D5D inhibitors.....	11
4. An overview of free radical reactions in LA peroxidation.....	13
5. COX-catalyzed DGLA and AA peroxidation.....	17
6. The structures of three classic and common spin traps.....	21
7. LC/ESR/MS combined technique.....	24
8. Synthesis of d ₉ -POBN.....	31
9. Hydroxylamine-sorbent interactions on Oasis MAX sorbent.....	41
10. Proposed mechanism of COX-catalyzed AA peroxidation.....	53
11. Proposed mechanisms of COX-catalyzed DGLA peroxidation.....	55
12. Reduction of POBN-trapped radical adducts and detection of hydroxylamines by LC/MS.....	64
13. Proposed mechanism of the synergistic effect of DGLA and 5-FU.....	102

LIST OF ABBREVIATIONS

AA.....	arachidonic acid
AC.....	adenylate cyclase
ACN.....	acetonitrile
ALA.....	α -linolenic acid
APS.....	ammonium persulfate
ANOVA.....	analysis of variance
cAMP.....	cyclic 3', 5'-adenosine monophosphate
COX.....	cyclooxygenase
CREB.....	nuclear cAMP response element binding protein
CYP450.....	cytochrome P450
DGLA.....	dihomo- γ -linoleic acid
DHA.....	docosahexenoic acid
DMPO.....	5, 5-dimethyl-1- pyrroline N-oxide
DMSO.....	dimethyl sulfoxide
DTT.....	DL-dithiothreitol
D5D.....	Δ -5 desaturase
D6D.....	Δ -6 desaturase
EET.....	epoxy eicosatrienoic acid
EGFR.....	epidermal growth factor receptor
ELOVL5.....	very long chain fatty acid protein 5
EIC.....	extracted ion chromatogram
ESR.....	electron spin resonance

EPA.....eicosapentaenoic acid

EPR.....electron paramagnetic resonance

ERK.....extracellular-signal-regulated kinase

FBS.....fetal bovine serum

GLA..... γ -linolenic acid

HCl.....hydrogen chloride

HETE.....hydroxyeicosatetraenoic acid

HETrE.....hydroxyeicosatrienoic acid

HOAc.....glacial acetic acid

HPLC/LC.....high performance liquid chromatography

IL.....interleukin

LA.....linoleic acid

LOX.....lipoxygenase

LT.....leukotriene

MAX.....mixed-mode anion exchange

MBD.....membrane binding domain

MDA.....malondialdehyde

M₁DG.....cyclic pyrimido [1,2 α] purin-10(3H)-one

MNP.....2-methyl-2- nitrosopropane

MRM.....multiple reaction monitoring

MS.....mass spectrometry

MS².....tandem MS

MTS.....3-(4,5-dimethylthiazol-2-yl)-5-(3-carboxymethoxyphenyl)-
2-(4-sulfophenyl)-2H-tetrazolium

NaCl.....sodium chloride
NaOH.....sodium hydroxide
NFκB.....Nuclear factor kappa B
NH₄OH.....ammonium hydroxide
NSAIDs.....non-steroidal anti-inflammatory drugs
H₂O.....water
PBS.....phosphate buffered saline
PES.....phenazine ethosulfate
POBN.....α-[4-pyridyl-1-oxide]-*N-tert*-butyl nitron
PG.....prostaglandin
PKA.....protein kinase A
PI.....propidium iodide
PLA₂.....Phospholipases A2
PPAR.....peroxisome proliferator-activated receptor
PUFA.....polyunsaturated fatty acid
SD.....standard deviation
SDS.....sodium dodecyl sulfate
SPE.....solid phase extraction
TBS.....Tris buffered saline
TGF.....transforming growth factor
THF.....tetrahydrofuran
TIC.....total ion chromatogram
TNF.....tumor necrosis factor

t_Rretention time
TX.....thromboxane
4-HNE.....4-hydroxy-2-nonenal
5-FU.....5-fluorouracil
15-PGDH.....15-prostaglandin dehydrogenase

CHAPTER 1. INTRODUCTION

1.1. Polyunsaturated Fatty Acids, Eicosanoids and Inflammation-Related Diseases

1.1.1. *Metabolism of dietary polyunsaturated fatty acids*

Fatty acids that contain more than one double bond in their carbon atom chain are referred to as polyunsaturated fatty acids (PUFAs) [1-5]. The nutritionally important PUFAs are classified as ω -6 and ω -3 on the basis of the position of the first double bond counting from the methyl end of the molecule [1-5]. For example, dihomo- γ -linolenic acid (20:3, ω -6) has twenty carbon atoms and three double bonds, with the first double bond at the sixth carbon atom counted from the methyl end of the acyl chain. ω -6 PUFAs include linoleic acid (LA, 18:2), γ -linolenic acid (GLA, 18:3), dihomo- γ -linolenic acid (DGLA, 20:3), and arachidonic acid (AA, 20:4), and ω -3 PUFAs include α -linolenic acid (ALA, 18:3), eicosapentaenoic acid (EPA, 20:5), and docosahexenoic acid (DHA, 22:6) [1-5].

Plant seed oils are frequently rich in PUFAs. Sunflower, safflower, corn and soybean oil all contain high amounts of LA [3-5]. Evening primrose oil, borage oil, black currant oil, and hemp seed oil contain substantial amounts of GLA [6, 7]. Although meat and egg yolks are direct dietary sources of AA [8], dietary LA is considered to be the main source of tissue AA [9]. Canola oil, perilla oil, flaxseed oil, linseed oils and walnuts contain abundant ALA [6]. EPA and DHA are mostly found in oil from deep, cold water fatty fish [10, 11]. In the absence of fish oil, ALA is the principle source of dietary ω -3 PUFAs [12].

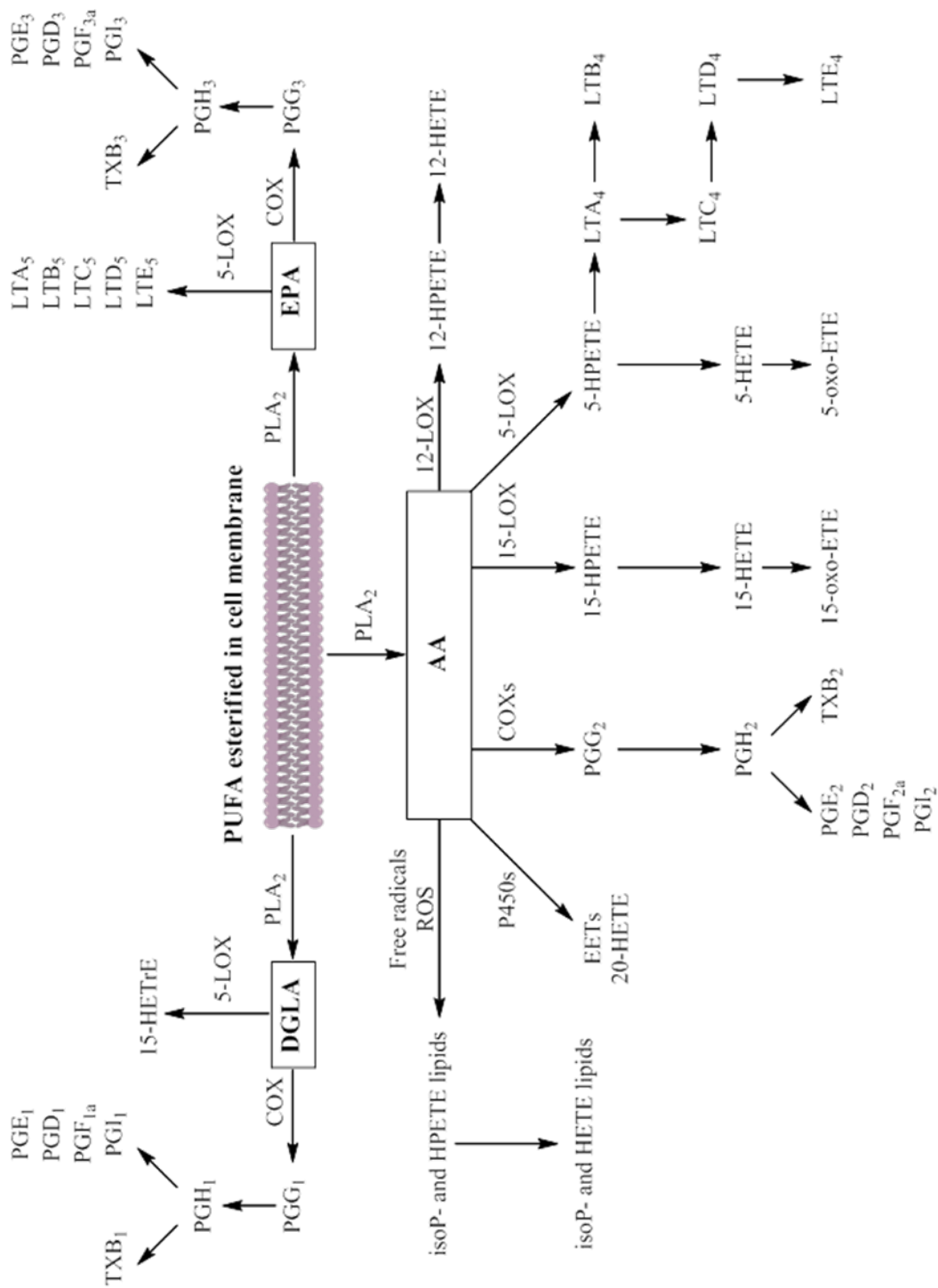
LA and ALA are considered to be essential fatty acids, which must be obtained from the diet because mammals lack the ability to introduce double bonds into fatty acids beyond carbons 9 and 10 counted from the carboxyl end [3-5]. LA is the precursor of the ω -6 PUFAs and ALA is the precursor of the ω -3 PUFAs. Once consumed, LA and ALA can be metabolized to their

down-stream PUFAs by the combined action of desaturation and elongation enzymes [2]. Desaturation enzymes introduce a new double bond in the carbon atom chain and elongation enzymes introduce two new carbon atoms. LA (18:2) is converted into GLA (18:3) by Δ -6 desaturase (D6D), followed by a two carbon atom chain elongation through a fatty acid elongase, elongation of very long chain fatty acid protein 5 (ELOVL5), to form DGLA (20:3) and finally undergoing desaturation by Δ -5 desaturase (D5D) to generate AA (20:4). Using the same series of enzymes as those used to metabolize ω -6 PUFAs, ALA is converted into EPA (20:5). Further conversion of EPA into DHA (22:6) involves two elongation steps to form docosapentaenoic acid (22:5) and tetracosapentaenoic acid (24:5), respectively; then desaturation to form tetracosahexaenoic acid (24:6) and removal of two carbons by β -oxidation to yield DHA [3] (Scheme 1). Among the series of elongation and desaturation steps in the metabolism of ω -6 and ω -3 PUFAs, D6D and D5D control the rate-limiting steps [13]. D6D and D5D are expressed in the majority of human tissues, with the highest levels being found in the liver, brain and heart [14].

PUFAs are important constituents of all cell membranes. PUFA esterified in the cell membrane's phospholipid is released by the action of several phospholipase enzymes (predominantly Phospholipases A2, PLA2). The fatty acids released by this hydrolysis subsequently undergo enzymatic or non-enzymatic lipid peroxidation to form various lipid mediators (Scheme 2). Cyclooxygenase (COX), lipoxygenase (LOX) and the cytochrome P450s (CYP450) are three major enzymes which could metabolize PUFA to prostaglandins (PGs), thromboxanes (TXs), leukotrienes (LTs), monohydroxy fatty acids and epoxy fatty acids [15, 16]. Isoprostanes, isoleukotrienes, and other peroxidized fatty acid products are formed non-enzymatically [16].

eicosanoids include the 2-series of PGs, the 2-series of TXs formed by COX; the 4-series of TXs, 15- and 12-hydroxyeicosatetraenoic acids (HETEs) formed by LOX; and the epoxy eicosatrienoic acids (EETs) and 20-HETE formed by CYP450 [15]. DGLA and EPA are also the substrates for COXs (constitutive isoform COX-1 and inducible isoform COX-2) and various LOXs (5-LOX, 12-LOX, and 15-LOX). DGLA is the precursor of the 1-series of PGs, the 1-series of TXs and 15-hydroxyeicosatrienoic acid (15-HETrE) [17]. EPA is the precursor of the 3-series of PGs, the 3-series of TXs and the 5-series of LTs [18]. Those eicosanoids are synthesized *de novo* as required and act in an autocrine or paracrine manner on target cells [19].

The compositions of dietary PUFAs vary among countries. The typical western diet is considered to be a high fat, high energy diet but with low fiber intake [20, 21]. As a consequence of the increased intake of LA-enriched vegetable oils in the Western diet [22, 23], the ratio ω -6: ω -3 in the Western diet is around 10:1 to 20:1, while the recommended ratio is 1:1 to 4:1 [24-26]. Over the last few decades, epidemiological studies have suggested that the increased dietary intake of ω -6 PUFAs is associated with an increase in the incidence of diseases involving inflammatory processes such as cardiovascular diseases, rheumatoid arthritis, inflammatory bowel diseases, and cancer [2, 20, 27, 28]. On the other hand, dietary intakes of ω -3 PUFAs could ameliorate the symptoms of chronic inflammation and decrease cancer incidence [2, 11, 29, 30]. Eskimos and Japanese fisherman who have a high consumption of ω -3 PUFAs from fish and marine mammals have low rates of breast and colon cancers [23, 31]. Interestingly, some studies showed that DGLA may be an exceptional ω -6 PUFA which actually possesses anti-inflammatory and anti-cancer activities [32-34].



Scheme 2. An overview of eicosanoid biosynthesis pathways.

PUFA constitutes the phospholipid domain of most cell membranes and is liberated from the cellular membranes by PLA₂. Free fatty acids can be metabolized to eicosanoids through non-enzymatic pathways and through three enzymatic pathways: COXs, LOXs and CYP450s.

1.1.2. AA-derived eicosanoids and inflammation related diseases

As a result of the high intake of ω -6 PUFAs in Western diets, AA is the predominant PUFA in most cell membranes. AA is the precursor of the 2-series of PGs, the 2-series of TXs, and the 4 series of LTs. In general, the actions of eicosanoids derived from AA are more pro-inflammatory. Chronic inflammation is believed to be associated with an increase in cancer incidence. One of the strongest associations between chronic inflammation and cancer is the increased risk of colon cancer in individuals with inflammatory bowel diseases [35, 36]. Inflammation also plays an important role in the development of other cancers, *e.g.* prostate, bladder, pancreatic, and breast cancers [37-39]. Inflammation in the tumor microenvironment is now recognized as one of the hallmarks of cancer. Chronic inflammation causes the up-regulation of a number of pro-inflammatory cytokines including interleukin (IL)-1, IL-6 and tumor necrosis factor (TNF)- α . Nuclear factor kappa B (NF κ B) is a transcriptional factor which has a variety of pro-tumorigenic activities. The pro-inflammatory cytokine-induced activation of NF κ B leads to increased cell proliferation, stimulation of angiogenesis, and resistance to apoptosis [40, 41]. NF κ B is the key mediator of inflammation-induced carcinogenesis and evidence directly links the NF κ B pathway to increased tumor formation and inflammation in experimental mouse models of intestinal cancer [42, 43]. Because NF κ B regulates COX-2 expression at the transcriptional level, COX-2 expression is increased, and higher levels of inflammatory PGE₂ are formed [44-46]. Thus, inflammation and enhanced metabolism of AA by COX-2 are linked to the increased risk of cancer. Higher PG levels, mainly PGE₂, are observed in various tumors [47, 48]. In addition to regulation by COX, the PGE₂ level is also determined by 15-prostaglandin dehydrogenase (15-PGDH), a prostaglandin degradation enzyme. 15-PGDH

oxidizes the active PGE₂ into biologically inactive 15-keto PGE₂. The expression of 15-PGDH was reduced in many tumors, which also contributes to the increase of PGE₂ [49-51].

The biological effect of PGs is mediated by a family of G-protein coupled receptors, designated EP for PGE₂ receptors, FP for PGF_{2α} receptors, TP for the thromboxane receptor, and IP for PGI₂ receptors [52]. Some PGs are also ligands for nuclear receptors such as peroxisome proliferator-activated receptors (PPARs). For example, PGI₂ is a natural ligand for PPAR δ [53]. Due to the high concentrations of PGE₂ in tumors, EP receptors have been extensively studied [52]. Four subtypes of EP receptors have been identified, designated as EP1, EP2, EP3, and EP4 [52, 54-57]. The signaling pathways of the EP receptor subtypes are significantly different. The EP1 receptor couples to phospholipase C/inositol triphosphate *via* a Gq-protein, leading to increased intracellular calcium concentration. The EP2 and EP4 receptors couple to adenylate cyclase (AC) *via* a Gs-protein, resulting in increases in intracellular levels of cyclic 3', 5'-adenosine monophosphate (cAMP). The EP4 receptor couples to a Gi protein, leading to the reduction of intracellular cAMP [54]. Both EP2 and EP4 expression are up-regulated in azoxymethane-induced colorectal cancer tissue compared with adjacent normal mucosa [55]. The mRNA levels of the EP2 and EP4 receptors also increased in APC^{Δ716} mouse small intestinal and colonic polyps [56]. Activation of EP2 and EP4 receptors *via* PGE₂ has been linked to cell proliferation, invasion, apoptosis, and angiogenesis [57]. Signaling through EP2 leads to GSK-3 phosphorylation *via* a protein kinase A (PKA)-dependent mechanism, while the activation of EP4 also leads to GSK-3 phosphorylation, but *via* a phosphatidylinositol 3-kinase-dependent pathway [58, 59]. PGE₂ can also transactivate the epidermal growth factor receptor (EGFR) [60] and the PPAR δ receptor [61].

Numerous epidemiological, clinical, and animal and cell culture studies have documented that the use of COX inhibitors or non-steroidal anti-inflammatory drugs (NSAIDs) is effective at decreasing the incidence and mortality of colorectal cancer [62, 63]. Apart from colorectal cancer, NSAIDs have also been associated with a reduced risk of many other cancers, for example, breast, stomach, bladder, ovary, and lung cancers [48, 64, 65]. Despite the efficacy of NSAIDs as chemopreventive agents, the precise molecular mechanisms underlying the protective effects of NSAIDs are not well understood. One possible mechanism for their anti-cancer properties has been attributed to the altered metabolism of AA. Inhibition of COX leads to the reduced conversion from AA to the pro-inflammatory prostaglandins.

1.1.3. DGLA-derived eicosanoids and inflammation related diseases

Increasing evidence suggests that DGLA might be an exception among the ω -6 PUFA family members in its potential ability to suppress tumor growth and metastasis [66-68]. DGLA is shown to inhibit the motility and invasiveness of human colon cancer cells *via* increasing the expression of E-cadherin, a cell-to-cell adhesion molecule which suppress metastasis [66, 67]. In addition, DGLA reduces tumor-endothelium adhesion, a key factor in the establishment of distant metastases, partly by improving gap junction communication within the endothelium [66, 68].

Because DGLA and AA are competing for the lipid-peroxidizing enzymes such as COX and LOX, an increase in DGLA relative to AA is able to attenuate the biosynthesis of AA-derived eicosanoids, *e.g.* the 2-series of PGs and the 4-series of LTs, and exert an anti-inflammatory effect [69]. Depending on the cell type, DGLA is converted to members of the 1-series of PGs (mainly PGE₁) and/or 15-HETrE [27]. These two DGLA-derived eicosanoids have shown clinical efficacy in a variety of diseases, including suppression of chronic inflammation,

vasodilation and lowering of blood pressure, inhibition of smooth muscle cell proliferation associated with atherosclerotic plaque development, inhibition of cancer cell growth and the differentiation of tumor cells [70-73].

In comparison with PGE₂, PGE₁ may possess distinct anti-inflammatory and anti-proliferation action. GLA and DGLA supplementation studies conducted in humans and mouse models have shown that the synthesis of 1-series PGs, rather than the 2-series PGs, is selectively elevated by either GLA or DGLA [17, 74]. Although the increases in the tissue levels of PGE₁ after DGLA supplementation are modest relative to those of PGE₂, effects are noteworthy because select biological properties of PGE₁ are about 20 times stronger than those of PGE₂ [75]. In particular, PGE₁ triggers a series of intracellular responses by binding to select EP receptors and/or the IP receptor [76]. The EP2 and EP4 receptors couple to adenylate cyclase *via* a Gs-protein, and receptor activation results in increases in intracellular levels of cAMP. Elevation of cAMP stimulates the expression of numerous genes through the PKA-mediated phosphorylation of the nuclear cAMP response element binding proteins (CREB). Through this mechanism, PGE₁ has been shown to inhibit vascular smooth muscle cell proliferation *in vitro* [32, 77], reducing the migration and proliferation of vascular SMC which, in turn, arrests the formation of typical atherosclerotic plaque [78, 79]. Whether PGE₁ and PGE₂ act on the same or different receptors was still not clear. Some studies demonstrate that PGE₁ could compete with PGE₂ through binding to the same receptors, EP2 and EP4 [80-82].

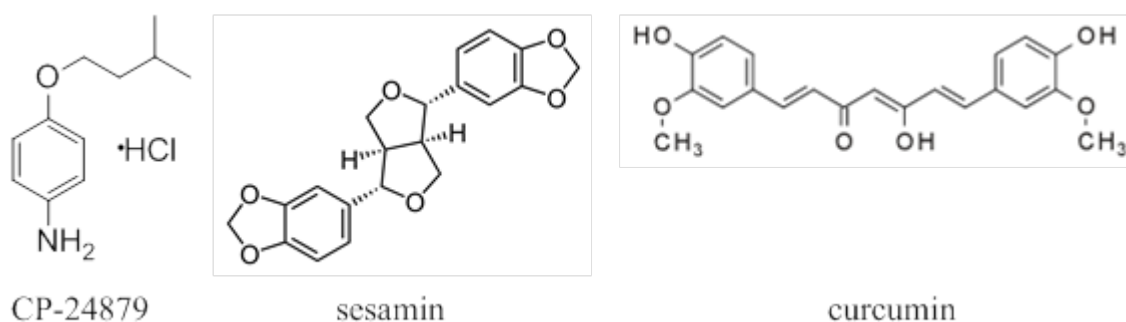
Several diseases may benefit from GLA or DGLA administration [17, 83]. It is reported that GLA and DGLA suppress human synovial cell proliferation by increasing PGE₁ synthesis and intracellular cAMP levels [84]. In addition, administration of GLA or DGLA is capable of suppressing human T-cell proliferation [83, 85]. Recent studies demonstrated that DGLA

produced by GLA feeding decreased the Th2 cytokine and immunoglobulin G1 antibody responses. GLA and DGLA was also able to induce T-regulatory cell activity, *e.g.*, transforming growth factor (TGF)-beta-producing T cells, and was able to reduce proinflammatory IL-1 and TNF- α production [86], indicating that the immunity mechanism is likely to participate in the anti-tumor effect.

However, the mechanism of DGLA-mediated effects has not been fully elucidated. It is worth noticed that in both *in vivo* and *in vitro* studies, the cellular content of AA, even after significant enrichment with DGLA, was still 2.5 ± 3.0 -fold higher than DGLA, mainly due to the effective desaturation of DGLA to AA by D5D [74, 87, 88]. For example, dietary supplementation of GLA or DGLA as ethyl esters or triglycerides leads to only a small increase in GLA or DGLA content in cell membrane lipids, often accompanied by a very significant increase in AA content. Moreover, the cellular ratio of PGE₁/PGE₂ in animals fed with GLA-enriched oils was shown to be substantially lower than the ratio of DGLA/AA [17, 74]. Similarly, in mouse fibrosarcoma cells treated with exogenous DGLA, the ratio of PGE₁/PGE₂ was considerably smaller than the cellular ratio of DGLA/AA [87, 89].

Therefore, an effective solution to accumulate DGLA is inhibiting the further conversion from DGLA to AA by D5D inhibitors. Sesame, curcumin and CP-24879 (a mixed D5D/D6D inhibitor) (Scheme 3) have been verified to exert anti-proliferative or anti-cancer effects *via* their ability to enhance the concentration of DGLA [74, 88, 90, 91]. The addition of GLA or DGLA together with CP-24879 inhibited D5D activity and blocked the biosynthesis of AA from DGLA. This led to a very substantial increase in the accumulation of DGLA from 2.3% to almost 12% of total fatty acids without a change in the level of AA in cells [74]. In addition, because addition of DGLA bypasses a rate-limiting enzymatic step (D6D desaturation) that controls the metabolism

of ω -6 PUFAs, it may generate a systemic decline in Δ 6 desaturation. A reduced capacity to convert LA to DGLA has been associated with various physiological and pathophysiological states, including diabetes, atopic dermatitis, rheumatoid arthritis, cardiovascular disease and cancer [17, 33, 92]. Therefore, supplementation of DGLA with inhibitors of D5D may be valuable in alleviating some of the symptoms of these diseases. The biosynthesis of DGLA-derived eicosanoids is dependent primarily on the abundance of free DGLA, so increasing the administration of DGLA and/or targeting the D5D may be a good strategy to treat some inflammation diseases.



Scheme 3. Structure of tested D5D inhibitors.

The typical Western diet enriched in ω -6 PUFAs has been suggested to be associated with an increased risk of cancer and other inflammation-related diseases. However, DGLA might be an exceptional ω -6 which may have anti-cancer and anti-inflammatory effects. As the most abundant ω -6 PUFA in mammalian cells, AA is metabolized to the pro-carcinogenic and pro-inflammatory 2-series of PGs through COX. DGLA, the upstream fatty acid of AA, is also a substrate of COX and is converted to the anti-carcinogenic and anti-inflammatory 1-series of PGs. The PUFA-derived eicosanoids such as the PGs have been extensively studied. However, eicosanoids are not the only metabolites generated from COX-catalyzed PUFA peroxidation.

Many other lipid mediators have been discovered, such as the PUFA-derived free radical metabolites and the degradation end products.

1.2. Lipid Peroxidation and Lipid Mediators in Inflammatory Diseases

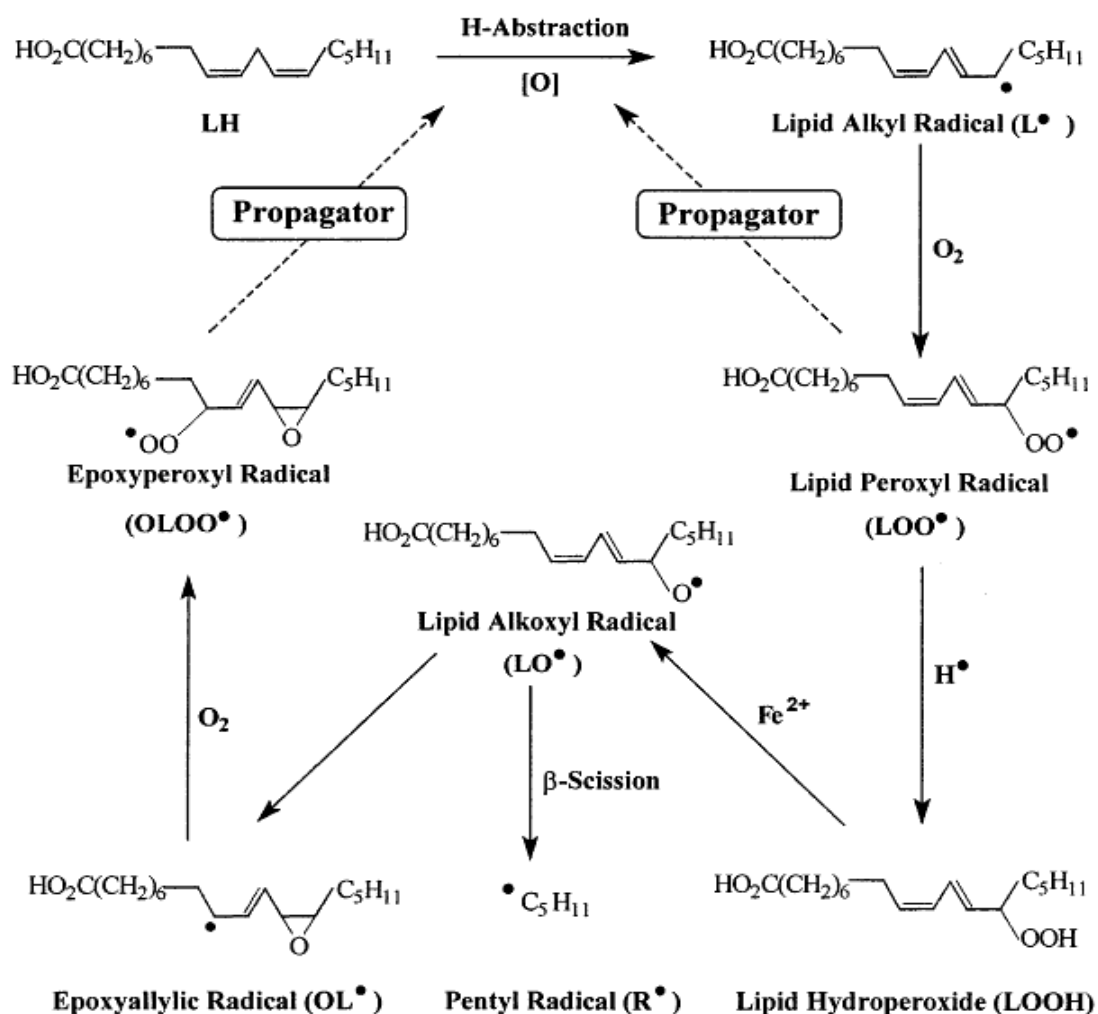
PUFAs with methylene-interrupted double bonds are highly susceptible to oxidative decomposition, or what is commonly known as lipid peroxidation. LOX and COX are two lipid-peroxidizing enzymes that metabolize dietary and membrane lipids (PUFAs) through a series of free radical reactions [93-95]. The lipid metabolites generated from both LOX- and COX-catalyzed peroxidation of PUFAs, such as LA (18:2, ω -6), AA (20:4, ω -6), EPA (20:5, ω -3), and DHA (22:6, ω -3), have been of great interest due to their potent and diverse biological activities. Lipid peroxidation and PUFA metabolites are implicated in tumor growth, angiogenesis, and metastasis by the change in expression of various LOXs (5-LOX, 12-LOX, and 15-LOX) and COX-2 (inducible COX isoform) in a variety of cancers [96-99].

COX-/LOX-catalyzed PUFA peroxidation is a well-known free radical chain reaction consisting of three major steps-initiation (reaction 1), propagation (reactions 2-3), and termination (reactions 4-5):



Here L-H represents a lipid molecule, *e.g.* PUFA; L^\bullet represents a carbon-centered lipid (PUFA) radical, and X^\bullet represents radicals from oxidants, *e.g.* hydroxyl radical, ferryl and perferryl species, and oxidative species in activated COX/LOX enzymes. The weakest carbon-

hydrogen bonds, at the *bis*-allylic methylene position of PUFAs, are typically vulnerable to oxidation since they have a much lower dissociation energy (~75 kcal/mol) than that of a typical alkyl C-H bond (101 kcal/mol [100, 101]). During propagation (reactions 2-3), peroxy radical (LOO^\bullet , propagator) forms from the reaction of L^\bullet with oxygen, and further attacks another lipid or PUFA molecule. Peroxy radical can also be converted into other types of free radicals through H-abstraction, Fe^{2+} -mediated Fenton-type reactions, and β -scission (Scheme 4) [2, 93, 102].



Scheme 4. An overview of free radical reactions in LA peroxidation.

Adapted from Qian et al. [102].

Apart from eicosanoids, lipid peroxidation products are the most investigated bioactive molecules of PUFA metabolism. Through lipid peroxidation, many highly reactive lipid radicals are produced and degraded to a series of lipid peroxidation end products including malondialdehyde (MDA) and 4-hydroxy-2-nonenal (4-HNE) [103-105]. These end products of lipid peroxidation participate in the signal transduction cascade and in control of cell proliferation and differentiation, as well as in apoptosis pathways [106-108].

MDA is the most mutagenic degradation product of PUFA peroxidation. Dietary intake of PUFAs increases intestinal MDA production *in vivo* [109]. MDA then reacts with the guanine in DNA to form a cyclic pyrimido [1,2 α] purin-10(3H)-one (M₁dG) adduct, which is the major MDA-DNA adduct detected in human and rodent tissues. If the DNA repair system does not replace the M₁dG with a normal DNA base, cells will undergo apoptosis, or genetic mutation will be induced. M₁dG genetic mutation is one of the possible reasons for the carcinogenic features of MDA. MDA together with 4-HNE also forms adducts with elongation factor two in ribosomes, consequently disturbing or reducing protein synthesis, which has often been observed during ageing and cancer development [110].

The MDA level is significantly elevated in colitis, an inflammatory and preneoplastic state of colorectal cancer, and antioxidants decrease the MDA concentration in animal models and ameliorate the severity of colitis [111]. Increased plasma or urine MDA concentration has also been observed in many other cancers, such as skin, breast and also colorectal cancer [112]. In patients with advanced colorectal cancer, the serum MDA concentration is much higher than in those with primary colorectal cancer [113]. Surinenaite et al. [114] found that the serum MDA level was more elevated in stage III than stage II colorectal cancer patients. After the tumor tissue was removed by surgery, the serum MDA level was significantly decreased [115]. These

observations suggest a close correlation between MDA and colorectal cancer carcinogenesis and progression, and MDA is thus a potential biomarker for clinical prognosis and use as an index of surveillance of treatment effects. On the other hand, increased levels of reactive oxygen species and MDA lead to mitochondrial dysfunction. This cytotoxic effect may be attributed to the inhibitory effect of PUFAs in colorectal cancer cell growth [116].

Recently, increasing evidence from animal and *in vitro* studies suggests that unlike the other ω -6 PUFAs and their lipid mediators, which generally possess pro-inflammatory and pro-cancer activity, DGLA might inhibit carcinogenesis [70]. A supplement of DGLA significantly increased the formation of free radicals and lipid peroxides in tumor cells and induced apoptosis [117, 118], suggesting that DGLA-derived free radicals and lipid peroxides may be responsible for its anti-tumorigenic effect by influencing apoptosis and genes/oncogenes that regulate the apoptotic process [117]. Previous studies have shown that under certain conditions some PUFAs were able to induce apoptosis of tumor cells with little or no cytotoxic action on normal cells [117, 119, 120]. It was observed that among all the tested fatty acids, DGLA was the most effective in selectively killing tumor cells [117]. These results suggested that DGLA shows selective tumoricidal action *in vitro*. Through suppressing the expression of oncogenes Her-2/neu and Bcl-2 and enhancing p53 activity, DGLA could induce apoptosis of tumor cells [119, 121-123]. Further study found that the COX inhibitor and anti-oxidants had opposite effects on the anti-tumorigenic action of DGLA. It was found that COX inhibitors blocked the tumoricidal action of DGLA on human cervical carcinoma, whereas anti-oxidants inhibited the cytotoxic action of DGLA on human breast cancer cells [124-126]. These results suggested that the COX metabolism of DGLA may play a role in the anti-cancer effect of DGLA.

In some cancer cells, GLA or DGLA led to only a partial inhibition of cancer cell growth in the presence of a COX inhibitor, which indicates that PGE₁, the COX product of DGLA, cannot completely account for its anti-tumor effect [17, 33, 74]. Recent research revealed that free radicals and lipid peroxidation are related to the cytotoxicity of PUFAs on cancer cells, which could be completely arrested by anti-oxidants such as vitamin E and superoxide dismutase. On the other hand, it has been reported that vitamin E only partially arrests the growth inhibition of cancer cells mediated by PUFAs [122, 127]. The different experimental results may be because of the use of various cell lines. Another reason is that almost all the cytotoxic effects against cancer cells depend on the concentration of the metabolic products from PUFAs. Therefore, it is possible that DGLA exerts its anti-tumor cytotoxic effects *via* a combination of the free radicals, lipid peroxidation and the non-radical metabolites, which probably inhibit cell proliferation, promote apoptosis and even make cancer cells differentiate and mature.

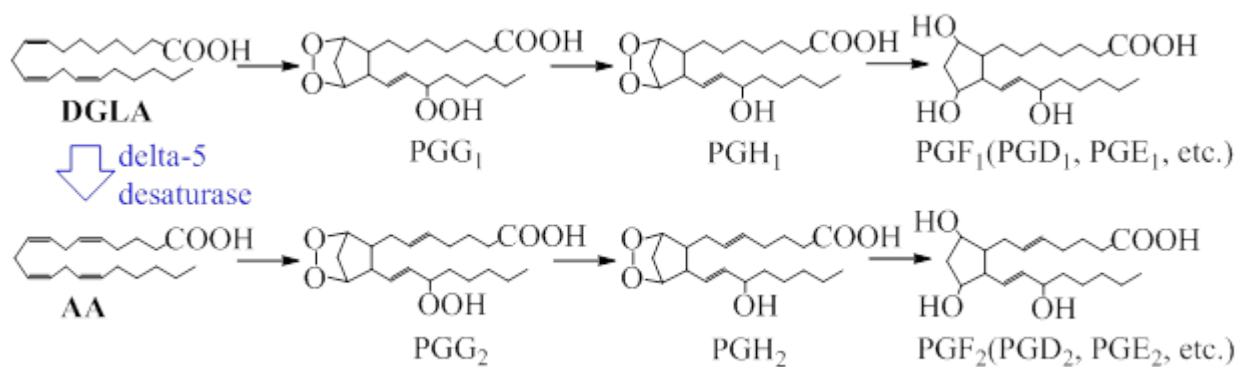
Through a series of free radical reactions, various bioactive lipid mediators were generated from COX-catalyzed PUFA peroxidation, among which the role of the free radical metabolites in inflammatory diseases was still not clear. AA and DGLA are both substrates of COX. Due to the differences in their structures and the substrate-enzyme conformations in the active site, COX may catalyze AA and DGLA's peroxidation through different free radical reactions, thus resulting in different free radical metabolites [171, 173].

1.3. The Catalytic Mechanism of COX

COX (also referred as prostaglandin endoperoxide H) is a lipid peroxidizing enzyme that catalyzes the committed step in prostaglandin biosynthesis. There are two COX isoforms: COX-1 and COX-2 [128]. COX-1 is constitutively expressed in most mammalian tissues. The prostaglandins produced by COX-1 in response to hormone stimulation play a housekeeping role

in normal physiological processes, including the regulation of renal water and sodium metabolism, stomach acid secretion, parturition, and hemostasis [19, 129]. COX-2 is induced by various cytokines, growth factors, inflammation mediators and tumor promoters, and is involved in cell replication and differentiation [19]. COX-1 and COX-2 are therapeutic targets for NSAIDs, including aspirin, ibuprofen, and the specific COX-2 inhibitors [48, 130-132]. NSAIDs inhibit the production of lipid metabolites through COX, reduce inflammation, fever, and pain, and lower the risk of mortality from cardiovascular disease and various cancers [48, 130-133].

COX converts fatty acids, *e.g.* DGLA and AA, to PGH in two reactions: 1) its prostaglandin H synthase activity (the cyclooxygenase activity) incorporates two oxygen molecules into DGLA and AA to generate PGG and 2) its peroxidase activity, generally coupled with a reducing agent, reduces PGG to form PGH, which can be further converted to a second series of PGs (PGD, PGE, and PGF) (Scheme 5).



Scheme 5. COX-catalyzed DGLA and AA peroxidation.

DGLA is converted to AA *via* D5D.

These two reactions occur at distinct but structurally and functionally interconnected sites. The cyclooxygenase catalysis requires the enzyme to be activated first, a process which is peroxide-dependent [134-136]. In contrast, the peroxidase activity is independent of the cyclooxygenase [134-136]. At the cyclooxygenase site, the reaction begins with abstraction of the 13-pro-*S*-hydrogen from AA by a tyrosyl radical positioned on Tyr-385; this step is the rate-

determining step and generates an AA radical [3, 134]. The tyrosyl radical is formed due to oxidation of the heme group at the peroxidase site of the enzyme [134].

Although there are some subtle kinetic differences between COX-1 and COX-2 in terms of hydroperoxide activator requirements and substrate and inhibitor specificities [137, 138], the two isoforms are closely related structurally and mechanistically. Both isoforms are signal peptides with different lengths. COX-1 contains 576 amino acids and COX-2 contains 587 amino acids [134, 135, 137, 138]. COX-1 and COX-2, which are encoded by separated genes, showed a 60%-65% sequence identity in the same species, and individual isoforms from different species showed an 85%-90% sequence identity. The crystal structures of COX isoforms are structurally homologous and superimposable~~[134, 135, 137, 138]~~. Each monomer consists of three domains: an epidermal growth factor (EGF) domain of about 50 amino acids in length at the N terminus, a neighboring membrane binding domain (MBD) of about 50 amino acids in length, and a large C-terminal globular catalytic domain of about 460 amino acids in length. The EGF domain is essential for folding [134, 135, 137, 138]. The MBDs of COX contain four amphipathic helices, the last of which merges into the catalytic domain [134, 135, 137, 138]. These helices surround an opening into the COX active site through which fatty acid substrates and NSAIDs are believed to enter~~[134, 135, 137, 138]~~. The globular catalytic domain has a hydrophobic channel protruding into the core of this domain [134, 135, 137, 138].

Both COX-1 and COX-2 are located on the luminal surfaces of the ER and of the inner and outer nuclear membranes [137, 138]. COX-2 appears to be relatively more concentrated within the nuclear membrane thus the products formed through COX-2 may have greater access to the nucleoplasm to influence nuclear events *via* nuclear receptors [137, 138].

X-ray crystallographic studies indicate that the COX catalysis occurs in a hydrophobic channel which extends from the MBD of the enzyme into the core of the globular domain [139]. The fatty acid substrate, such as AA or DGLA, is positioned in this site in an extended L-shaped conformation [139, 140]. Crystallographic [139] and mutagenic [141, 142] analyses of the interaction of AA within the COX active site assigned active site residues to functional categories [141, 142] as follows: (a) Tyr-385 residues directly involved in abstraction of the 13-pro-*S*-hydrogen (Tyr-385); (b) residues essential for positioning C-13 for hydrogen abstraction (Tyr-348 and Gly-533); (c) residues essential for the high binding affinity of AA (Arg-120); and (d) residues critical for positioning AA such that following abstraction of the 13-pro-*S*-hydrogen the AA radical is converted to PGG₂ at the cyclooxygenase active site (Val-349, Trp-387, and Leu-534).

Most studies of COX activities have utilized AA as the substrate. Although AA is the preferred substrate, both COX isoforms will oxygenate ω -3 and ω -6 C18, C20, and C22 fatty acids *in vitro* with catalytic efficiencies in the range of 0.05–0.7 that of AA [143]. Some of these alternative substrates, including DGLA, are also oxygenated *via* COX activity when added exogenously to intact cells [74]. Substrates other than AA typically have higher K_m values than AA [143] but can compete with AA for the COX active site, thereby inhibiting formation of the 2-series PGs.

A mutational and crystallographic analysis of the interaction of DGLA with the COX active site identified the active site residues that determine COX fatty acid substrate specificity [140]. DGLA binds in the COX active site channel in an extended L-shaped conformation generally similar to that seen for AA [140]. Despite their similar L-shaped conformations in the COX active site, the positions of the carboxyl halves of the DGLA and AA molecules differ

significantly [139, 140]. The locations for C-3, C-4, and C-6 through C-8 of DGLA in the COX active site are the two regions showing the largest deviations from AA [140]. Specifically, the relative positions of C-2 through C-10 differ considerably between AA and DGLA due to the absence of the C-5/C-6 double bond in DGLA [140].

The differences in the catalytic mechanism of COX-mediated DGLA and AA peroxidation suggested that there may be different free radical metabolites formed through different free radical reactions. However, due to their high activity and short lifetimes, the free radical metabolites had not been identified and characterized until recently [171, 173], not to mention their association with PUFA's bioactivity. The development of an appropriate technique for characterization of PUFA-derived radicals during lipid peroxidation greatly advances the understanding of COX and PUFA peroxidation in inflammatory diseases.

1.4. PUFA-Derived Free Radical's Detection and Characterization

1.4.1. Electron spin resonance and spin-trapping

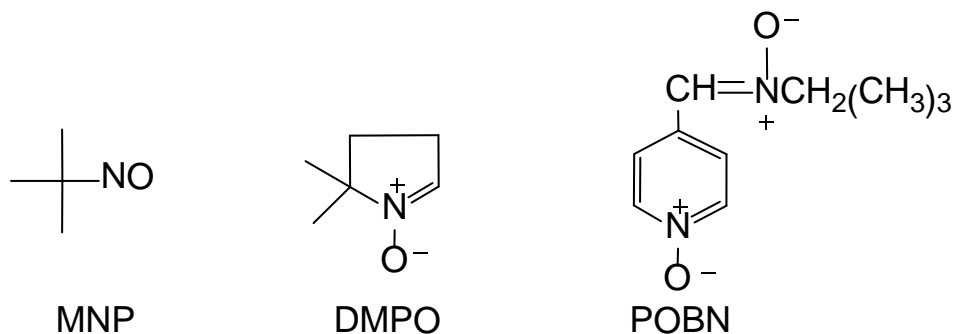
The most common and traditional technique to measure free radicals is electron spin resonance (ESR), also known as electron paramagnetic resonance (EPR). ESR is designed to detect chemical species containing unpaired electron(s), which are detected in a magnetic field as they transition between different energy levels [144]. The ESR spectrum gives the distinctive ESR parameters of each radical, hyperfine couplings and g values, which give information about the structures of radicals.

Unfortunately, in living systems, almost all free radicals that are generated are very reactive and have very short lifetimes. The short lifetimes of free radicals make them undetectable by ESR due to poor signal-to-noise. In order to overcome this problem, the ESR spin trapping technique was developed in the late 1960's [145-147]. In this technique, primary

and short-lived free radicals in a living system could react with either a nitron or nitroso compound (spin trapping agent) to form spin adducts or radical adducts (reaction 6) that have a much longer lifetime and can be measured by ESR.



Three classic and common spin trapping agents are listed in Scheme 6: 2-methyl-2-nitrosopropane (MNP), α -[4-pyridyl 1-oxide]-N-*tert*-butyl nitron (POBN), and 5, 5-dimethyl-1-pyrroline N-oxide (DMPO). MNP and POBN are spin trapping agents that preferentially trap carbon-centered free radicals [148-152]. DMPO has more trapping flexibility since it can trap different types of unstable free radicals, including oxygen-centered, carbon-centered, and sulfur-centered free radicals [153-155]. These spin traps had all been broadly used to assist ESR measurement of PUFA-derived radicals formed from many chemical and biological systems [156-159].



Scheme 6. The structures of three classic and common spin traps.

Due to its good spin trapping ability and appropriate solubility in biological media, the nitron compound POBN has been widely used in many ESR studies to detect PUFA-derived free radicals formed from *in vitro* and *in vivo* lipid peroxidation. It has so far been the most successful spin trap used to trap PUFA-derived free radicals in both cellular peroxidation and *in vivo* peroxidation [101, 160-162]. However, like all other spin trapping agents used with the

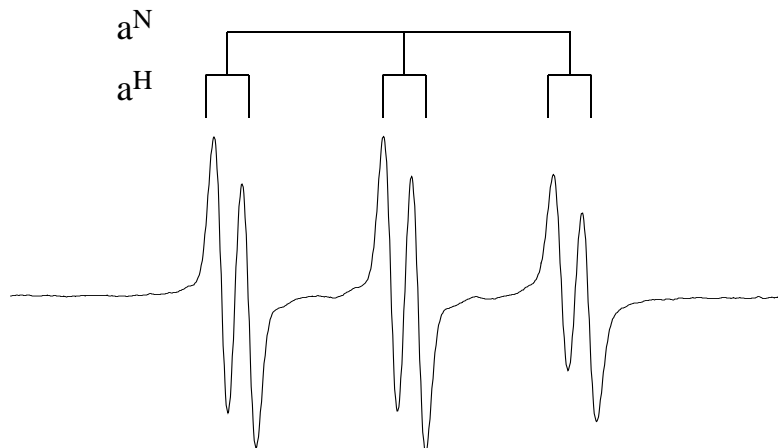


Fig. 1. Typical ESR spectrum of POBN radical adduct.

Note, $a^N \approx 14.4\text{-}16.1$ G; $a^H \approx 2.2\text{-}2.8$ G.

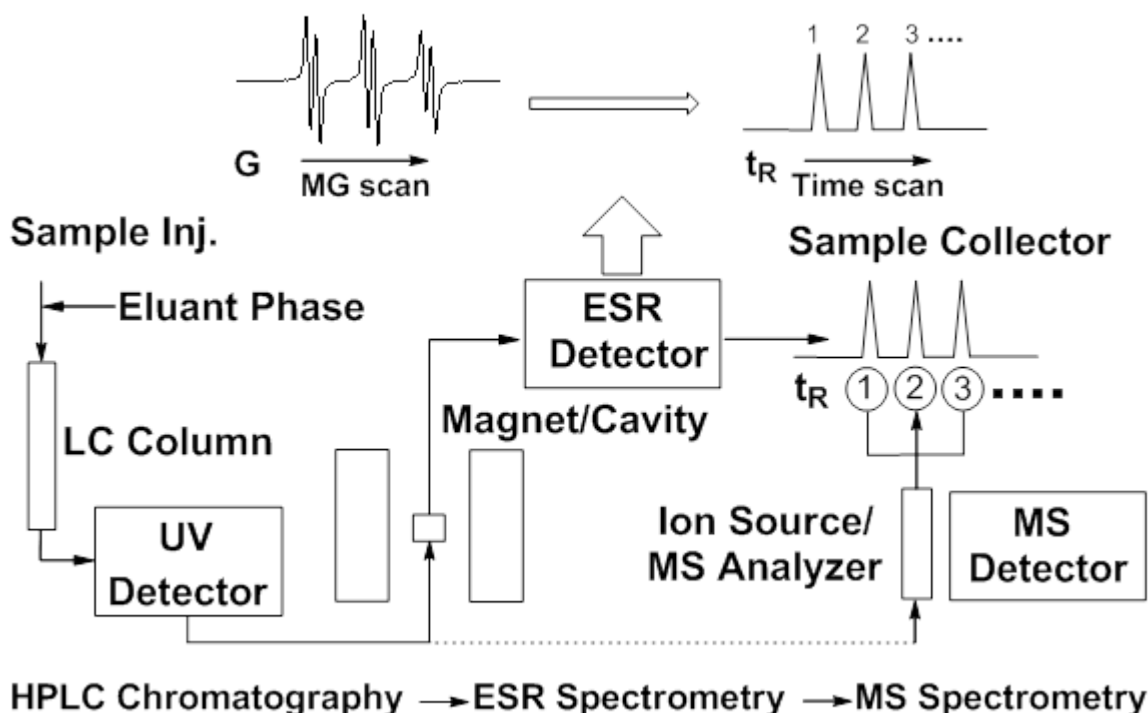
with many factors such as solvent, temperature, and even the individual ESR instrument. Thus, in most previous studies, PUFA-derived free radicals had never been structurally identified with the traditional ESR method. Their structures were either proposed based on the presumed mechanism or ambiguously termed PUFA-derived free radicals.

1.4.2. Development of the combined HPLC/ESR/MS and spin-trapping technique

In order to characterize individual PUFA-derived free radicals generated from complicated lipid peroxidation, many researchers had combined ESR with high-performance liquid chromatography (HPLC) as well as mass spectrometry (MS) and/or tandem MS (MS^2). A typical combination system is displayed in Scheme 7, in which spin trapped free radicals with the same and/or similar spectra (*e.g.* the six-line spectrum of the POBN adduct) were separated by a chromatography column according to their polarities, monitored by ESR, and collected and/or directly eluted to the MS detector for structure identification.

In the on-line ESR system, instead of running a magnetic field scan to get a six-line ESR spectrum for POBN adduct(s), a time scan would be conducted with the magnetic field fixed on the top of the first or third line of the POBN adduct spectrum. In this way one would observe a

number of absorption peaks vs. retention time, with each peak representing a POBN adduct with a different structure and/or a different isomer.



Scheme 7. LC/ESR/MS combined technique.

Spin trapped radical adducts that have identical or similar ESR spectra are separated with an HPLC column, detected by on-line ESR under a time scan model with a fixed magnetic field, and then identified by MS. The dashed line represents an LC/MS refinement that offers much higher detection sensitivity and reliability since all three redox forms of a radical adduct can be measured.

In the late 1980's, Iwahashi et al. made great efforts to develop an LC/ESR and LC/MS combination to characterize free radicals formed from PUFA peroxidation, epoxidation and β -scission hydroperoxidation [163, 164]. However, since many technologies, *e.g.*, the fast resolution LC column and the soft ionization MS analyzer, were unavailable or not yet used in research, several problems were encountered in the characterization of free radicals *via* a combination of LC/ESR and LC/MS: (1) although HPLC was used to separate POBN adducts in an LC/ESR on-line system, the UV chromatogram of the analyte had never been reported due to

very poor chromatography resolution; (2) the ESR-active LC fractions (*e.g.* POBN radical adducts) were not detected as the corresponding m/z ions. The product ions of the reduced forms of spin adducts were detected for ESR-active peaks, which raised questions about the method's reliability; (3) some POBN radical adducts, particularly the radicals with $-COOH$ ($\sim pK_a$ 5.0), had very poor retention behavior due to the pH range (5-6) of the mobile phase (ammonium acetate) used for chromatographic separation; (4) a semi-preparative LC column and very large amounts of samples were required for these experiments, thus it was not a suitable protocol for most biological reactions, in which analytical sampling and performance are demanded [74-75]; and (5) a serious ESR tuning problem was encountered due to poor chromatograph resolution and low sensitivity arising from interface issues between the LC and ESR. The ESR tuning problem often creates artificial on-line ESR peak(s) during LC/ESR detection, thus also raising the question of the method's reliability.

Benefiting from many new developments and improvements in LC and MS technology in the early 2000's, Qian et al. finally made a breakthrough in combining the LC/ESR and LC/MS methods to characterize PUFA-derived free radicals in many biological systems [156, 165]. The interface issues present in the combination of the HPLC, ESR, and MS techniques (Scheme 7) were dealt with, and most problems encountered in previous applications have been resolved. This refined combination of LC/ESR and LC/MS [165-167] was able to optimize several aspects of the chromatography and MS conditions: (1) adding 1.0 - 0.01% acetic acid (HOAc) into the mobile phase to maintain a weakly acidic pH greatly improved the retention behavior of all types of POBN adducts; (2) replacing the classic ODS column with a rapid resolution Eclipse column not only achieved the best chromatographic resolution and sensitivity, but also allowed experiments to be conducted with analytic sampling and performance; (3) applying soft MS

ionization to allow all ESR-active peaks to be detected as the corresponding m/z ions significantly improved the method's reliability; and (4) adding a very small amount of tetrahydrofuran (THF) in the mobile phase improved LC resolution. In fact, THF can also stabilize the ESR tuning during HPLC/ESR measurement [165-167], perhaps due to its low dielectric constant. However, due to its corrosiveness, which could potentially damage the instrument, THF was not used as a mobile phase component in later combination LC/ESR and LC/MS systems [168-173]. The current combination of spin trapping, LC/ESR and LC/MS refined by Qian et al. not only greatly improves the reliability of radical identification, but also optimizes the method's sensitivity and resolution.

1.4.3. Detection of free radical from COX-catalyzed AA and DGLA peroxidation via spin-trapping and LC/ESR/MS

Using the refined combination technique (Scheme 7), Qian et al. have recently characterized the carbon-centered radicals formed from ovine COX-catalyzed DGLA and AA peroxidation *in vitro* [171, 173]. These studies suggested that both similar and different free radical reactions occur in the COX-catalyzed peroxidation of AA vs. DGLA. Due to the common structural moiety (C-8 to C-20) in DGLA and AA, COX can catalyze their free radical peroxidation by the same pathway, *i.e.*, C-15 oxygenation, to form the same or similar free radicals and non-radical metabolites. The different structural moiety (C-1 to C-7) in DGLA forms distinctive free radicals and non-radical products from its unique C-8 oxygenation.

In the study of COX-catalyzed AA peroxidation, three major types of radical adducts (from β and β' -scission) with numerous isomers were observed [171], including three isomers of POBN/ \bullet C₁₄H₂₁O₄ (m/z 448), two isomers of POBN/ \bullet C₆H₁₃O (m/z 296), etc. The radical species \bullet C₁₄H₂₁O₄ (as m/z 448 for the radical adduct) is a novel double-bonded carbon-centered

radical that is derived (special β' -scission) from PGF_2 during COX/AA peroxidation *via* C-15 oxygenation. Two isomers of $\text{POBN}/\bullet\text{C}_6\text{H}_{13}\text{O}$ (m/z 296) also form from the same special β' -scission. However, a normal β -scission of PGF_2 -type alkoxy results in formation of the $\bullet\text{C}_6\text{H}_{11}$ radical as an m/z 266 ion. The special β' -scission (forming two radicals instead of one) was found to be preferred over β -scission in COX/AA peroxidation [171].

Just as in AA, β -scission also takes place in COX/DGLA *via* C-15 oxygenation, but only forms two isomers of $\text{POBN}/\bullet\text{C}_6\text{H}_{13}\text{O}$ (m/z 296). The carbon double-bond radical was not generated, most likely due to this β' -scission taking place during PGH synthesis instead of during PGF_1 synthesis [173]. In addition, two exclusive radicals are generated from C-8 oxygenation in COX-catalyzed DGLA peroxidation, radical products of m/z 324 as $\text{POBN}/\bullet\text{C}_7\text{H}_{13}\text{O}_2$ and m/z 354 as $\text{POBN}/\bullet\text{C}_8\text{H}_{14}\text{O}_3$. This successful characterization of novel and exclusive free radicals from similar and different radical reactions between COX-catalyzed peroxidation of AA and DGLA laid a foundation for our new investigations of COX biology and the role of PUFAs in inflammatory diseases, especially in cancer.

1.4.4. Refining the approach to ESR spin-trapping and LC/MS to detect free radicals under normal biological conditions.

COX can metabolize DGLA and AA through free radical-mediated lipid peroxidation to form the 1-series and 2-series of PGs, respectively. Unlike the pro-carcinogenic and pro-inflammatory PGs2, the PGs1 may possess anti-carcinogenic and anti-inflammatory activity. Our previous studies have demonstrated that in ovine (cell-free) COX-mediated DGLA and AA peroxidation, there are similar free radicals formed through similar reactions (hereafter called common) and different ones formed through different free radical reactions (hereafter called

exclusive). However, it was still unclear whether the differences are associated with the contrasting bioactivity of AA vs. DGLA.

The overall objective of the present research was to identify AA and DGLA-derived free radical metabolites and also elucidate their roles in colon cancer progression and/or prevention. We hypothesized that the differences in COX-catalyzed free radical peroxidation between DGLA vs. AA correspond to a conflict between the bioactivities of DGLA and AA; and that maintaining a balanced and/or beneficial ratio of DGLA vs. AA in the culture medium could control and slow the growth and progression of colon cancer cells.

In order to investigate the possible association between cancer cell growth and exclusive free radicals generated from COX/AA vs. COX/DGLA, we refined our combined spin-trapping/LC/MS method to include solid phase extraction (SPE) in order to characterize free radicals in their reduced forms (hydroxylamines) in the human colon cancer cell line HCA-7 colony 29, which has a high expression of COX-2. For the first time, we were able to profile free radical formation in the experimental settings in which cell proliferation (*via* the MTS assay) and cell cycle distribution (*via* PI staining) could also be assessed. We identified and characterized both common and exclusive free radicals as their reduced forms in cellular COX-catalyzed AA vs. DGLA peroxidation. Our results showed that DGLA- and AA-derived exclusive free radicals, rather than PGE₁ and PGE₂, were more consistent with the opposing bioactivities of DGLA vs. AA.

Due to rapid conversion from DGLA to AA via D5D, the anti-proliferative effect of DGLA in our treatments was limited. Thus, double doses of DGLA and D5D inhibitors were introduced. Treatment with double doses of DGLA or the co-treatment of DGLA with D5D inhibitors increased the DGLA levels in cells and further increased the formation of DGLA-

derived exclusive free radicals. The increased DGLA competed with AA at the enzyme site, thus controlling the generation of AA-derived exclusive free radical metabolites. Among DGLA, double-dose DGLA, and combined DGLA/D5D treatments, the latter exerted the most anti-proliferative effect on colon cancer cell growth. Co-treatment of DGLA with D5D inhibitors greatly limited the formation of exclusive AA-derived free radicals and increased the exclusive DGLA-derived free radicals, thus causing significant cell G₂/M arrest and inhibition of cell proliferation. HCA-7 colony 29 transfected with siRNA to silence the expression of D5D was used to further investigate the possible mechanism underlying the anti-proliferative effect of DGLA on cell growth. According to the Western blot analysis, D5D expression was completely blocked. Our results suggested that targeting D5D was able to reciprocally alter the levels of DGLA and AA in cells, resulting in a profound increase in anti-proliferative DGLA-derived free radical metabolites and a simultaneous decrease in the pro-proliferative AA-derived free metabolites. In addition, the combined treatment with DGLA and D5D inhibitors increased the susceptibility of colon cancer cells to the chemotherapy drug 5-fluorouracil (5-FU). In the D5D knockdown cells, the synergistic effects of DGLA and 5-FU on growth inhibition and cytotoxicity were even greater.

In summary, our refined LC/MS technique along with SPE allowed us for the first time to characterize free radicals in cells under normal growth conditions in which cell response, *i.e.*, proliferation and cell cycle distribution, could also be assessed. Our results suggest that the exclusive free radical metabolites correspond to the contrasting effects of AA vs. DGLA on cancer cell growth. Increasing DGLA levels (by double doses of DGLA or targeting D5D) and concurrently decreasing AA in cells could be a novel approach to controlling AA-dependent cancer development. Our study allowed us to directly study free radical-associated PUFA

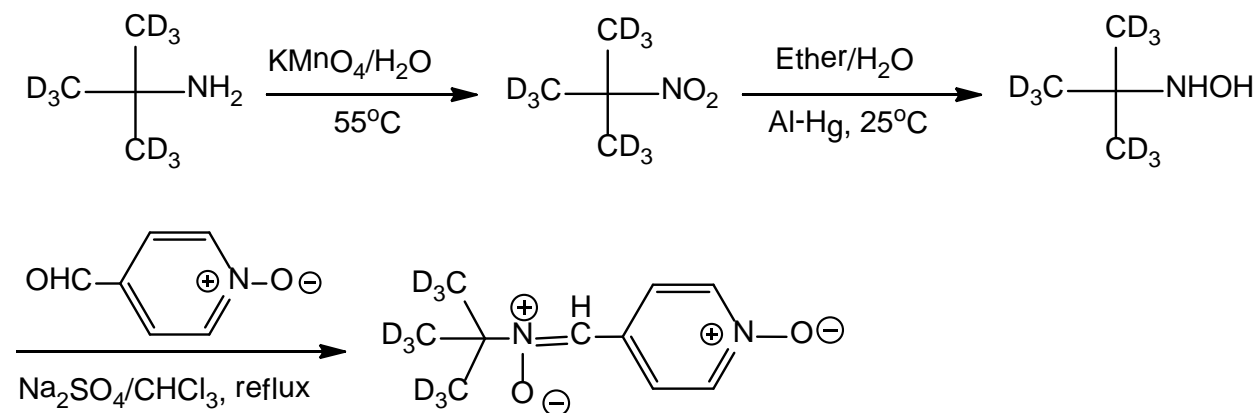
bioactivity, thus improving our understanding of COX-catalyzed lipid peroxidation in cancer biology.

CHAPTER 2. MATERIALS AND METHODS

2.1. Chemicals and Reagents

High-purity POBN was purchased from Alexis Biochemicals (San Diego, CA, USA).

Deuterated POBN (d_9 -POBN, Scheme 8) was synthesized by the core synthesis facility at North Dakota State University.



Scheme 8. Synthesis of d_9 -POBN.

Under three equivalents of potassium permanganate, the d_9 -*tert*-butylamine was oxidized to d_9 -2-methyl-2-nitropropane, which was then subjected to a controlled reduction (with Al-Hg as reductant) to form *N*- d_9 -*tert*-butylhydroxylamine. The final product, d_9 -POBN, was obtained from a dehydration reaction between *N*- d_9 -*tert*-butylhydroxylamine and 4-pyridinecarboxaldehyde-1-oxide. The overall yield of the current d_9 -POBN synthesis is $\sim 30\%$.

OmniPur[®] 10× Phosphate Buffered Saline (PBS) Liquid Concentrate was purchased from EMD Millipore (Billerica, MA, USA). AA and DGLA were purchased from Nu-Chek-Prep (Elysian, MN, USA). Ethanol (200 proof, for molecular biology) was purchased from Sigma-Aldrich (St. Louis, MO, USA). Heptanoic acid, 1-hexanol and 8-hydroxyoctanoic acid were purchased from Sigma-Aldrich (St. Louis, MO, USA).

CP-24879, sesamin and curcumin were purchased from Cayman Chemicals (Ann Arbor, MI, USA). 5-FU was purchased from Sigma-Aldrich (St. Louis, MO, USA). Dimethyl sulfoxide (DMSO) was purchased from Alfa Aesar (Ward Hill, MA, USA).

Acetonitrile (ACN, HPLC grade), water (H₂O, HPLC grade), methanol and ethyl alcohol pure (200 proof) were purchased from EMD Chemicals (Gibbstown, NJ, USA). Ammonium hydroxide (NH₄OH, 5.0 N) and glacial acetic acid (HOAc) were purchased from Sigma-Aldrich (St. Louis, MO, USA). NH₄OH (5 %) was freshly prepared by diluting the 5.0 N solution with deionized water.

TRIS (base) was purchased from J.T. Baker (Phillipsburg, NJ, USA). Hydrogen chloride (HCl, 12.1 N) was purchased from EMD Chemicals (Gibbstown, NJ, USA). Sodium chloride (NaCl) was purchased from VWR International (West Chester, PA, USA). cOmplete Protease Inhibitor Cocktail Tablets were purchased from Roche Applied Science (Indianapolis, IN, USA). Triton[®] X-100, glycerol and DL-dithiothreitol (DTT) were purchased from Sigma-Aldrich (St. Louis, MO, USA).

Bovine serum albumin solution (2.0 mg/mL) was purchased from Thermo Scientific (Rockford, IL, USA). The DC[™] BCA protein assay, glycine, Sodium dodecyl sulfate (SDS), and Precision Plus Protein[™] Kaleidoscope Standards were purchased from Bio-Rad Laboratories (Hercules, CA, USA). Acrylamide/bis-acrylamide (30 % solution), 2-mercaptoethanol and CAPS were purchased from Sigma-Aldrich (St. Louis, MO, USA). Ammonium persulfate (APS) was purchased from AMRESCO (Solon, OH, USA). TEMED was purchased from Research Organics (Cleveland, OH, USA). Tween[®] 20 was purchased from G-Bioscience (St. Louis, MO, USA). Bromophenol was purchased from EMD Chemicals (Gibbstown, NJ, USA). Sodium hydroxide (NaOH) was purchased from J.T. Baker (Phillipsburg, NJ, USA).

Polyclonal anti-COX-2 antibody produced in rabbits was purchased from Abcam (Cambridge, MA, USA). Polyclonal anti-FADS1 antibody produced in rabbits and monoclonal Anti-Actin antibody produced in mice were purchased from Sigma-Aldrich (St. Louis, MO,

USA). Horseradish peroxidase-conjugated goat anti-rabbit IgG and horseradish peroxidase-conjugated goat anti-mouse IgG were purchased from Cayman Chemicals (Ann Arbor, MI, USA). Pierce ECL Western Blotting Substrate was purchased from Thermo Scientific (Logan, UT, USA).

CellTiter 96[®] AQueous One Solution Cell Proliferation Assay was purchased from Promega (Madison, WI, USA). Ribonuclease A from bovine pancreas (RNase A, 30 mg/mL) was purchased from Sigma-Aldrich (St. Louis, MO, USA). Propidium iodide (PI, 10 mg/mL) was purchased from Life Technologies (Grand Island, NY, USA).

Opti-MEM[®] Reduced Serum Medium (GlutaMAX[™]), Lipofectamine[™] RNAiMAX reagent, Silencer[®] Select siRNA (5 nmol) for FADS1 and negative control #1 (5 nmol) were purchased from Life Technologies (Grand Island, NY, USA).

2.2. Cell Culture

The human colon cancer cell line HCA-7 colony 29 was purchased from the European Collection of Cell Cultures (Porton Down, Salisbury, UK). Fetal bovine serum (FBS) and 0.25% trypsin-EDTA was obtained from Thermo Scientific (Logan, UT, USA). DMEM high glucose medium (phenol-red free) was obtained from ScienCell Research Laboratories (Carlsbad, CA, USA). Cells were grown in DMEM high glucose medium (phenol red-free) supplemented with 10% FBS in an incubator containing a 95% humidified atmosphere of 5% CO₂ at 37°C. Cells were sub-cultured at a ratio of 1:5 after they had reached ~90% confluency. Final concentrations of all treatments including controls were prepared with an appropriate volume of cell culture medium to attain a concentration of 0.1% (v/v) ethanol or DMSO.

2.3. Preparation of Reaction Solution

2.3.1. Stock solutions

Stock solutions of POBN and d₉-POBN (500 mM) were freshly prepared in PBS buffer.

Stock solutions of AA and DGLA (100 mM) were prepared in ethanol. PGE₂, PGE₁, PGE₂-d₉, PGE₁-d₄, AA-d₈, DGLA-d₆ were purchased from Cayman Chemicals (Ann Arbor, MI, USA). Stock solutions of the PGE₂, PGE₁, PGE₂-d₉, PGE₁-d₄, AA-d₈, and DGLA-d₆ (100 ng/μL) were prepared in ethanol.

Stock solutions of heptanoic acid, 1-hexanol and 8-hydroxyoctanoic acid (500 μM) were prepared in ethanol. All of the stock solutions were stored in aliquots at -80 °C. A series of the corresponding working solutions was freshly prepared by diluting the stock solutions with ethanol.

Stock solutions of CP-24879 (50 mM), sesamin (100 mM), curcumin (50 mM) and 5-FU (1.0 M) were prepared in DMSO. All of the stock solutions were stored in aliquots at -80 °C. A series of corresponding working solutions was freshly prepared by diluting the stock solutions with DMSO.

2.3.2. Cell lysis buffer

HCl (10.0 N) was prepared by transferring 1 mL of HCl to a 15 mL centrifuge tube. 11.1 mL of deionized water was added and the solution vortexed to mix completely. The volume was then made up to 12.1 mL with deionized water.

NaCl (5.0 M) was prepared by transferring approximately 14.6 g of NaCl to a 50 mL centrifuge tube. 45 mL of deionized water was added and the solution vortexed to dissolve it completely. The volume was made up to 50 mL with deionized water.

The protease inhibitor (5× stock solution) was prepared by transferring 9.0 mL of ice cold deionized water to a 15 mL centrifuge tube. One tablet of cOmplete Protease Inhibitor Cocktail was added and the solution vortexed to dissolve it completely. 1.0 mL aliquots were stored at -20 °C.

DTT (1.0 M) was prepared by transferring approximately 1.5 g of DTT to a 15 mL centrifuge tube. 9.0 mL of deionized water was added and vortexed to dissolve it completely. The volume was made up to 10 mL. 1.0 mL aliquots for each were stored at -20 °C.

Tris buffer (1.0 M, pH 7.4) was prepared by transferring approximately 12.1 g of Tris base into a 100 mL reagent bottle. 90 mL of deionized water was added and stirred to dissolve completely. The pH was adjusted to 7.4 ± 0.05 with HCl (10.0 N) and the volume made up to 100 mL with deionized water.

The cell lysis buffer was prepared on ice by transferring 1.0 mL of deionized water to a 15 mL centrifuge tube. 216 μ L of 5.0 M NaCl solution, 1.8 mL of protease inhibitor stock solution, 9.0 μ L of 1.0 M DTT, 4.5 mL of 1.0 M Tris buffer (pH 7.4), 900 μ L of glycerol and 450 μ L of Triton[®] X-100 were added. The volume was made up to 10 mL with deionized water. The contents were mixed by vortexing and 1.0 mL aliquots stored at -20 °C.

2.3.3. Protein assay

Protein standard solutions: Bovine serum albumin solution (2 mg/mL) was diluted with deionized water to prepare a series of protein standard solutions of 0.25, 0.5, 0.75, 1, 1.5 to 2.0 mg/mL. 1.0 mL aliquots of the standard solutions were stored at -20 °C.

Coloring reagent (a mixture of DC[™] BCA protein assay reagents A and S) was prepared fresh just before use. 1.0 mL of protein assay reagent A and 20 μ L of protein assay reagent S were mixed in a 1.5 mL centrifuge tube.

2.3.4. SDS-polyacrylamide gel electrophoresis (SDS-PAGE)

Reagents for gel preparation: APS (10%) was freshly prepared by dissolving approximately 0.1 g of APS in 1 mL deionized water. SDS (10%) was prepared by dissolving approximately 1.0 g of SDS in 10 mL deionized water.

Tris buffer (1.5 M, pH 8.8) was prepared by transferring approximately 18.2 g of Tris base into a 100 mL reagent bottle. 90 mL of deionized water was added and stirred to dissolve completely. The pH was adjusted to 8.8 ± 0.05 with HCl (10 N). The volume was made up to 100 mL with deionized water.

Tris buffer (1.0 M, pH 6.8) was prepared by transferring approximately 12.1 g of Tris base into a 100 mL reagent bottle. 90 mL of deionized water was added and stirred to dissolve completely. The pH was adjusted to 6.8 ± 0.05 with concentrated HCl (10 N). The volume was made up to 100 mL with deionized water.

Reagents for PAGE: NaOH (10 N) was prepared by transferring approximately 100.0 g of NaOH to 100 mL reagent bottle. 200 mL of deionized water was added and stirred to dissolve completely. The volume was made up to 250 mL with deionized water.

Tris buffer (0.5 M, pH 6.8) was prepared by transferring approximately 6.1 g of Tris base into a 100 mL reagent bottle. 90 mL of deionized water was added and stirred to dissolve completely. The pH was adjusted to 6.8 ± 0.05 with HCl (10 N). The volume was made up to 100 mL with deionized water.

Sample buffer (4× stock solution) was prepared by transferring 20 mL of 0.5 M Tris buffer (pH 6.8) into a 50 mL centrifuge tube. 20 mL glycerol, 2.0 g SDS, 2 mL 2-mercaptoethanol, and approximately 16.0 mg bromophenol blue were added and vortexed to

dissolve and mix the contents completely. The volume was made up to 50 mL with deionized water. 1.0 mL aliquots were stored at -20 °C.

Electrophoresis buffer (10× stock solution) was prepared by transferring approximately 30.3 g of Tris base into a 1000 mL reagent bottle. Approximately 144.0 g glycine, 10.0 g SDS and 900 mL of deionized water were added and stirred to dissolve completely. The volume was made up to 1000 mL with deionized water and stored at 4 °C.

Running buffer (1× working solution) was prepared by transferring 100 mL of 10× electrophoresis buffer into a 1000 mL reagent bottle. The volume was made up to 1000 mL with deionized water and stored at 4 °C. The buffer was reused three times.

Transfer buffer (10× stock solution) was prepared by transferring approximately 22.1 g of CAPS into a 1000 mL reagent bottle. 900 mL of deionized water was added and stirred to dissolve completely. The pH was adjusted to 11.0 ± 0.05 with NaOH (10 N). The volume was made up to 1000 mL with deionized water and stored at 4 °C.

Transfer buffer (1× working solution) was prepared by transferring 100 ml of 10× buffer to a 1000 mL reagent bottle. 200 mL methanol was added. The volume was made up to 1000 ml with ice cold deionized water and stored at 4 °C. The buffer was reused three times.

Tris buffered saline (TBS, 10× stock solution) was prepared by transferring approximately 12.1 g of Tris base to a 1000 mL reagent bottle. 87.7 g of NaCl and 900 mL of deionized water was added and stirred to dissolve, and the pH adjusted with HCl (10 N) to 7.6 ± 0.05 . The volume was made up to 1000 mL with deionized water and stored at 4 °C.

Washing Buffer (TBS-T, 1× working solution) was prepared by transferring 100 mL of 10× TBS in a 1000 mL reagent bottle. 1 mL Tween-20 was added. The volume was made up 1000 mL with deionized water and stored at 4 °C.

Blotting buffer (reusable) was prepared by transferring approximately 5.8 g of Tris base and 2.9 g of glycine in a 1000 mL reagent bottle. 700 mL deionized water was added and stirred to dissolve completely. 200 mL methanol was added. The volume was made up to 1000 mL with deionized water.

Blocking Solution (5% Non-fat Dry Milk) was prepared by transferring approximately 5 g of non-fat dry milk in a 100 mL reagent bottle. 90 mL of 1× TBS-T was added and stirred to dissolve and the volume made up to 100 mL with 1× TBS-T. It was used fresh.

2.3.5. Immunoblotting

Incubation Solution (for dilution of primary and secondary antibodies) was prepared by transferring 1 mL of blocking solution in a 15 mL centrifuge tube. The volume was made up to 10 ml with 1× TBS-T. Use it fresh. Polyclonal anti-COX-2 antibody produced in rabbit was used at a 1: 600 dilution. Polyclonal anti-FADS1 antibody produced in rabbit was used at a 1:400 dilution and monoclonal Anti-Actin antibody produced in mouse was used at a 1:4000 dilution. Horseradish peroxidase-conjugated goat anti-rabbit IgG and Horseradish peroxidase-conjugated goat anti-mouse IgG were used at a 1:4000 dilution.

2.3.6. Cell cycle distribution

RNase A (10 mg/mL stock solution) was prepared by transferring 1.0 mL Rnase A (30 mg/mL) to 1.5 mL centrifuge tube. 2.0 mL deionized water was added and vortexed to mix completely. 200 µL aliquots were stored at -20 °C.

PI (50 µg/mL working solution) was prepared by transferring 40 µL PI (10 mg/mL) to 15 mL centrifuge tube. 8.0 mL deionized water was added and vortexed to mix completely. PI was prepared away from light and used fresh.

2.3.7. Transfection with siRNA

FADS1 siRNA and negative control #1 (100 μ M stock solution) was prepared by centrifuging the tube to ensure that the dried siRNA was at the bottom of the tube. 100 μ L of Nuclease-free Water was added and vortexed to dissolve completely. 10 μ L aliquots were stored at -20 °C.

2.4. **Spin-Trapping Experiments in Cell-PBS Suspension**

To measure ESR-active free radical spin adducts, HCA-7 colony 29 cells at ~90% confluency were trypsinized, harvested, and suspended in PBS at $\sim 10^8$ cells/mL. POBN and PUFAs at final concentrations of 50 and 1.0 mM, respectively, were then added to 200 μ L of cell-PBS suspension to start the peroxidation and spin-trapping reaction. This complete reaction mixture was then incubated at 37°C in the absence of light. After a 30 min incubation, the reaction was stopped by mixing with ACN (1:1, v/v). The reaction mixture was centrifuged for 15 min at 14,000 rpm using a Microfuge[®] 22R Centrifuge (Beckman Coulter) and the supernatant was collected. The supernatant was condensed by removing ACN *via* a Vacufuge[®] 5301 Centrifugal Vacuum Concentrator (Eppendorf) for later offline ESR, LC/ESR and LC/MS analysis.

2.5. **Spin-Trapping Experiments under Normal Cell Growth Conditions**

Cells were seeded at the density of 4×10^6 cells per 100 mm petri dish to obtain 30 ~ 40% confluency. After a one-night incubation that allowed the cells to attach to the dish, the cell culture medium was replaced with fresh, and then POBN and PUFAs at final concentrations of 20 mM and 100 μ M, respectively, were added to start the peroxidation and spin-trapping reaction.

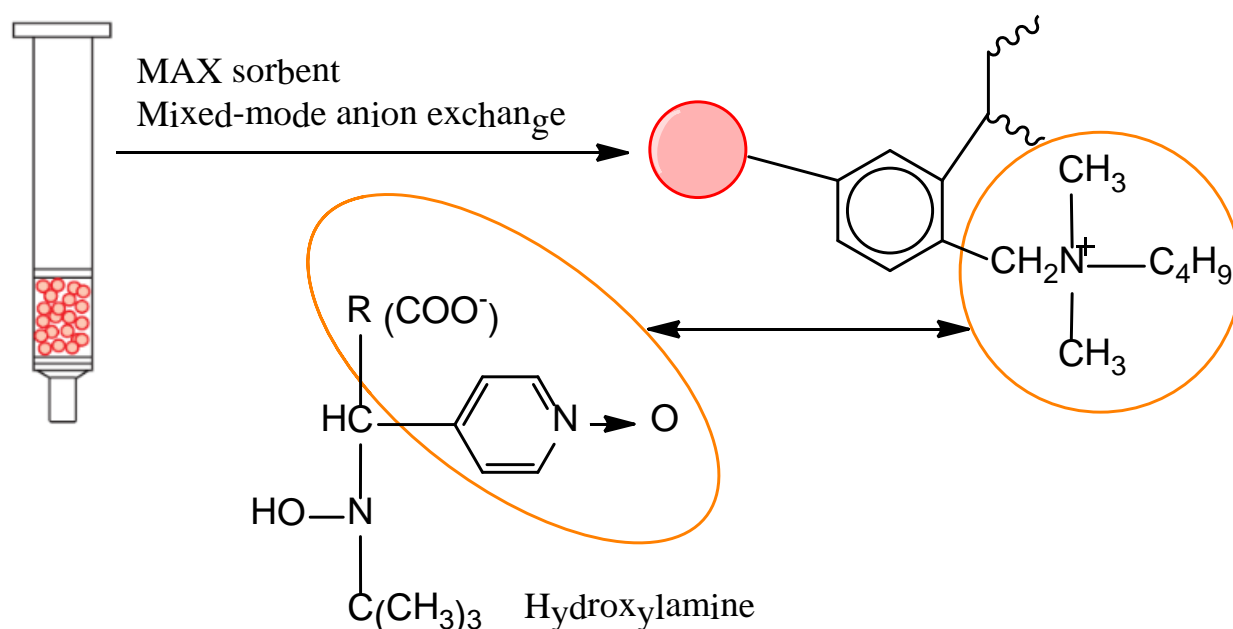
Unlike the overdosing with POBN and PUFA in the spin-trapping experiments performed in cell-PBS suspension, which could cause cell death in as short a time as just over 30 min, much lower concentrations of POBN and PUFA were introduced into the cell culture medium in our refined spin-trapping experiment. Instead of detecting the ESR-active POBN radical adduct, the reduced POBN radical adducts (hydroxylamines) were measured since they are a more stable redox form and could accumulate during incubation. After 0.5, 2, 4, 8, 12, 24 and 48 h of treatment, both the cell culture medium and cell homogenate (cells were scrubbed and homogenized with a Sonifier 150, Branson Ultrasonics) were collected. The reaction was stopped by adding ACN (1:1, *v/v*) into the mixture of the cell culture medium and cell homogenate. Then the mixture was vortexed and centrifuged for 15 min at 3000 rpm. The supernatant (4.0 mL) was subjected to SPE, followed by LC/MS and LC/MS² analysis.

In the spin-trapping experiments when dual spin traps (a mixture of *d*₀- and *d*₉-POBN, 50:50, *v/v*) were used to confirm the structural assignments of the hydroxylamines, all reaction conditions were the same as in the corresponding POBN spin-trapping reaction system.

2.6. Extraction and Analysis of Hydroxylamines

A mixed-mode anion exchange (MAX) SPE cartridge (Oasis[®], Waters) was employed to separate the hydroxylamine from the supernatant obtained from spin-trapping experiments under normal cell growth conditions. The sorbent of the MAX cartridge (N-vinylpyrrolidone-DVB copolymer, -CH₂N(CH₃)₂C₄H₉⁺) could interact with negatively charged groups (Scheme 9), *e.g.*, the pyridyl-oxide group in POBN's structure and the carboxyl and/or hydroxyl groups in the structures of PUFA-derived radicals. This highly selective interaction enabled the separation of hydroxylamines from the matrices. The MAX SPE cartridge was preconditioned with 2.0 mL methanol and 2.0 mL water and then 4.0 mL supernatant was loaded. The MAX SPE cartridge

was washed with 1.0 mL 5% NH_4OH and 1.0 mL methanol, and then hydroxylamines were eluted with 2 mL ACN:methanol (60:40, v/v, 2% formic acid). The elution was condensed to dryness with a concentrator and reconstituted in 100 μL methanol:water (10:90, v/v) for LC/MS and LC/MS² analysis.



Scheme 9. Hydroxylamine-sorbent interactions on Oasis MAX sorbent.

MAX is a strong mixed-mode anion exchange, water-wettable, polymeric sorbent stable from pH 0-14. SPE procedures using MAX sorbent enable separation of hydroxylamines from complex matrices including biological fluids.

2.7. Spin-Trapping of Hydroxyethyl Radical (Test of POBN's Trapping Ability)

In our refined spin-trapping experiment, the reaction was performed for days under normal cell growth conditions. To determine whether POBN would still be able to trap radicals under such conditions, we tested POBN's trapping ability for hydroxyethyl radicals ($\bullet\text{C}_2\text{H}_4\text{OH}$) for up to 48 h. POBN in DMEM high glucose medium (phenol-red free) was put in an incubator containing a 95% humidified atmosphere of 5% CO_2 at 37°C. After 2, 4, 24 and 48 h, the POBN in cell culture medium was mixed with ethanol and an Fe^{2+} stock solution (1.0 mM, prepared from ferrous ammonium sulfate in redistilled water, with the pH kept around 2.5 [174]). The final

concentrations of POBN, ethanol and Fe^{2+} in the reaction mixture were 20 mM, 1.0 mM and 0.1 mM, respectively. The reaction mixture was used directly for offline ESR analysis with an ESR flat cell for magnetic field scans.

2.8. Extraction and Analysis of PUFAs and PGEs in Cell Culture Medium

Cells were seeded at a density of 4×10^6 cells per 100 mm petri dish to obtain 30 ~ 40% confluency. After a one-night incubation that allowed the cells to attach to the dish, the cell culture medium was replaced with fresh, and then PUFAs at final concentrations of 100 μM were added to start the peroxidation reaction. After 0.5, 2, 4, 8, 12, 24 and 48 h of treatment, the cell culture media were collected. PUFAs and PGs in cell culture medium were extracted *via* SPE. Two mL of cell culture medium was collected after treatment and the internal standards (PGE₁-d₄, PGE₂-d₉, AA-d₈ and DGLA-d₆) were added. Then the medium was mixed with methanol and water to make a total of 3 mL of 15% methanol solution and vortexed for 1 min. The mixture was set on ice for 30 min and centrifuged for 15 min at 3000 rpm. The supernatant was collected and transferred to a new tube. After the pH was adjusted to 3.0 using 0.2 N HCl, the supernatant was loaded on a reverse phase SPE cartridge (SampliQ Silica C18 ODS, Agilent, preconditioned with 2 mL methanol and 2 mL water). The reverse phase SPE cartridge was washed with 1 mL of water, and then PUFAs and PGEs were eluted with 2 mL ethyl acetate. The elution was condensed by concentrator to dryness and reconstituted with 100 μL ethanol for LC/MS analysis.

2.9. Offline ESR

For the complete reaction system and relevant control experiments, reaction solutions (after mixing with ACN, 50% *v/v*) were transferred to the same ESR flat cell for magnetic field scans. ESR spectra were recorded with a Bruker EMX spectrometer equipped with a super high

Q cavity operating at 9.78 GHz at room temperature. Other ESR spectrometer settings were magnetic field center, 3497.4 G; magnetic field scan, 70 G; modulation frequency, 100 kHz; microwave power, 20 mW; modulation amplitude, 1.0 G; receiver gain, 5.0×10^4 ; time constant, 0.655 s; and conversion time, 0.164 s.

2.10. LC/MS and LC/MS²

2.10.1 LC/MS and LC/MS² for identification of free radical adducts and hydroxylamines

The LC/MS system consisted of an Agilent 1200 series HPLC system and an Agilent LC/MSD SL ion trap mass system. The outlet of the UV detector in LC was connected to the MS system with red PEEK HPLC tubing (0.005 i.d.). LC separations were performed on a C18 column (Zorbax Eclipse-XDB, 4.6×75 mm, 3.5 μm) equilibrated with 90% A (H₂O-0.1% HOAc) and 10% B (ACN-0.1% HOAc). A forty microliter condensed sample from a spin-trapping experiment in a cell-PBS suspension or under normal cell growth conditions was injected into the HPLC system by autosampler and eluted at a 0.8 mL/min flow rate with a combination of gradient and isocratic elution: (i) 0-5 min, 90 to 73% A and 10 to 27% B; (ii) 5-25 min (isocratic), 73% A and 27% B; (iii) 25-40 min, 73 to 30% A and 27 to 70% B; (iv) 40-43 min, 30 to 5% A and 70 to 95% B; and (v) 43-50 min (isocratic), 5% A and 95% B. The LC flow rate (0.8 mL/min) into the MS inlet was adjusted to 60 μL/min *via* a splitter. Electrospray ionization in positive mode was used for all LC/MS measurements. Total ion current (TIC) chromatograms in full mass scan mode (m/z 50 to m/z 600) were performed to profile all products formed in the reaction of COX-catalyzed AA/DGLA in the presence of POBN. Other MS settings were capillary voltage, -4500 V; nebulizer press, 20 psi; dry gas flow rate, 8 L/min; dry temperature, 60 °C; compound stability, 20%; and number of scans, 50. An extracted ion current chromatogram (EIC) from the above full scan experiment was obtained to acquire the MS profile

of the individual POBN trapped radical adduct. Normally an isolation width of ± 0.5 Da was selected for EIC.

LC/MS² analysis in multiple reactions monitoring (MRM) mode was performed to confirm the structural assignment of hydroxylamine. A four-Da width was typically used to isolate parent ions of interest. Other settings of the MS were: mass range, m/z 50-600; capillary voltage, -4500 V; nebulizer press, 20 psi; dry gas flow rate, 8 L/min; dry temperature, 60°C; compound stability, 20%; and number of scans, 5. The LC/MS² studies of reduced products of d₉-POBN radical adducts were performed to confirm the structures of reduced products of POBN radical adducts. All reactions for the POBN and the d₉-POBN spin trap systems were performed under identical conditions.

2.10.2. LC/MS for quantification of hydroxylamine

LC/MS settings for quantification were identical to the above full scan methods. A small and known amount of d₉-POBN was used purely as an internal standard in LC/MS quantification. Unlike the above LC/MS² procedure in which d₉-POBN was used as a spin trap for purposes of radical detection and structure identification, here it was not added until the mixture of cell culture medium and cell homogenate was mixed with blocking agent (1:1, v/v) to stop the reaction. Based on the average abundance of several types of POBN radical adducts observed in our reaction system and publications [169, 170], we chose 2.0 $\mu\text{g/ml}$ as the quantity of internal standard d₉-POBN to add to the ACN-sample mixture. To quantify the abundance of molecule ions of interest, the integrated EIC peak of m/z 204 for d₉-POBN was always used as the standard.

2.10.3. LC/MS for PUFAs and PGEs detection and quantification

Five microliters of sample was injected into the HPLC system and eluted with a combination of gradient and isocratic elution: (i) 0-12 min (isocratic), 68% A and 32% B; (ii) 12-14 min, 68 to 44% A and 32 to 56% B; (iii) 14-28 min (isocratic), 44% A and 56% B; (iv) 28-30 min, 44 to 14% A and 56 to 86% B; (v) 30-38 min, 14 to 4% A and 86 to 95% B; and (vi) 38-44 min (isocratic), 5% A and 95% B. Electrospray ionization in negative mode was used for all LC/MS measurements. Other MS settings were nebulizer pressure, 15 psi; dry gas flow rate, 5 L/min; dry temperature, 325 °C.

For quantification, m/z 351, 360, 353, 357, 305, 303, 311 were used for measuring PGE₂, PGE₁, AA, DGLA, PGE₁-d₄, PGE₂-d₉, AA-d₈ (m/z 311) and DGLA-d₆ (m/z 311), respectively. The concentrations of PUFAs in the samples were calculated by comparing the ratios of the peak areas of the compounds to those of the internal standards using the internal standard curve. The standard curve was constructed from a series of concentrations of PGE₂, PGE₁, AA, DGLA and the same concentrations of PGE₁-d₄, PGE₂-d₉, AA-d₈ and DGLA-d₆, which were added into the cell culture medium.

2.11. Transfecting HCA-7 Colony 29 Cells with FADS1 siRNA

HCA-7 colony 29 cells were transfected with FADS1 siRNA according to the manufacturer's protocol. Cells were seeded at 2×10^5 cells per well in a 6-well plate. After a 12 h incubation to allow the cells to attach, the cell culture medium was removed and cells were washed with PBS. Then the transfection mix was generally prepared and added. Briefly, for each well to be transfected, FADS1 siRNA stock solution (100 μM, in RNase free water) was diluted in 250 μL Opti-MEM reduced serum medium (Invitrogen) to final concentrations of 50, 100 and 150 nM and mixed with 15 μL of each transfection reagent (Lipofectamine™ RNAiMAX) pre-

diluted in 250 μ L Opti-MEM. After a 5 min incubation at room temperature, the transfection mixes were added to the cells in a final volume of 2.5 mL medium. The cells were incubated for 48 hours at 37°C in a CO₂ incubator until ready to assay for gene knockdown. Cells transfected with a non-target control siRNA were used as controls. The gene knockdown results were evaluated by Western blot.

This procedure was used to reverse transfect siRNA into HCA-7 colony 29 cells in a 6-well format. For cells transfected in different cell culture formats, *e.g.* a 96-well plate or a 100 mm petri dish, the amounts of Lipofectamine[™] RNAiMAX, siRNA, cells, and medium were scaled up or down according to Table 1.

Table 1. Scaling Up or Down Transfections.

Culture Vessel	Multiplication Factor
96-well plate	0.04×
6-well plate	1×
100 mm petri dish	2.2×

The multiplication factor in the table was used to scale the volumes for transfection experiments. The factor is based on the relative surface area of a single well from a 6-well plate.

If the volume of Lipofectamine[™] RNAiMAX was too small to dispense accurately, Lipofectamine[™] RNAiMAX was pre-diluted 10-fold in Opti-MEM[®] I Reduced Serum Medium, and a 10-fold higher amount was dispensed (at least 1.0 μ L per well).

2.12. Western Blot Analysis

Preparation of cell lysate: Cell lysis buffer was placed on ice and all steps carried out at 4 °C. 150 μ L of cell lysis buffer was added to each well of the Petri dish. Cells in the whole area of the Petri dish were scraped with a plastic scraper. The lysate was collected in 1.5 mL centrifuge tubes, passed through a syringe (25 gauge, BD) 5-6 times to make the lysate

homogeneous, and then centrifuged at 2000 rpm for 2 min at 4 °C. The supernatant was collected and stored at -80 °C for further analysis.

Protein quantification: The protein concentration in the cell lysates was measured using a DCTM protein assay kit according to the manufacturer's instructions. Briefly, 5 uL of protein standard or diluted cell lysate and the DCTM protein assay reagents were added into each well in a 96-well plate. Solutions were incubated at room temperature for 15 min in the dark. The optical density was then read at 750 nm using a Microplate Reader (SpectraMax M5, Molecular Devices). The protein amount in each sample was calculated by the standard curve.

Preparation of samples for loading: Each sample was normalized to the same concentration and then the sample prepared to load onto the gel by mixing with the sample buffer (sample:4× sample buffer = 3:1). Samples were vortexed and spun down, denatured at 95 °C for 5 min, and stored at -20 °C for further analysis.

Preparation of gel: The required concentrations of resolving gel and stacking gel were prepared according to Table 2, avoiding any bubble formation in the wells.

Table 2. Volume of components required to cast gels.

	Resolving Gel (10%)	Stacking Gel (4%)
	2 mL	1.25 mL
	1.5 M Tris buffer (pH 8.8)	1.0 M Tris buffer (pH 6.8)
H₂O	7.8 mL	7.55 mL
acrylamide/bis-acrylamide (30 % solution)	4 mL	1 mL
10% SDS	160 μL	100 μL
10 % APS	160 μL	100 μL
TEMED	16 μL	10 μL
Total	16 mL	10 mL

Running the gel after sample loading: Samples (maximum 40 μ L) were loaded in the wells and run at constant voltage, first at 90 V, while the samples passed by the stacking gel, then increasing the voltage to 120 V. The voltage was switched off just before the blue line reached the bottom to prevent overrun.

Transferring: Sponges and filter paper were soaked in blotting buffer for 15 min. The Immobilon-P transfer membrane (PVDF, Millipore) was first soaked in methanol (activation step) for 15 min and then in blotting buffer. The proteins were transferred electrophoretically to the PVDF membrane at constant voltage (80 V) for 2 h on ice.

Blotting: Membranes were blocked for non-specific binding by rocking gently in 5% non-fat dry milk (diluted in 1 \times TBS-T) for 1 h and washed for 5 min in 1% non-fat dry milk (diluted in 1 \times TBS-T), then incubated with primary antibody for 1 hr at room temperature or overnight at 4 $^{\circ}$ C (with dilution in incubation solution as required) with continuous rocking.

Membranes were washed 3 times for 5 min each in 1 \times TBS-T and twice for 5 min each in 1% non-fat dry milk (diluted in 1 \times TBS-T). The secondary antibody was added (diluted in incubation solution as required) and incubated for 1 h at room temperature, with continuous rocking.

Membranes were washed 3 times for 5 min each in 1 \times TBS-T, incubated in ECL western blot substrates (Pierce) for 1 min, and exposed to X-ray film (Phoenix Research), taking care that all the chemiluminescent exposure should be as fast as possible to avoid loss of signal.

Luminescent signals were captured on a Mini-Medical Automatic Film Processor (Imageworks).

2.13. Cell Proliferation Assay via MTS

The CellTiter 96[®] AQueous One Solution Cell Proliferation Assay is a colorimetric method for determining the number of viable cells in proliferation or cytotoxicity assays. The

CellTiter 96[®] AQueous One Solution Reagent contains a novel tetrazolium compound [3-(4,5-dimethylthiazol-2-yl)-5-(3-carboxymethoxyphenyl)-2-(4-sulfophenyl)-2H-tetrazolium, inner salt; MTS] and an electron coupling reagent (phenazine ethosulfate; PES). PES has enhanced chemical stability that allows it to be combined with MTS to form a stable solution. The MTS tetrazolium compound is bio-reduced by cells into a colored formazan product that is soluble in tissue culture medium. This conversion is presumably accomplished by NADPH or NADH produced by dehydrogenase enzymes in metabolically active cells. The quantity of formazan product as measured by the absorbance at 490nm is directly proportional to the number of living cells in culture.

A cell proliferation assay was performed according to the manufacturer's instructions. Briefly, cells were seeded at 5000 cells per well into 96-well plates. After overnight incubation to allow the cells to attach, different treatments were added. The cells were incubated in an incubator containing a 95% humidified atmosphere of 5% CO₂ at 37°C for 48 h and then 20 µL per well of CellTiter[®] 96 Aqueous One Solution Reagent was added into each well. After the plate was incubated for 4 h in an incubator, the absorbance at 490 nm was recorded with a 96-well plate reader. Values were normalized to the value in the control group.

2.14. Cell Cycle Distribution Analysis *via* PI Staining

PI is a fluorescent dye that binds specifically to DNA. This property has led to its common use in evaluation of cell cycle, aneuploidy and apoptosis by flow cytometry. When excited by a laser light at 488 nm, PI emits a signal that can be monitored by the red wavelength detector typically reserved for phycoerythrin (usually FL2).

The effect of different treatment on cell cycle distribution was determined by flow cytometry after staining the cells with PI. Briefly, 4×10⁶ cells were seeded, allowed to attach by

overnight incubation, and exposed to different treatments for 8 and 24 h. Cells were trypsinized, washed with PBS and fixed in ice-cold 70% ethanol at 1×10^6 cells/mL for 30 min at 4 °C. The cells were then treated with 10 μ L ribonuclease A (10 mg/mL) and 400 μ L PI (50 μ g/mL) for 30 min and measured on a Cell Lab Quanta™ SC (Beckman Coulter, CA). The percentage of cells in different phases of the cell cycle was computed using Flow Jo (TreeStar, OR). At least 10,000 cells were analyzed.

2.15. Statistics

Data were expressed as mean \pm standard deviation (SD). Statistical differences between the mean values for two groups (at least three experiments per group for all experiments) were evaluated by analysis of variance (ANOVA) and Tukey's post hoc test. Correlation relationships were determined by correlation/regression analysis in which *P* values less than 0.05 were considered statistically significant.

CHAPTER 3. DETECTION AND IDENTIFICATION OF FREE RADICALS FORMED FROM CELLULAR COX-CATALYZED AA AND DGLA PEROXIDATION

3.1. Introduction

The major ω -6 PUFA found in tissues is AA, which is converted from dietary LA through a series of desaturation and elongation enzymes ([2] Scheme 1). LA (18:2) is converted into GLA by D6D, followed by a two-carbon-atom chain elongation by ELOVL5 to form DGLA, and finally undergoing desaturation by D5D to generate AA. Both AA and its upstream fatty acid, DGLA, are substrates of COX, one of the most studied mammalian oxygenases. COX catalyzes the lipid peroxidation of PUFAs to form PGHs, the precursors of such bioactive lipid mediators as PGs (PGE, PGD, and PGF, Scheme 2). COX has two isoforms, the constitutive isoform COX-1 and the inducible isoform COX-2 [94]. Unlike COX-1, which is expressed in nearly all mammalian tissues, COX-2 is often up-regulated at the inflammation site and in various tumor tissues, thus it has received much research attention in connection with inflammation-related diseases including cancer [19, 175-178]. It was reported that COX-2 is overexpressed by ~40% in human adenomas and ~80% in adenocarcinomas relative to normal mucosa in colon tissues [179, 180].

COX catalyzes AA peroxidation to the pro-inflammatory and pro-carcinogenic PGs₂. PGE₂, one form of PGs₂, is the major COX product that could stimulate colorectal carcinogenesis by activating elements of the pro-survival signaling pathway such as the extracellular-signal-regulated kinases (ERK), cAMP/PKA and EGFR [181-183]. Unlike its downstream product AA, DGLA may be the exceptional ω -6 PUFA which may perform anti-inflammatory and anti-cancer activities by increasing PGs₁ through COX. For example, PGE₁, one form of PGs₁, was reported to inhibit vascular smooth muscle cell proliferation, reduce

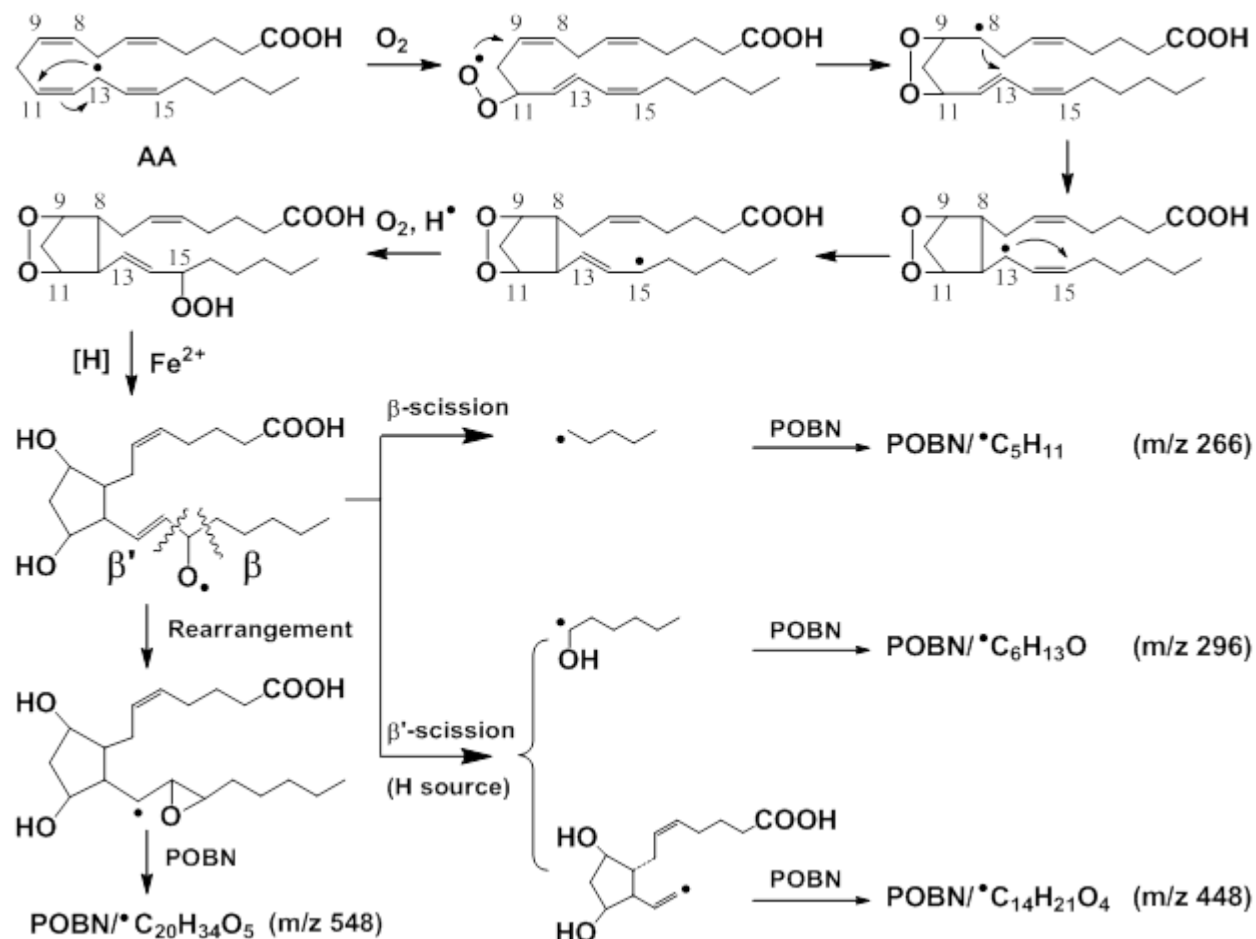
vascular cell adhesion, and attenuate the development of atherosclerosis [32, 76, 184]. PGE₁ also exerted an inhibitory effect on the growth of melanoma cells and HeLa cells [70, 185-187].

It is well-known that COX catalyzes PUFAs to PGs through a series of free radical reactions [134]. As the most reactive intermediates, however, the PUFA-derived free radicals formed during COX-catalyzed peroxidation have never been identified and characterized due to the lack of appropriate methodology. Thus, the possible role of these free radical metabolites in inflammation related diseases including cancer are still not clear. Recently, the novel technique of combined LC/ESR/MS and spin-trapping allowed us to detect and characterize the free radicals formed from COX-catalyzed AA and DGLA peroxidation (ovine COX in a cell-free *in vitro* system [171, 173]). Our previous studies suggested that both similar and different free radical reactions occurred in COX-catalyzed peroxidation of AA vs. DGLA ([171, 173] Scheme 10 and 11). For example, COX can catalyze their free radical-mediated peroxidation through the same pathways, *e.g.* C-15 oxygenation, to form the same or similar free radicals and non-radical metabolites due to the common structural moiety (C-8 to C-20) in AA and DGLA. In contrast, the different structural moiety (C-1 to C-7) in DGLA generated exclusive free radicals and non-radical products *via* its unique C-8 oxygenation pathway. This unique C-8 oxygenation in the COX/DGLA reaction may be attributed to the different relative positions of C-2 through C-10 in DGLA compared to AA due to the absence of the C-5/C-6 double bond in DGLA [188].

In the study of COX-catalyzed AA peroxidation, three types of POBN radical adducts with numerous isomers were observed [171], including three isomers of POBN/[•]C₁₄H₂₁O₄ (m/z 448), two isomers of POBN/[•]C₆H₁₃O (m/z 296) and ten isomers of POBN/[•]C₂₀H₃₄O₅ (m/z 548) (Scheme 10). The radical species POBN/[•]C₁₄H₂₁O₄ (m/z 448) contains a novel carbon-carbon double bond radical ([•]C=C) that is derived from the special β'-scission PGF₂ type alkoxyl radical

during COX/AA peroxidation *via* C-15 oxygenation (Scheme 10). Two isomers of POBN/ \bullet C₆H₁₃O (m/z 296) also form from the same special β' -scission. This special β' -scission (breaking the carbon bond on the opposite side of the normal β -scission) was found to be preferred over the normal β -scission in COX/AA peroxidation ([171], Scheme 10).

Pathway of C-15 oxygenation and free radicals that are trapped and identified



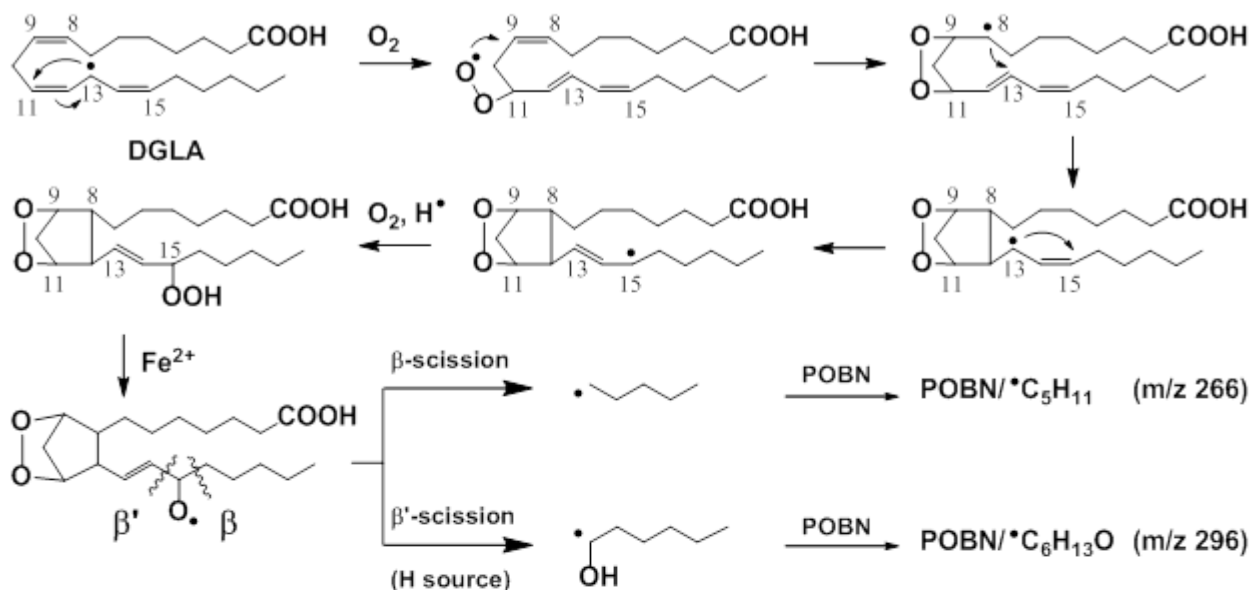
Scheme 10. Proposed mechanism of COX-catalyzed AA peroxidation.

Free radical reactions including formation of C-13 radicals, C-9/C-11 endoperoxide bridging (adding the first O₂ *via* the cyclooxygenase activity of COX), C-8 and C-12 cyclization, and C-15 oxygenation (adding the second O₂ *via* the peroxidase activity of COX). A total of four types of free radicals, \bullet C₅H₁₁, \bullet C₆H₁₃O, \bullet C₁₄H₂₁O₄ and \bullet C₂₀H₃₄O₅, were formed and trapped by POBN as m/z 266, 296, 448 and 548 ions.

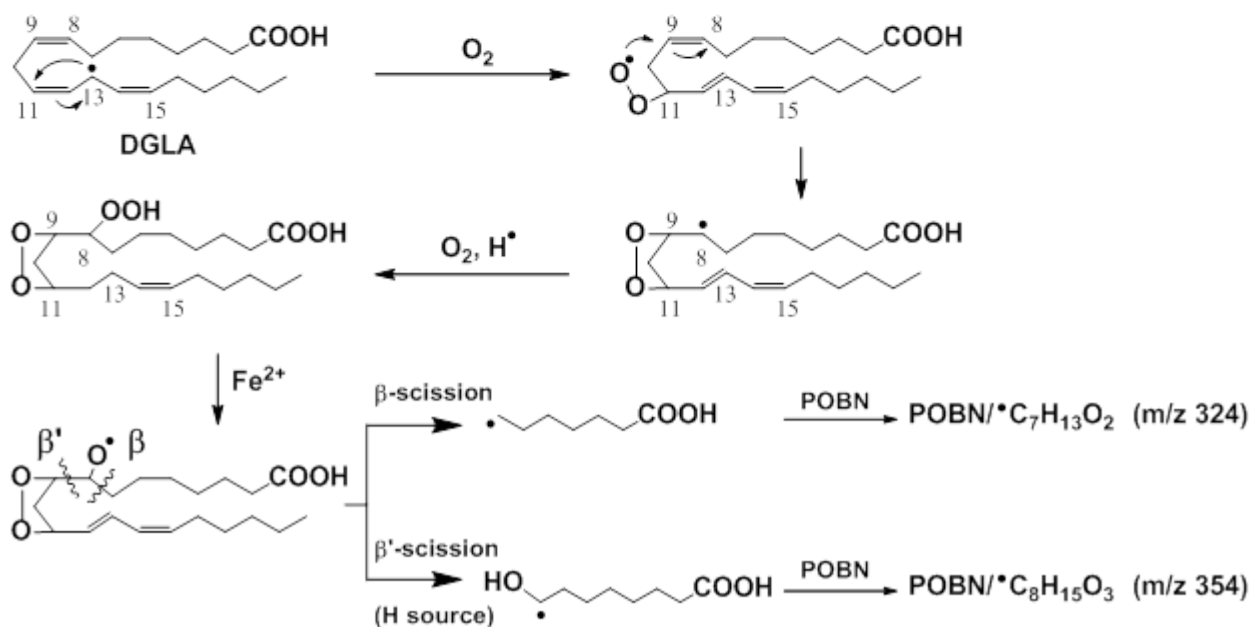
Similarly, β' -scission also takes place in COX/DGLA *via* C-15 oxygenation, but two isomers of POBN/ \bullet C₆H₁₃O (m/z 296) were formed without detection of their co-products; *i.e.*, \bullet C=C was not generated [173]. Such a pattern probably results because this β' -scission takes place in the PGH₁-type alkoxy radical instead of the PGF₁-type alkoxy radical ([173], Scheme 11). Another radical adduct of POBN/ \bullet C₅H₁₁ (m/z 266) from β -scission in the C-15 oxygenation pathway was observed [173]. In addition, two exclusive DGLA-derived free radicals are generated from C-8 oxygenation in COX-catalyzed DGLA peroxidation (cell-free), radical products of m/z 324 as POBN/ \bullet C₇H₁₃O₂ (from β -scission) and m/z 354 as POBN/ \bullet C₈H₁₄O₃ (from β' -scission, Scheme 11).

In order to confirm whether those radicals were actually formed from cellular COX peroxidation and thus to assess the association between those novel free radical metabolites and cell growth, we made the first effort in this study to characterize free radicals formed from cellular COX-catalyzed AA and DGLA peroxidation using the human colon cancer cell line HCA-7 colony 29, a cell line with high COX-2 expression. Our refined LC/MS method along with SPE allowed us for the first time to detect and characterize free radicals as the reduced form (hydroxylamines) derived from the cellular COX metabolism of AA and DGLA in an experimental setting in which cell growth responses such as proliferation and cell cycle distribution could also be assessed. Therefore, our new protocol should allow us to further study the free radical-based mechanism associated with PUFA bioactivity and improve our knowledge of COX in cancer biology.

A. Pathway of C-15 oxygenation and free radicals that are trapped and identified



B. Pathway of C-8 oxygenation and free radicals that are trapped and identified



Scheme 11. Proposed mechanisms of COX-catalyzed DGLA peroxidation.

(A) Free radical reaction, *e.g.* C-15 oxygenation (similar to that of COX/AA), formed two free radicals, $\cdot C_5H_{11}$ and $\cdot C_6H_{13}O$, which were trapped by POBN as m/z 266 and 296 adducts. (B) Free radical reaction, *e.g.*, C-8 oxygenation (another way to add the second O_2 , occurring after formation of the C-13 radical and C-9/C-11 endoperoxide bridge), formed two exclusive free radicals, $\cdot C_7H_{13}O_2$ and $\cdot C_8H_{15}O_3$, which were trapped by POBN as the m/z 324 and m/z 354 ions.

3.2. Results and Discussion

3.2.1. *COX-2 expression in HCA-7 colony 29 cells*

The human colon carcinoma cell line HCA-7 colony 29 (a subpopulation isolated from the HCA-7 cell line) is a new addition to the colorectal collection. Due to its higher expression of COX-2, the HCA-7 colony 29 cell line is very useful for studying COX-catalyzed PUFA peroxidation. In our study, the expression of COX-2 in HCA-7 colony 29 was evaluated by Western blot analysis as described in Chapter 2, after cells were treated with 0.1% ethanol (control), 100 μ M of DGLA or 100 μ M of AA. HCA-7 colony 29 cells showed a strong COX-2 expression that was not altered by treatment with DGLA and AA (Fig. 2). The unchanged COX-2 expression indicated that the substrates did not affect the enzyme expression; thereby AA- and DGLA-derived metabolites through COX were comparable.

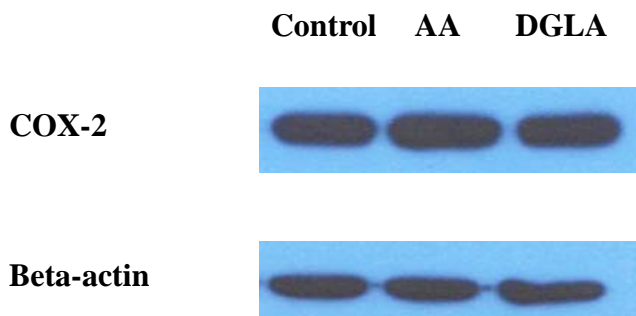


Fig. 2. Western blot analysis of COX-2 expression with PUFA treatment.

HCA-7 colony 29 cells were treated with 0.1% ethanol, 100 μ M of AA or 100 μ M of DGLA, respectively, for 24 h. Ten micrograms of protein per sample was separated by SDS-PAGE, transferred to PVDF membrane, and immunoblotted using a COX-2 specific antibody. Beta-actin served as the loading control.

3.2.2. *Offline ESR detection of free radicals*

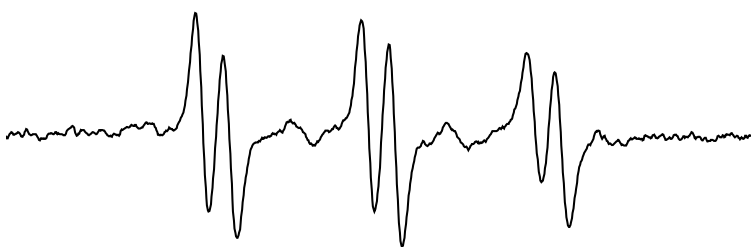
Free radicals generated and spin-trapped by POBN from COX-catalyzed PUFA peroxidation in HCA-7 colony 29 cells were measured by offline ESR. In the control experiment in the absence of PUFA in cell-PBS suspension, no ESR signal of POBN radical adducts was

observed (Fig. 3A). A typical six-line ESR signal of POBN radical adducts with hyperfine coupling constants of $a^N \approx 15.69$ G and $a^H \approx 2.68$ G (Fig. 3B and 3C) was observed after cells were incubated with 1.0 mM of AA or DGLA. Although AA is generally considered to be the more favored substrate for COX, the ESR signal of POBN radical adducts between AA and DGLA treatment did not show any significant difference in G value or signal height.

A. Spin-trapping in Cell-PBS suspension



B. Spin-trapping in Cell-PBS suspension with AA



C. Spin-trapping in Cell-PBS suspension with DGLA



3465 3480 3495 3510 3525
Magnetic Field (G)

Fig. 3. Offline ESR spectra of spin-trapping experiments in cell-PBS suspensions.

(A) ESR spectra of spin-trapping experiments in cell-PBS suspension without PUFA. (B) ESR spectra of spin-trapping experiments in cell-PBS suspension with a supplement of 1.0 mM of AA. (C) ESR spectra of spin-trapping experiments in cell-PBS suspensions with a supplement of 1.0 mM of DGLA. ESR field scans were performed with an ESR flat cell and the hyperfine couplings of the spectra were $a^N \approx 15.69$ G and $a^H \approx 2.68$ G.

However, this offline ESR measurement can provide only an overall signal intensity of POBN radical adducts, not specific information in terms of types, numbers, and structures, because many of the POBN spin adducts tend to have the same or similar a^N and a^H hyperfine couplings [146].

Although this experiment demonstrated the generation of free radicals formed from cellular COX-catalyzed PUFA peroxidation, it must be performed in the presence of a large excess of cells ($>10^8$), and high concentrations of POBN (> 50 mM) as well as PUFA (> 1 mM) in PBS for very short incubation time (< 30 min).

3.2.3. LC/ESR/MS identification of free radicals in cell-PBS suspension

In order to obtain detailed structural information for the individual POBN radical adducts from COX-catalyzed PUFA peroxidation in cell-PBS suspensions, samples were subjected to LC/ESR and LC/MS analysis. Although no ESR-active peak was observed in online LC/ESR chromatograms (data not shown), almost all radical adducts including isomers observed in the cell-free system [171, 173] in our previous publications were detected in cells *via* LC/MS (Fig. 4).

For example, the EIC chromatogram of four protonated molecular ions of m/z 266, m/z 296, m/z 448 and m/z 548 could be projected from the full MS scan (m/z 50 to m/z 600, Fig. 4A) of the cellular COX/AA spin-trapping reaction. The EIC peak of the m/z 266 ion corresponded to the POBN radical adduct of the pentyl radical, which was the product of the β -scission occurring away from the double bond ($\text{POBN}/\bullet\text{C}_5\text{H}_{11}$, $t_R \approx 24.0$ min, Fig. 4A, Scheme 10). The EIC peaks of the m/z 296 ion corresponded to the POBN radical adduct of two isomers of hexanol radicals ($\text{POBN}/\bullet\text{C}_6\text{H}_{13}\text{O}$, $t_R \approx 12.4$ min and 17.8 min, Fig. 4A). The EIC peaks of the m/z 448 ion corresponded to the POBN radical adducts of three isomers of $\text{POBN}/\bullet\text{C}_{14}\text{H}_{21}\text{O}_4$ ($t_R \approx 11.9$ min,

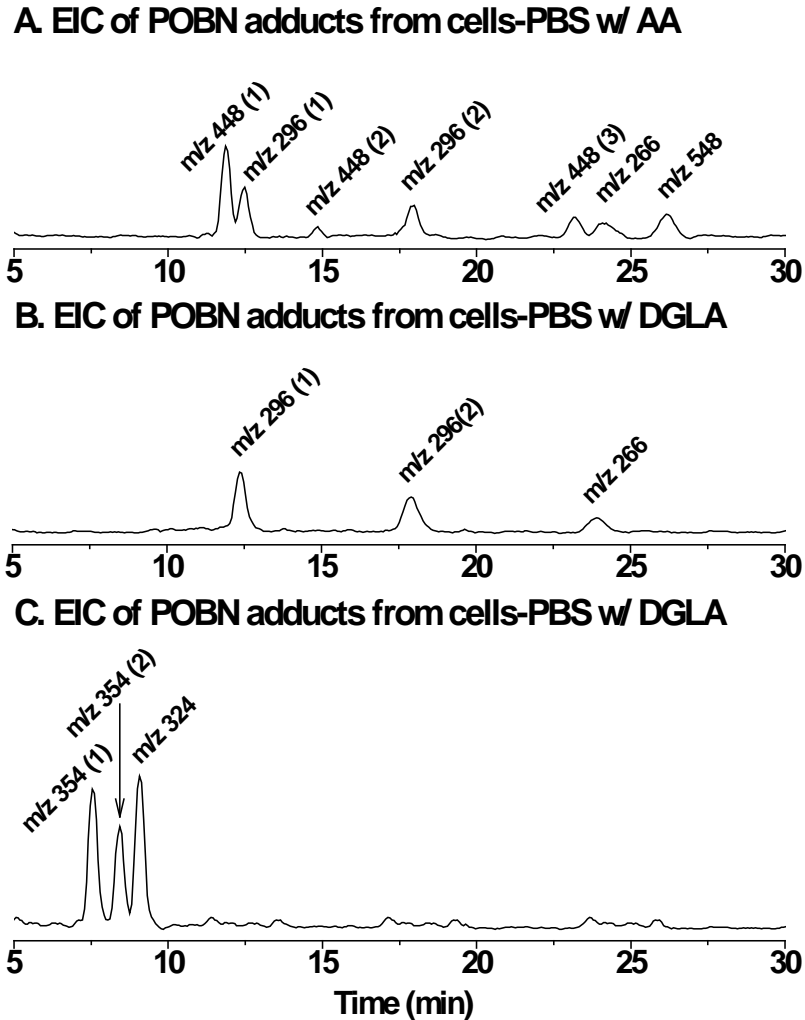


Fig. 4. LC/MS chromatogram (EICs) of POBN adducts formed from cellular COX-catalyzed AA and DGLA peroxidation.

Spin-trapping experiments in cell-PBS suspension with a supplement of 50 mM POBN and 1.0 mM PUFA for 30 min. (A) EICs of m/z 296, m/z 448, m/z 266 and m/z 548 as POBN/ \bullet C₅H₁₁, POBN/ \bullet C₆H₁₃O, POBN/ \bullet C₁₄H₂₁O₄ and POBN/ \bullet C₂₀H₃₄O₅ formed from C-15 oxygenation of COX/AA. (B) EICs of m/z 266 and m/z 296 as POBN/ \bullet C₅H₁₁ and POBN/ \bullet C₆H₁₃O formed from C-15 oxygenation of COX/DGLA. (C) EICs of m/z 324 and m/z 354 as POBN/ \bullet C₇H₁₃O₂ and POBN/ \bullet C₈H₁₅O₃ from C-8 oxygenation of COX/DGLA.

14.8 min and 23.3 min, Fig. 4A). POBN/ \bullet C₆H₁₃O and POBN/ \bullet C₁₄H₂₁O₄ were derived from a special β -scission labeled ' β ' in Scheme 10, where β -scission occurred toward the double bond near the PGF ring. All three radicals were generated from the C-15 oxygenation of COX/AA peroxidation and spin-trapped by POBN (Scheme 10). POBN/ \bullet C₂₀H₃₄O₅ (m/z 548, $t_R \approx 26.2$ min, Fig. 3A) was formed from the rearrangement of a PGF₂-type alkoxy radical (Scheme 10).

Due to the shared structural moiety (C8-C20) of AA and DGLA, cellular COX-catalyzed DGLA peroxidation undergoes the same C-15 oxygenation pathway (Scheme 11A). Thus, the EIC peaks of the m/z 266 ion (POBN/ \bullet C₅H₁₁, $t_R \approx 24.0$ min, Fig. 4B) and the m/z 296 ion (POBN/ \bullet C₆H₁₃O, $t_R \approx 12.4$ min and 17.8 min, Fig. 4B) were both observed. However, the formation of \bullet C=C as the second radical of the β' -scission in addition to \bullet C₆H₁₃O was not observed in COX/DGLA peroxidation. The β' -scission appears to preferentially occur at the PGH1 stage, which results in the rearrangement of the \bullet C=C to form an oxygen-centered radical that could not be trapped by POBN [171]. C-8 oxygenation in COX-catalyzed DGLA peroxidation also formed two exclusive free radicals corresponding to the protonated molecule ions of m/z 354 and m/z 324 (Fig. 4C). The EIC of m/z 354 was projected at $t_R \approx 7.5$ min and 8.4 min, and appeared to be two isomers of POBN/ \bullet C₈H₁₅O₃ that formed from the β' -scission of a DGLA-derived alkoxy radical with a carboxyl end (Scheme 11B). The molecule at m/z 324 ($t_R \approx 9.1$ min) was the POBN radical adduct of the \bullet C₇H₁₃O₂ radical with the carboxyl end formed from the β -scission of the DGLA-derived alkoxy radical as proposed in Scheme 11B.

When a lower concentration of POBN (20 mM) as well as PUFA (100 μ M) was used, the signal intensity of the offline ESR was significantly decreased and not all the POBN radical adducts were observed in the LC/MS chromatogram (data not shown).

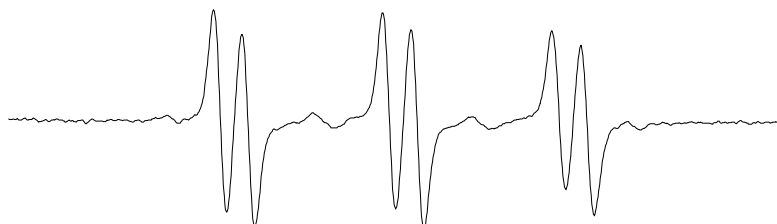
Although our Fig. 4 demonstrated radical identification in cellular COX-catalyzed AA and DGLA peroxidation for the first time, its biological application was problematic for several reasons: (1) in order to observe the EIC peaks of POBN adducts as in Fig. 4, peroxidation and spin-trapping experiments must be conducted with a large number of cells ($>10^8$ /mL); (2) an excessive amount of POBN (> 50 mM) as well as PUFA (> 1 mM) must also be introduced, even though such high doses of supplements could lead to cell death within 1 h, and (3) the spin-trapping and peroxidation were taking place in PBS instead of cell culture medium and the incubation time was very short (< 30 min). All these facts indeed restrict the biological application of the detection method in Fig. 4, since common parameters of cell growth, *e.g.* proliferation, apoptosis, and cell cycle distribution, must be assessed after a long incubation time.

3.2.4. Assessment of POBN's trapping ability

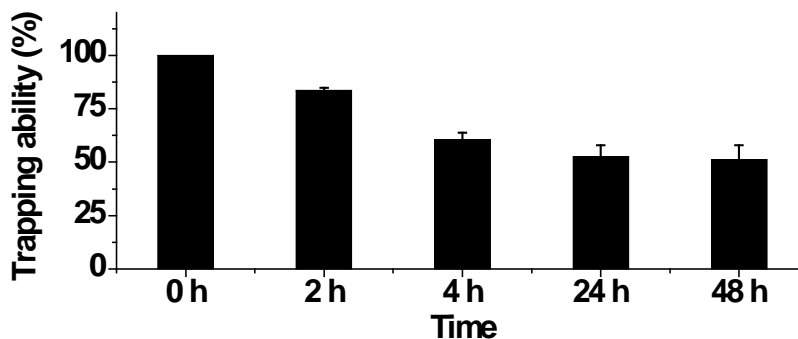
Due to its appropriate solubility in biological fluids, POBN has been widely used in many lipid peroxidation studies to detect free radicals formed *in vivo* and *in vitro*. POBN has normally been administered *via* acute injection in animal models and the samples analyzed by ESR after a short period of time (~ 0.5 to 1 h) [168, 189]. For *in vitro* studies, the time of the reaction in the presence of POBN was also very short (less than 0.5 h) [169-173]. Whether POBN is able to trap free radicals after a days-long incubation in complete growth medium has never been studied.

Methods for evaluating a cell population's response to external factors such as cell proliferation and apoptosis usually require a long incubation time, varying from hours to days, when cells are cultured under normal growth conditions (cells grown in a recommended complete growth medium in an incubator containing a 95% humidified atmosphere of 5% CO₂ at 37°C). In order to investigate the possible association between PUFA-derived free radical metabolites and cell growth, the free radical formation from cellular COX-catalyzed PUFA

A. Offline ESR spectrum of POBN/ \bullet C₂H₄OH



B. Trapping ability of POBN in cell culture medium



C. Concentration of POBN in cell culture medium

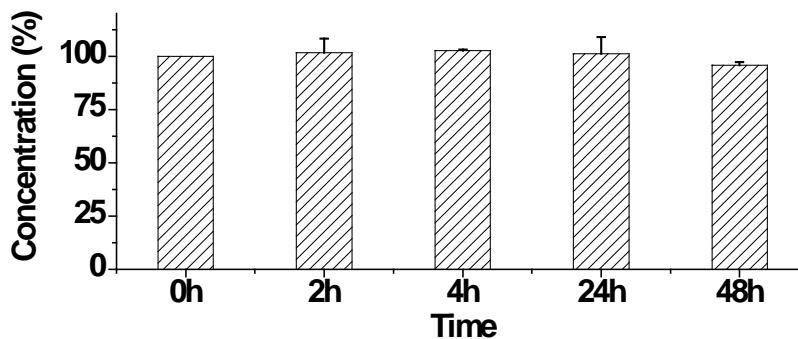


Fig. 5. POBN's trapping ability and stability in cell culture medium.

POBN in culture medium was mixed with ethanol and Fe²⁺ stock solution and subjected to offline ESR measurement. The final concentrations of POBN, ethanol and Fe²⁺ in the reaction mixture were 20 mM, 0.1 mM and 0.1 mM, respectively. (A) Offline ESR spectra of POBN/ \bullet C₂H₄OH, (B) Trapping ability of POBN in cell culture medium after 2, 4, 24 and 48 h incubation, (C) Concentration of POBN in cell culture medium after 2, 4, 24 and 48 h incubation. ESR field scans were performed with an ESR flat cell and the hyperfine couplings of the spectra were $a^N \approx 15.71$ G and $a^H \approx 2.62$ G.

peroxidation should be assessed under the same conditions as the cell proliferation and apoptosis assays (*i.e.*, a long incubation time such as 24 or 48 h is normally needed).

Thus, we investigated the potency of POBN as a spin trap after 2, 4, 24 and 48 h of incubation in a complete culture medium. At the end of each time point, ethanol and Fe^{2+} were added to a POBN/medium solution to start the spin-trapping reaction, and the reaction mixture was immediately subjected to off-line ESR analysis. Ethanol was oxidized to hydroxyethyl radical ($\bullet\text{C}_2\text{H}_4\text{OH}$) in the presence of Fe^{2+} and trapped by POBN to form $\text{POBN}/\bullet\text{C}_2\text{H}_4\text{OH}$. A six-line spectrum of $\text{POBN}/\bullet\text{C}_2\text{H}_4\text{OH}$ ($a^{\text{N}} \approx 15.71 \text{ G}$ and $a^{\text{H}} \approx 2.62 \text{ G}$) was detected *via* offline ESR (Fig. 5A). The signal intensity of $\text{POBN}/\bullet\text{C}_2\text{H}_4\text{OH}$ quickly decreased to ~50% after a 4 h incubation and remained at around the same level up to 48 h (Fig. 5B).

This result suggested that POBN was able to continually and effectively trap radicals after incubations lasting up to several days. POBN's concentration was also measured *via* LC/MS. Interestingly, the concentration of POBN in the medium was almost unchanged during the 48 h incubation.

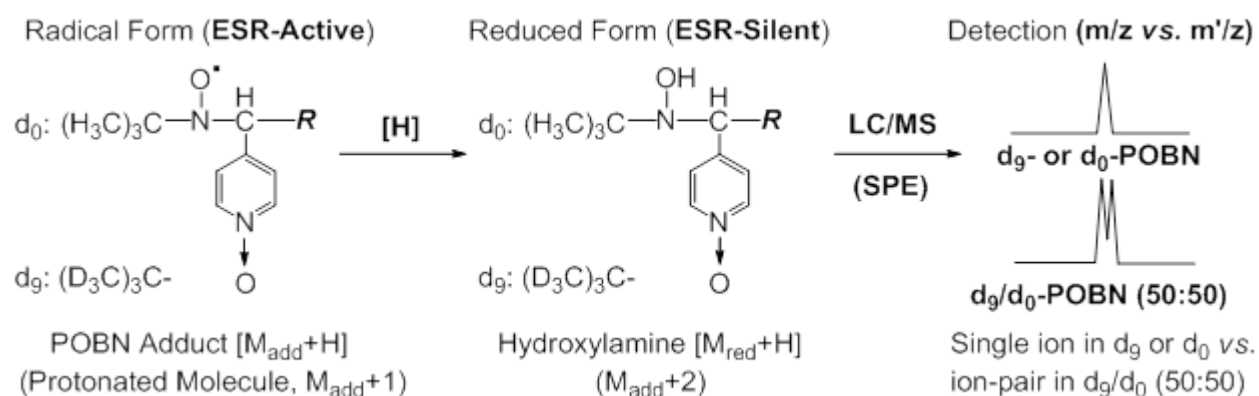
3.2.5. LC/MS and dual spin-trapping in detection of free radicals as hydroxylamines

Since POBN is able to trap free radicals under cell culture conditions for up to 48 h, we conducted the peroxidation and spin-trapping reactions with lower concentrations of POBN (20 mM) as well as PUFA (100 μM); cells were cultured in complete growth medium in an incubator containing a 95% humidified atmosphere of 5% CO_2 at 37°C. After a 30 min incubation, the supernatant was extracted through a MAX SPE cartridge and subjected to offline ESR as well as LC/ESR analysis.

Although no offline ESR signal was observed in offline ESR spectra and no ESR-active peak was detected *via* LC/ESR (data not shown), we proposed that the ESR-active POBN radical

adducts could be readily reduced to their ESR-silent forms as hydroxylamines due to the cellular reducing environment, *e.g.* the presence of the antioxidant GSH and the antioxidant enzymes GSH peroxidase, GSH reductase and superoxide dismutase [190, 191].

Hydroxylamines are more stable redox forms than the related radical forms of POBN adducts, and they could accumulate during incubation to a concentration that is detectable by LC/MS (Scheme 12). The reduction of any given POBN adduct corresponded to the structural changes +1 Da for the protonated molecules during MS ionization. For example, $\bullet\text{C}_6\text{H}_{13}\text{O}$ was trapped by POBN as the m/z 266 ion, thus the corresponding reduced POBN adduct (hydroxylamine) was the m/z 297 ion (+1 Da).

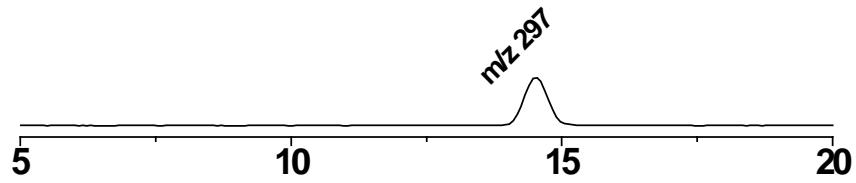


Scheme 12. Reduction of POBN-trapped radical adducts and detection of hydroxylamines by LC/MS.

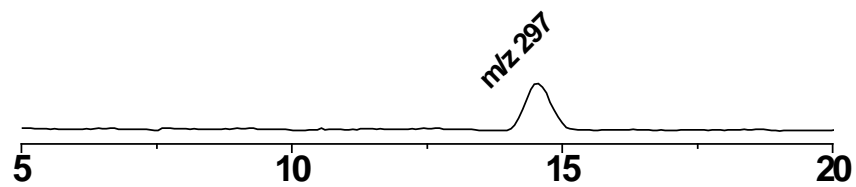
The reduced radical adducts (*e.g.* hydroxylamines) in dual spin-trapping experiments in cells were able to accumulate and be singled out in LC/MS as 9-Da ion pairs. Note that R: free radicals.

In order to characterize AA- and DGLA-derived free radicals formed under normal cell growth conditions, we examined the reduced forms of the adducts. In cellular COX-catalyzed AA peroxidation, one isomer of POBN/ $\bullet\text{C}_6\text{H}_{13}\text{O}$'s reduced form was projected at $t_R \approx 14.5$ min as a molecule ion of m/z 297 (Fig. 6A). In fact, m/z 297 was the only reduced POBN radical adduct that was observed after 30 min of incubation. After an 8 h incubation, in addition to POBN/ $\bullet\text{C}_6\text{H}_{13}\text{O}$, another reduced POBN radical adduct was observed, which corresponded to

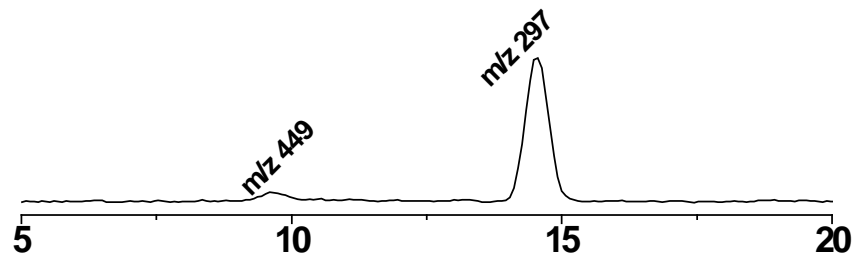
A. Hydroxylamine from cells w/ AA, 0.5 h



B. Hydroxylamine from cells w/ DGLA, 0.5 h



C. Hydroxylamines from cells w/ AA, 8 h



D. Hydroxylamines from cells w/ DGLA, 12 h

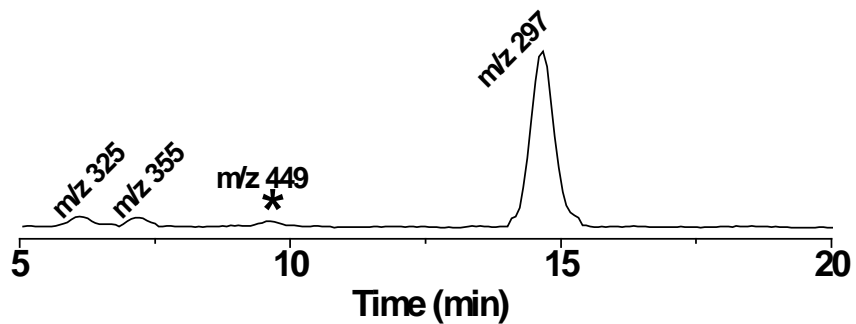


Fig. 6. LC/MS chromatogram (EICs) of hydroxylamines formed from cellular COX-catalyzed PUFA peroxidation.

HCA-7 colony 29 cells were cultured under normal cell growth conditions in the presence of 20 mM POBN and 100 μ M PUFA. (A) EIC of m/z 297 from cells treated with AA for 30 min. (B) EIC of m/z 297 from cells treated with DGLA for 30 min. (C) EIC of m/z 297 and m/z 449 from cells treated with AA for 8 h. (D) EIC of m/z 297, m/z 325 and m/z 355 from cells treated with DGLA for 12 h. (*) m/z 449 was the hydroxylamine generated from COX/AA peroxidation.

one isomer of POBN/ \bullet C₁₄H₂₁O₄'s reduced form as a protonated molecular ion of m/z 449. The EIC chromatography of m/z 449 was projected at $t_R \approx 9.6$ min (Fig. 6C). The signal intensity of m/z 297 increased from 0.5 to 8 h and the appearance of m/z 449 after 8 h suggests that POBN radical adducts were reduced to their corresponding hydroxylamine products and accumulated during incubation. However, the signal intensity of m/z 449 was much lower than that of m/z 297.

In cellular COX-catalyzed DGLA peroxidation, similar to what we observed in the COX/AA reaction, one isomer of POBN/ \bullet C₆H₁₃O's reduced form as a molecule ion of m/z 297 was projected at $t_R \approx 14.5$ min (Fig. 6B), and m/z 297 was the only reduced POBN radical adduct observed after 30 min of incubation. When the incubation time was extended to 12 h, two more hydroxylamine products were observed: POBN/ \bullet C₇H₁₃O₂ and POBN/ \bullet C₈H₁₅O₃'s reduced form as protonated molecular ions of m/z 325 and m/z 355 were profiled at $t_R \approx 6.1$ min and $t_R \approx 7.1$ min, respectively (Fig. 6D). There was an increase of the signal intensity of m/z 297 from 0.5 to 12 h, and m/z 297 was still the major hydroxylamine that was detected after a 12 h incubation compared to m/z 325 and m/z 355. Interestingly, m/z 449, the reduced POBN adduct of the special \bullet C=C derived from the COX/AA reaction, was also observed at 12 h, which indicated that DGLA was converted to AA in cells.

3.2.6. *LC/MS, LC/MS² and dual spin-trapping in characterization of hydroxylamines*

Because the POBN radical adducts were reduced to the ESR-silent hydroxylamines in cells, ESR no longer served as a detector. In order to confirm the structural assignment of hydroxylamines, the dual spin trap technique (d₀ and d₉-POBN) was applied. Dual spin-trapping experiment along with LC/MS detection [170-173] was used for recognition and also identification of a number of isomers of radical adducts and their structures. In this technique, the nine hydrogen atoms on the tert-butyl group were replaced by deuterium in d₉-POBN. The

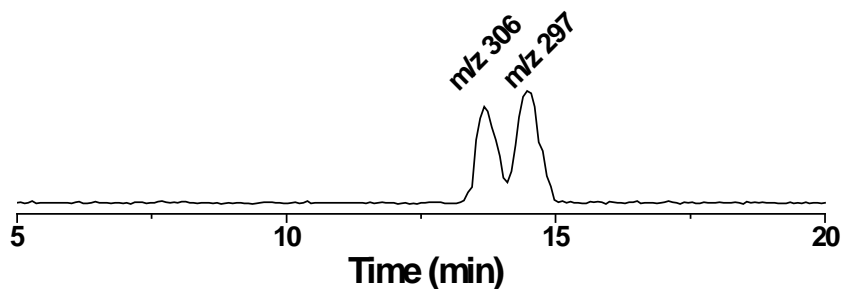
commercially unavailable spin trap d₉-POBN has been recently synthesized starting from commercially available d₉-*tert*-butylamine (Scheme 8). When a 50:50 mixture of POBN and d₉-POBN was applied in a cellular spin-trapping experiment, hydroxylamine could be singled out in LC/MS as an ion pair with a 9-Da difference (Scheme 12), and then the corresponding d₀/d₉-POBN fragmentation should be observed by LC/MS².

The dual spin-trapping experiments were performed with a 12 h incubation because at that time all four reduced products, POBN/[•]C₆H₁₃O, POBN/[•]C₁₄H₂₁O₄, POBN/[•]C₇H₁₃O₂ and POBN/[•]C₈H₁₅O₃, were observed. Under the same chromatographic conditions, the polarity and molecular differences between the structures of the reduced products of d₀- and d₉-POBN radical adducts resulted in a shorter retention time for the reduced d₉-POBN adduct than for the reduced d₀-POBN adduct, as shown in Figs. 7A, 8A, 9A and 10A.

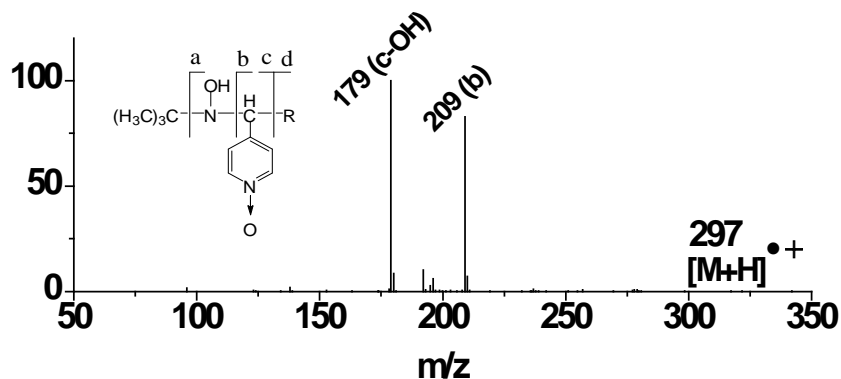
In the cellular COX/AA reaction using dual spin traps, two ion pairs of m/z 306/297 and m/z 458/449 were observed. The ion pair of m/z 297/306 (*t_R* ≈ 14.5 min and *t_R* ≈ 13.8 min) represented d₀/d₉-POBN/[•]C₆H₁₃O's reduced products (Fig. 7A). LC/MS² studies confirmed these assignments by showing a unique fragmentation pattern of m/z 179 and m/z 209 ions from POBN/[•]C₆H₁₃O (Fig. 7B). LC/MS analysis of m/z 188 and m/z 209 from d₉-POBN/[•]C₆H₁₃O further verified the assignments (Fig. 7C).

Another ion pair of m/z 449/458 (*t_R* ≈ 9.6 min and *t_R* ≈ 9.3 min) represented d₀/d₉-POBN/[•]C₁₄H₂₁O₄'s reduced products (Fig. 8A). LC/MS² studies confirmed these assignments by showing a unique fragmentation pattern of m/z 179, m/z 342, m/z 360 and m/z 431 ions from POBN/[•]C₁₄H₂₁O₄ (Fig. 8B). LC/MS analysis of m/z 179, m/z 342, m/z 360 and m/z 440 from d₉-POBN/[•]C₁₄H₂₁O₄ further verified the assignments (Fig. 8C).

A. EIC of m/z 306 and m/z 297 ion pair



B. LC/MS² of m/z 297 from POBN[•] C₆H₁₃O



C. LC/MS² of m/z 306 from d₉-POBN[•] C₆H₁₃O

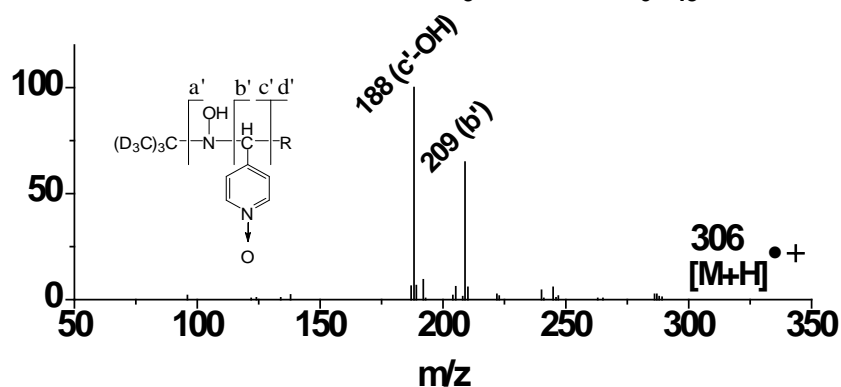
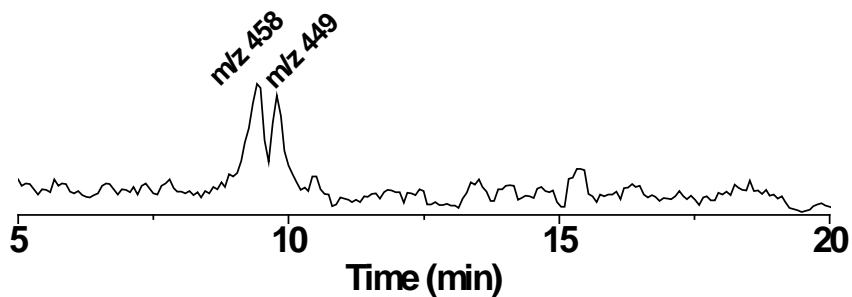


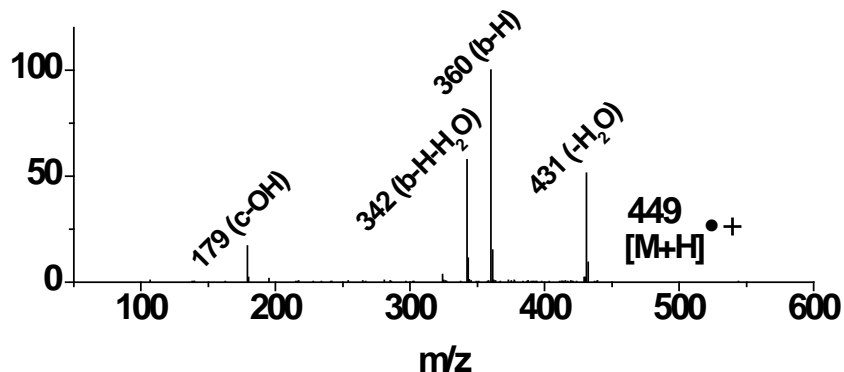
Fig. 7. LC/MS chromatogram (EICs) and LC/MS² analysis of m/z 306 and m/z 297 in dual spin-trapping experiment.

HCA-7 colony 29 cells were cultured under normal cell growth conditions in the presence of 20 mM d₀/d₉-POBN and 100 μ M AA for 12 h. (A) EIC of m/z 306 and m/z 297 from cells treated with AA. (B and C) LC/MS² of m/z 297 and m/z 306 from cells treated with AA. Each chromatographic fraction with m/z 297 in the POBN experiment had a counterpart in the d₉-POBN spin-trapping experiment (a', b', c', and d' ions).

A. EIC of m/z 458 and m/z 449 ion pair



B. LC/MS² of m/z 449 from POBN[•] C₁₄H₂₁O₄



C. LC/MS² of m/z 458 from d₉-POBN[•] C₁₄H₂₁O₄

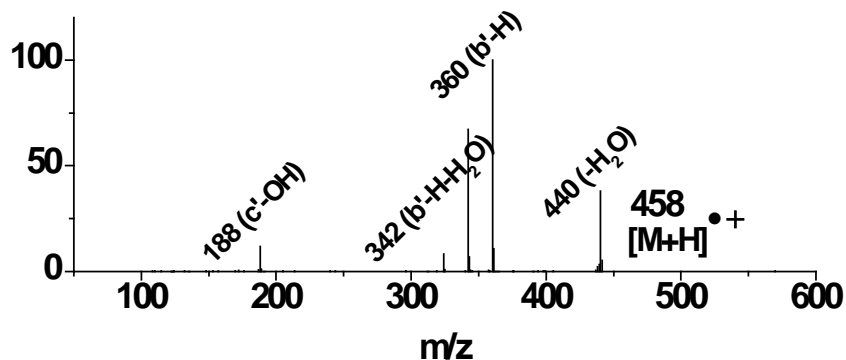


Fig. 8. LC/MS chromatogram (EICs) and LC/MS² analysis of m/z 458 and m/z 449 in dual spin-trapping experiment.

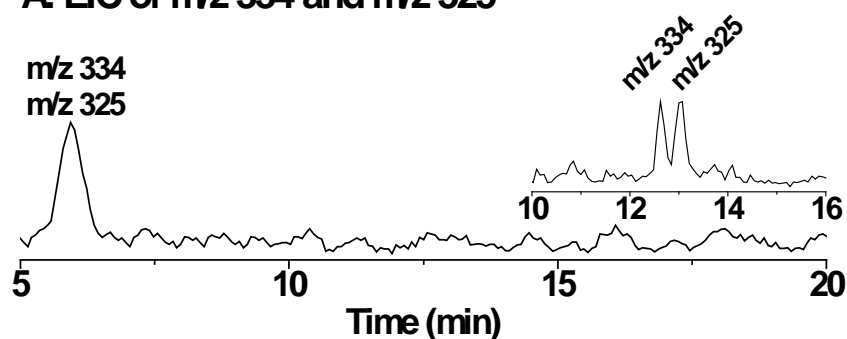
HCA-7 colony 29 cells were cultured under normal cell growth conditions in the presence of 20 mM d₀/d₉-POBN and 100 μ M AA for 12 h. (A) EIC of m/z 458 and m/z 449 from cells treated with AA. (B and C) LC/MS² of m/z 449 and m/z 458 from cells treated with AA. Each chromatographic fraction with m/z 449 in the POBN experiment had a counterpart in the d₉-POBN spin-trapping experiment (a', b', c', and d' ions).

In a cellular COX/DGLA reaction using dual spin traps, the ion pair of m/z 306/297 was also observed and the results of EICs and LC/MS² analysis was similar to that observed in the COX/AA reaction (data not shown). Another two ion pairs of m/z 325/234 and m/z 355/264 were observed as shown in Figs. 9A and 10A. The ion pair of m/z 325 /334 represented d_0/d_9 -POBN/ \bullet C₇H₁₃O₂'s reduced product. The LC/MS² studies confirmed these assignments by showing a unique fragmentation pattern of m/z 122 and m/z 237 ions from POBN/ \bullet C₇H₁₃O₂ (Fig. 9B). LC/MS analysis of m/z 122 and m/z 237 from d_9 - POBN/ \bullet C₇H₁₃O₂ further verified the assignments (Fig. 9C). The ion pair of m/z 355/364 represented d_0/d_9 -POBN/ \bullet C₈H₁₅O₃'s reduced product. LC/MS² studies confirmed these assignments by showing a unique fragmentation pattern of m/z 138, m/z 179, m/z 250 and m/z 266 ions from POBN/ \bullet C₈H₁₅O₃ (Fig. 10B). LC/MS analysis of m/z 138, m/z 188, m/z 250 and m/z 266 from d_9 - POBN/ \bullet C₈H₁₅O₃ further verified the assignments (Fig. 10C).

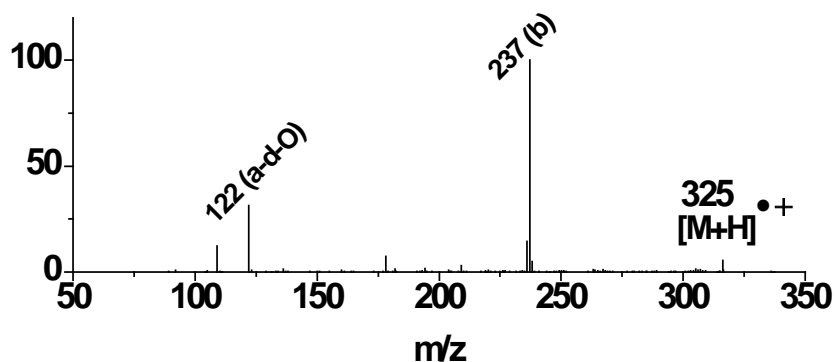
However, under the same chromatographic conditions, the ion pairs of m/z 325/234 and m/z 355/264 were not observed as double peaks because the retention times of these ion pairs were too short ($t_R \approx 6$ min) as shown in Figs. 9A and 10A. In fact, when we changed the chromatographic conditions and extended the retention time of the analytes, the double peaks of m/z 325 and m/z 334 ($t_R \approx 12.6$ and 13.0 min) as well as m/z 355 and m/z 364 ($t_R \approx 14.9$ and 15.2 min) were both detected as shown in the inset of Figs. 9A and 10A.

In conclusion, our refined LC/MS method along with the SPE allowed us to detect and characterize free radicals formed from cellular COX metabolism of AA and DGLA as their reduced form (hydroxylamines). Since hydroxylamines were accumulated products, they could be detected under the experimental setting in which cell growth response such as proliferation and cell cycle distribution could also be assessed. Thus, for the first time, common and exclusive

A. EIC of m/z 334 and m/z 325



B. LC/MS² of m/z 325 from POBN•C₇H₁₃O₂



C. LC/MS² of m/z 334 from d₉-POBN•C₇H₁₃O₂

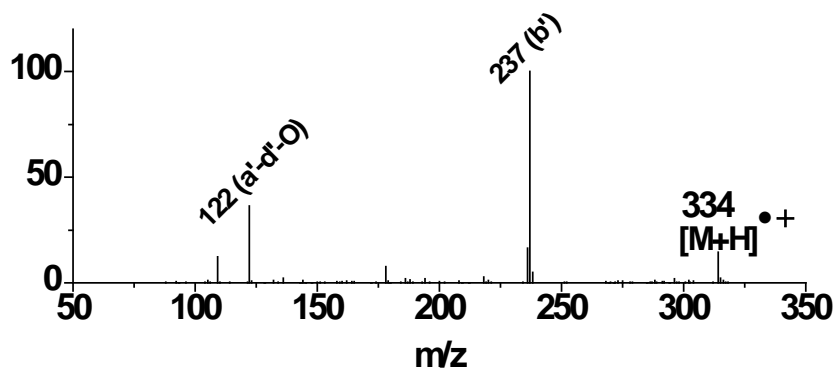
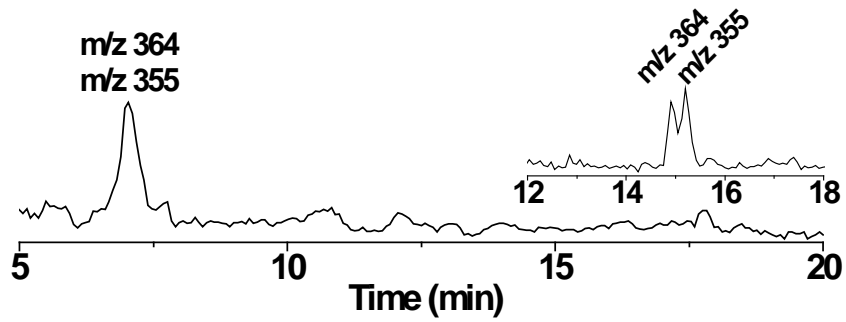


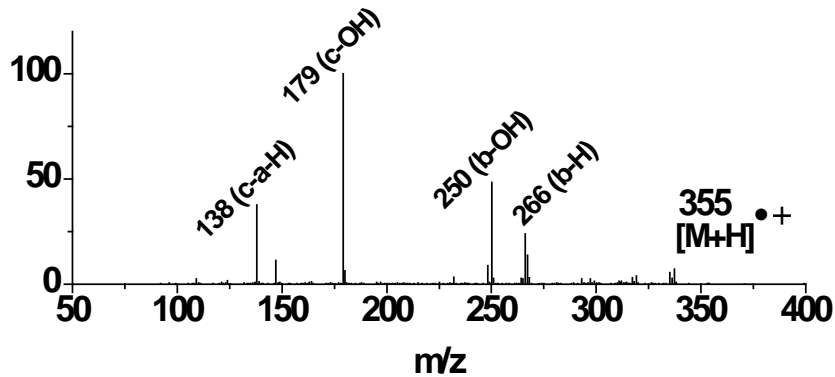
Fig. 9. LC/MS chromatogram (EICs) and LC/MS² analysis of m/z 334 and m/z 325 in dual spin-trapping experiment.

HCA-7 colony 29 cells were cultured under normal cell growth conditions in the presence of 20 mM d₀/d₉-POBN and 100 μM DGLA for 12 h. (A) EIC of m/z 334 and m/z 325 from cells treated with DGLA. (B and C) LC/MS² of m/z 325 and m/z 334 from cells treated with DGLA. Each chromatographic fraction with m/z 325 in the POBN experiment had a counterpart in the d₉-POBN spin-trapping experiment (a', b', c', and d' ions). The inset in Fig. 9A was the EIC of m/z 334 and m/z 325 under different chromatographic condition: (i) 0-40 min, 0 to 60% B; (ii) 40-43 min, 60 to 95% B; and (iii) 43-50 min (isocratic), 5% A and 95% B.

A. EIC of m/z 364 and m/z 355



B. LC/MS² of m/z 355 from POBN• C₈H₁₅O₃



C. LC/MS² of m/z 364 from d₉-POBN• C₈H₁₅O₃

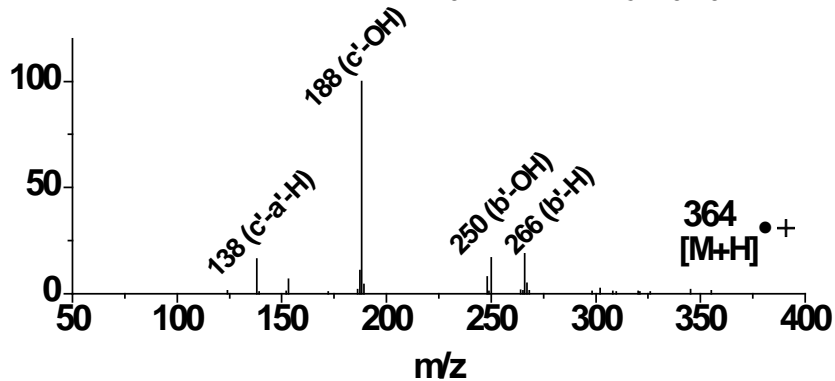


Fig. 10. LC/MS chromatogram (EICs) and LC/MS² analysis of m/z 364 and m/z 355 in dual spin-trapping experiment.

HCA-7 colony 29 cells were cultured under normal cell growth conditions in the presence of 20 mM d₀/d₉-POBN and 100 μM DGLA for 12 h. (A) EIC of m/z 364 and m/z 355 from cells treated with DGLA. (B and C) LC/MS² of m/z 355 and m/z 364 from cells treated with DGLA. Each chromatographic fraction with m/z 355 in the POBN experiment had a counterpart in the d₉-POBN spin-trapping experiment (a', b', c', and d' ions). The inset in Fig. 10A was the EIC of m/z 364 and m/z 355 under different chromatographic conditions: (i) 0-40 min, 0 to 60% B; (ii) 40-43 min, 60 to 95% B; and (iii) 43-50 min (isocratic), 5% A and 95% B.

free radicals as the reduced form were identified and characterized in COX-catalyzed AA vs. DGLA peroxidation in cells. The $\bullet\text{C}_6\text{H}_{13}\text{O}$ was the common free radical generated from both COX/AA and COX/DGLA peroxidation. The $\bullet\text{C}_{14}\text{H}_{21}\text{O}_4$ was the exclusive free radical from COX/AA and the $\bullet\text{C}_7\text{H}_{13}\text{O}_2$ and $\bullet\text{C}_8\text{H}_{14}\text{O}_3$ were exclusive free radicals from COX/DGLA.

CHAPTER 4. THE ASSOCIATION BETWEEN AA-/DGLA-DERIVED FREE RADICAL METABOLITES AND COLON CANCER CELL GROWTH

4.1. Introduction

AA, the major ω -6 PUFA in mammalian cells, has been associated with the enhancement of tumorigenesis and metastasis in the development of various cancers [72, 192-196].

Interestingly, increasing evidence from animal and *in vitro* studies suggests that DGLA, the upstream fatty acid of AA, may possess anti-inflammatory and anti-carcinogenetic activity [70-73]. Previous studies have showed that under certain conditions some PUFAs were able to induce apoptosis of tumor cells with little or no cytotoxic action on normal cells [117, 119, 120]. It was observed that among all the tested fatty acids, DGLA was the most effective in selectively killing tumor cells [117]. These results suggested that DGLA shows selective tumoricidal action *in vitro*. Through suppressing the expression of oncogenes Her-2/neu and Bcl-2 and enhancing p53 activity, DGLA could induce apoptosis of tumor cells [119, 121-123]. Further study found that the COX inhibitor and anti-oxidants had opposite effect on the anti-tumorigenic action of DGLA. It was found that COX inhibitors blocked the tumoricidal action of DGLA on human cervical carcinoma, whereas anti-oxidants inhibited the cytotoxic action of DGLA on human breast cancer cells [124, 125]. These results suggested that the COX metabolism of DGLA may play a role in the anti-cancer effect of DGLA.

COX catalyzes AA and DGLA peroxidation to form PGE₂ and PGE₁, respectively. PGE₂ and PGE₁ are well-known lipid signaling molecules that participate in various physiological and pathological actions by activating the PKA signaling pathway through EP receptors. In general, PGE₂ and PGE₁ were believed to be associated with the opposing effects of AA vs. DGLA. However, the structures of PGE₂ and PGE₁ are similar, with PGE₁ only missing one double bond

in the structure. If both of them bind to the same receptors, it was hard to believe that PGE₂ and PGE₁ could exert opposing activities. In COX-catalyzed PUFA peroxidation, in addition to PGEs, several free radicals, the most reactive intermediate metabolites, were formed. However, due to their highly reactive nature, the individual free radicals have not been characterized in cells and the role of those novel free radical metabolites in cancer progression and prevention still remains a mystery. Our new method has allowed us to study the exclusive free radical products of COX/AA *vs.* COX/DGLA for the first time, which may open a new door to advancing COX biology.

In our previous results (Chapter 3), free radicals formed in common from COX/AA and COX/DGLA peroxidation and those formed exclusively from one or the other were identified and characterized in colon cancer cell HCA-7 colony 29. We further investigated the association between the individual free radicals and the contrasting bioactivity of AA *vs.* DGLA. In this chapter, we profiled free radical products derived from the cellular COX metabolism of AA and DGLA under normal cell growth conditions and tested their association and effects on cell growth. Our results suggested that the free radical metabolites may be a better indicator for the opposite effects of AA *vs.* DGLA on cancer cell proliferation than PGE₂ *vs.* PGE₁. DGLA may attenuate colon cancer cell proliferation *via* its exclusive free radical metabolites through COX metabolism, and regulating DGLA, and its metabolites in cells could be used as a new approach to controlling colon cancer cell growth.

4.2. Results and Discussion

4.2.1. Quantification of hydroxylamines as free radicals in a single dose of PUFA treatment

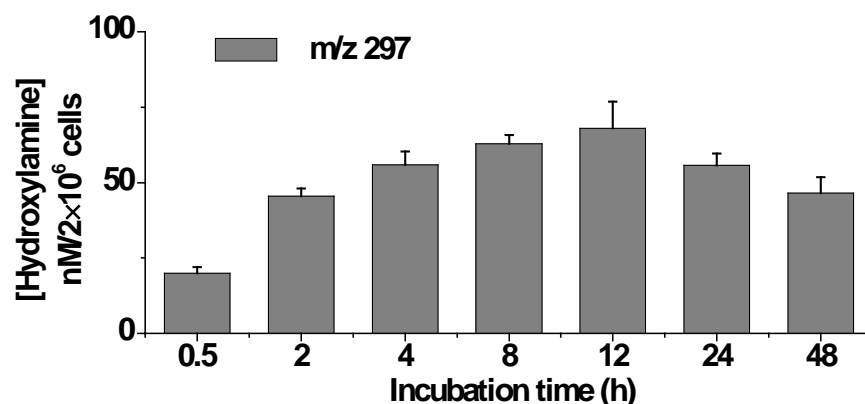
In order to find a possible association between free radical metabolites generated from COX-catalyzed PUFA peroxidation and cell growth, the time course of hydroxylamine (the

reduced form of POBN trapped radical adducts) formation was quantified for up to 48 h with d₉-POBN as an internal standard rather than a spin trap for radical identification. For this purpose, a small measured amount of d₉-POBN was added, but only after the mixture of cell culture medium and cell homogenate was mixed with ACN (1:1, v/v) to stop the peroxidation and spin-trapping reaction. The same amount of d₉-POBN was added to each sample and the concentration of each hydroxylamine was calculated by comparing their integrated peak areas in EICs to the peak area of the internal standard of d₉-POBN (m/z 204, t_R ≈ 3.6 min) with a known concentration at 2.0 μg/mL. The final concentrations of hydroxylamines were normalized to cell numbers and expressed as [hydroxylamines] per 2×10⁶ cells.

Hydroxylamines in cells treated with a single dose of AA: In cells treated with AA, the m/z 297 ion, as the reduced product of POBN/[•]C₆H₁₃O, was observed at all the time points (from 0.5 to 48 h). The concentration of the m/z 297 ion gradually increased and reached its peak concentration of ~ 68.0 nM at 12 h, then slightly decreased at 24 h and 48 h (Fig. 11A), possibly due to decreased POBN trapping ability after one day of the experiment. Before 8 h, the m/z 297 ion was the only hydroxylamine that was detected. The reduced product of POBN/[•]C₁₄H₂₁O₄, as the m/z 449 ion, was detected starting at 8 h (Fig. 11B). Its concentration increased from 8 to 12 h, followed by a decrease from 12 to 48 h. The peak concentration of the m/z 449 ion was ~ 7.0 nM, which was about 1/10 that of the m/z 297 ion.

Hydroxylamines in cells treated with a single dose of DGLA: In cells treated with DGLA, the m/z 297 ion was also observed from 0.5 to 48 h (Fig. 12A). From 0.5 to 12 h, its concentration increased to a peak of ~ 79.2 nM and decreased afterwards at 24 and 48 h. The reduced products of POBN/[•]C₇H₁₃O₂ and POBN/[•]C₈H₁₅O₃ as the m/z 325 and m/z 355 ions were observed at 8 h and clearly detected from 12 h to 48 h (Fig. 12B). At 24 h, the ions of m/z

A. Profile of common radical product from cells w/ AA



B. Profile of exclusive radical product from cells w/ AA

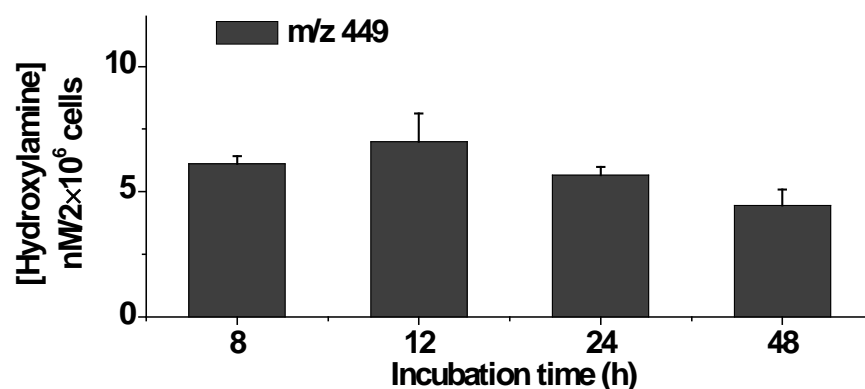
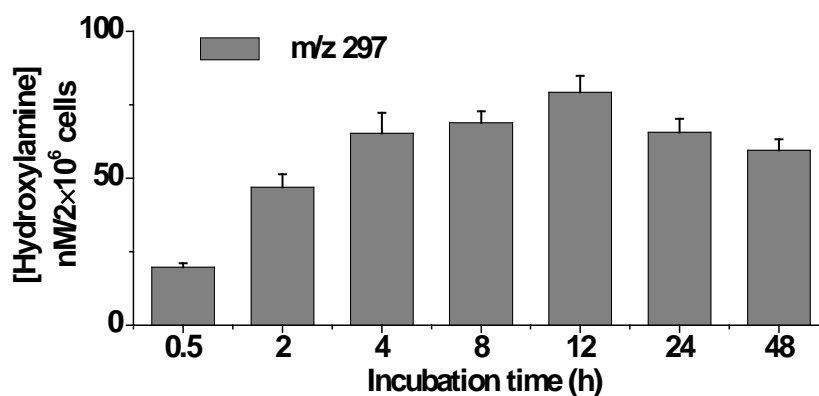


Fig. 11. Profiles of hydroxylamines with a single dose of AA treatment.

HCA-7 colony 29 cells were cultured under normal cell growth conditions for 0.5, 2, 4, 8, 12, 24 and 48 h in the presence of 20 mM POBN and 100 μ M AA. (A) Profile of common radical product (m/z 297) in cells treated with AA. (B) Profile of exclusive radical product (m/z 449) in cells treated with AA. Hydroxylamines were quantified with d₉-POBN (2 μ g/mL). Data are expressed as means \pm SD from n \geq 3.

325 and m/z 355 reached their peak concentrations at \sim 5.8 nM and 8.5 nM, respectively. The concentration of the m/z 325 ion did not show a significant difference from 12 h to 48 h. For the ion of m/z 355, there was a substantial increase from 12 h to 24 h and afterwards a decrease. Interestingly, the hydroxylamine of the m/z 449 ion (asterisked in Fig. 12B), which was the exclusive product from COX/AA peroxidation, was also observed in cells treated with DGLA. Its peak concentration (\sim 6.4 nM) was observed at 12 h.

A. Profile of common radical product from cells w/ DGLA



B. Profile of exclusive radical products from cells w/ DGLA

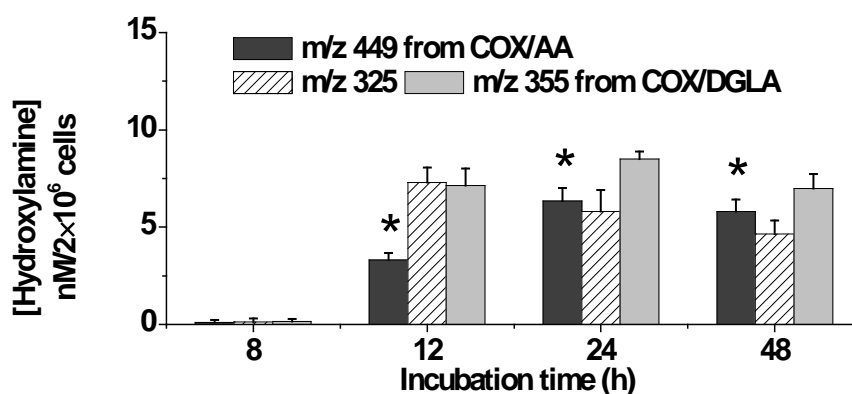


Fig. 12. Profiles of hydroxylamines with single dose of DGLA treatment.

HCA-7 colony 29 cells were cultured under normal cell growth conditions for 0.5, 2, 4, 8, 12, 24 and 48 h in the presence of 20 mM POBN and 100 μ M. (A) Profile of common radical product (m/z 297) in cells treated with DGLA. (B) Profiles of exclusive radical products (m/z 325 and m/z 355) in cells treated with DGLA. Hydroxylamines were quantified with d₉-POBN (2 μ g/mL). (*) m/z 449 was the exclusive radical product generated from COX/AA peroxidation. Data are expressed as means \pm SD from n \geq 3.

The concentration of the m/z 297 ion in cells treated with DGLA showed a trend similar to what we observed in cells treated with AA, but continued to become higher as the incubation time increased. At 0.5 and 2 h, the concentrations of the m/z 297 ion in COX/DGLA and COX/AA were at about the same level. From 4 to 48 h, it was higher in cells treated with DGLA. It is worth noticing that the peak concentration of the m/z 449 ion in cells treated with DGLA

was close to the level of that at 24 h and 48 h in cells treated with AA, which indicates a rapid conversion from DGLA to AA.

The most abundant hydroxylamine accumulated during a 48 h incubation in both the AA and DGLA treatments was the m/z 297 ion, whose concentration was about 10-fold greater than the m/z 449, m/z 325 and m/z 355 ions. In fact, in cell-free *in vitro* systems where ovine COX catalyzed AA and DGLA peroxidation [171, 173], the m/z 296 ion as POBN/ \bullet C₆H₁₃O was also the most abundant radical adduct in both reactions. It has been reported that the POBN adducts of the m/z 448 ion (POBN/ \bullet C₁₄H₂₁O₄) showed very low MS efficiencies compared to their ESR and UV detection during online separation due to the steric hindrance of protonation of the POBN. Similarly, the reduced product of POBN/ \bullet C₁₄H₂₁O₄ as the m/z 449 ion may have the same very low MS efficiencies as m/z 448.

In COX-catalyzed DGLA peroxidation, the free radicals were generated from two distinct pathways: C-15 oxygenation and C-8 oxygenation. The hydroxylamine, the m/z 297 ion as the reduced product of POBN/ \bullet C₆H₁₃O, was generated from the C-15 oxygenation pathway (Scheme 11), while the ions of m/z 325 and m/z 355, as the reduced products of POBN/ \bullet C₇H₁₃O₂ and POBN/ \bullet C₈H₁₅O₃, were generated from C-8 oxygenation (Scheme 11). However, which was the preferred DGLA peroxidation pathway was still unknown. The high abundance of the m/z 297 ion and the low abundance of the m/z 325 and m/z 355 ions suggest that maybe the C-15 oxygenation pathway is the preferred one. As a result, m/z 325 and m/z 355 will have accumulated more slowly than m/z 297 and would be detected later. Another reason for the low abundance of m/z 325 and m/z 355 was the rapid conversion of DGLA to AA in cells. COX competed with D5D for DGLA, and as the available substrate decreased, the radical formation would subsequently decrease.

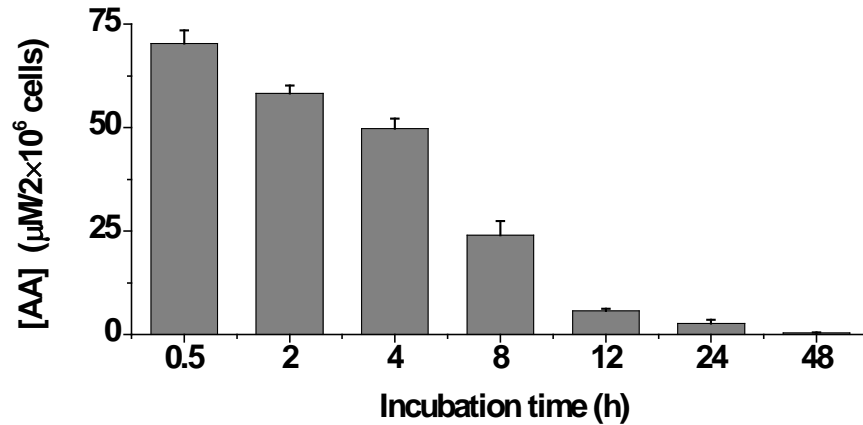
4.2.2. Profile of PUFAs and PGEs in a single dose of PUFA treatment

The presence of the hydroxylamine of the m/z 449 ion in the cellular spin-trapping experiment with a supplement of DGLA suggested that DGLA could be rapidly converted to AA in cells (by D5D). In order to verify our hypothesis and learn more about the metabolism of PUFA in cells, we used LC/MS to examine the time course of the concentrations of PUFAs and prostaglandins in cell culture medium after AA or DGLA treatment. The concentrations of AA, DGLA, PGE₂ and PGE₁ were quantified by the commercially available deuterated internal standards AA-d₃, DGLA-d₆, PGE₂-d₉ and PGE₁-d₄. The same amounts of internal standards with known concentrations were added to each sample and the concentrations of AA, DGLA, PGE₂ and PGE₁ were calculated according to the standard curves.

AA and PGE₂ in cells treated with a single dose of AA: When cells were incubated with AA, the concentration of AA in the cell culture medium gradually decreased in the first 4 h and significantly dropped at 8 h, almost reaching the control level after 24 h (Fig. 13A). In the meantime, a substantial production of PGE₂ was observed at 0.5 h, and the concentration of PGE₂ reached a peak at 8 h (~ 101.5 nM) and slightly decreased afterwards (Fig. 13B).

PUFAs and PGEs in cells treated with a single dose of DGLA: In the DGLA-treated cells, the trends of the uptake of DGLA and the formation of PGE₁ (Fig. 14) were similar to those observed in AA-treated cells. The uptake of DGLA was significantly higher at both 8 and 12 h and almost depleted in the medium at 48 h (Fig. 14A). The peak concentration of PGE₁ was ~ 81.3 nM at 8 h (Fig. 14B). As expected, AA was also detected in DGLA-treated cells and reached a peak (~ 4.0 nM) at 8 h (Fig. 14A), almost the same level as in AA-treatment at 12 h (Fig. 13A). The concentration of the metabolite of AA through COX metabolism, PGE₂, constantly increased from 0.5 to 48 h and the ratio of [PGE₁]:[PGE₂] decreased from ~ 1:6 to 1:1.

A. Profile of PUFA from cells treated w/ AA



B. Profile of PGE from cells treated w/ AA

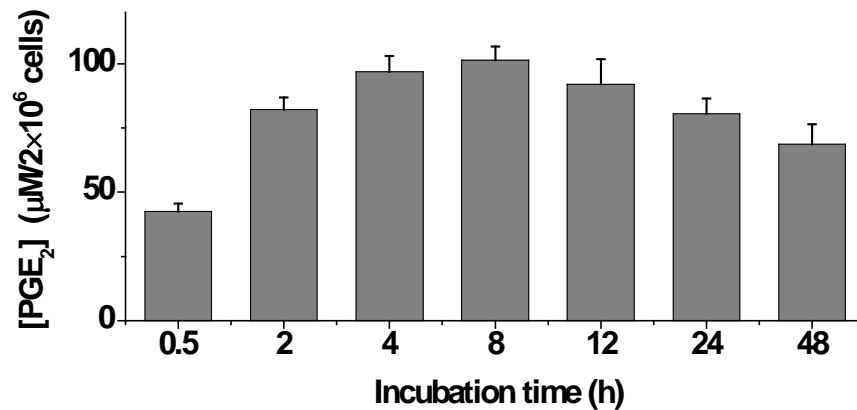
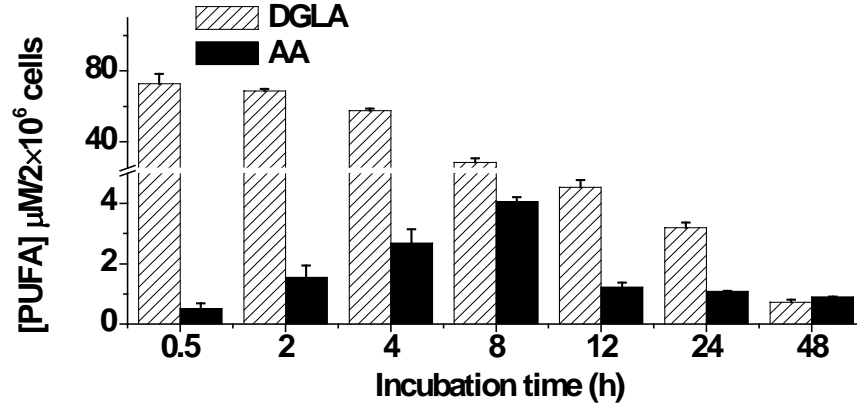


Fig. 13. Profiles of AA and PGE₂ with single doses of AA treatment.

HCA-7 colony 29 cells were cultured under normal cell growth conditions for 0.5, 2, 4, 8, 12, 24 and 48 h with a supplement of 100 μM of AA. (A) Profile of AA in cell culture medium, (B) Profile of PGE₂ in cell culture medium. AA and PGE₂ were quantified with the internal standards AA-d₈ and PGE₂-d₉, respectively. Data are expressed as means ± SD from n≥3.

A. Profile of PUFAs from cells treated w/ DGLA



B. Profile of PGEs from cells treated w/ DGLA

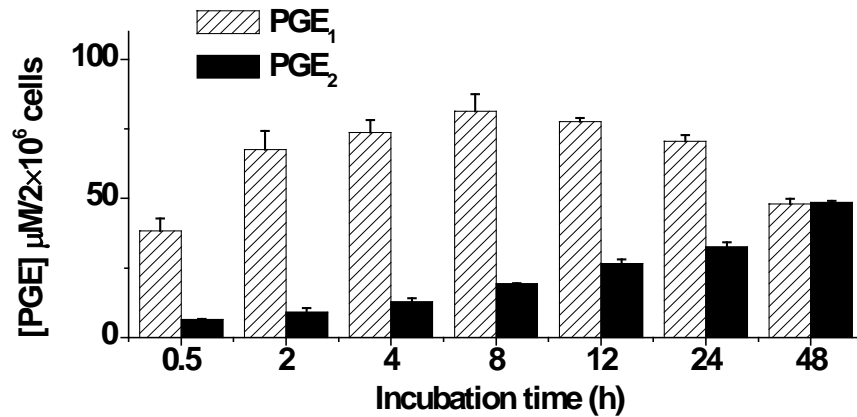


Fig. 14. Profiles of DGLA, AA, PGE₁ and PGE₂ with a single dose of DGLA treatment.

HCA-7 colony 29 cells were cultured under normal cell growth conditions for 0.5, 2, 4, 8, 12, 24 and 48 h with a supplement of 100 μM of DGLA. (A) Profiles of DGLA and AA in cell culture medium, (B) Profiles of PGE₁ and PGE₂ in cell culture medium. DGLA, AA, PGE₁ and PGE₂ were quantified with the internal standards DGLA-d₆, AA-d₈, PGE₁-d₄ and PGE₂-d₉, respectively. Data are expressed as means ± SD from n≥3.

The profiles of PUFAs in cell culture medium showed the rate of uptake of the exogenous PUFA by cells. The formation of PGEs as the end non-radical metabolites in COX-catalyzed PUFA peroxidation was closely related to the formation of the free radical metabolites and indicated the availability of the free fatty acid at the enzyme site in cells. The pattern of PGE formation was consistent with the formation of the free radical metabolites in this study. The significant drop of both AA and DGLA in the cell medium was observed at 8 h and 12 h, and the

maximum production of PGEs also occurred at 8 h. As observed in the time course of hydroxylamine formation, 8 h and 12 h are two critical time points at which the hydroxylamines reached their peak concentrations or started to show up.

In DGLA-treated cells, the detection of AA and PGE₂ confirmed the conversion from DGLA to AA. The appearance of AA in the cell culture medium was probably due to the diffusion of the free fatty acid through the membrane. Although AA concentration peaked at 8 h and decreased afterwards, there was a steady increase in PGE₂ up to 48 h. The production of PGE₂ did not decrease after 8 h but kept increasing, suggesting that the DGLA continuously converted to AA with the maximum conversion occurring at 8 h, and AA (converted from DGLA) even reached the same level as in the AA-treatment at 12 h.

The exogenous PUFA could be esterified into the phospholipid of the cell membrane. Due to the high concentration of PUFAs in the cell culture medium, the exogenous PUFA could also diffuse into the cells without being incorporated into the cell membrane. According to the results, the dramatic drop of AA and DGLA in the cell culture medium suggested that more than 90% of the uptake of the supplemental AA and DGLA was achieved by 12 h, which meant at 12 h, all the exogenous PUFA was either incorporated into the cell membrane's phospholipids or diffused into the cells as the free fatty acid. Those free AA and DGLA were subsequently metabolized to their corresponding metabolites (including PGEs and the free radical metabolites). The free DGLA also served as the substrate of D5D (the enzyme converting DGLA to AA) and was continuously converted to AA. As the pool of exogenous PUFA was exhausted at 12 h, the formation of PUFA-derived metabolites started to decrease (not increasing due to the decreased POBN trapping ability) because now the source of PUFA came from the membrane's

phospholipids and needed to be released into the cells as the free acid formed by the action of cPLA₂.

4.2.3. Effect of PUFAs on cell proliferation and cell cycle distribution

We have successfully characterized and profiled the common and exclusive free radical products generated from COX/AA and COX/DGLA peroxidation in HCA-7 colony 29 cells. In order to make a possible association between these novel free radical metabolites and the opposing bioactivity of AA vs. DGLA, first of all, the effects of PUFA on the proliferation of HCA-7 colony 29 were evaluated *via* the MTS assay.

The effect of AA or DGLA on cell growth was evaluated *via* the MTS assay. After a 48 h incubation, the cells supplemented with AA showed a slight increase in cell proliferation compared to the control treatment (Table 3). The DGLA-treated cells showed a similar pro-proliferation effect (Table 3), which was expected as we hypothesized. The DGLA should exhibit an inhibitory effect on cell growth compared to AA, but the constant conversion from DGLA to AA may abolish this effect because of the pro-proliferation effect of the exclusive AA-derived free radical metabolites ($\bullet\text{C}=\text{C}$).

Table 3. Effect on cell proliferation and cell cycle distribution from PUFAs.

HCA-7 Colony 29 treated w/	Cell Cycle Distribution				Cell Proliferation
	% in G ₁ Phase		% in G ₂ /M Phase		% viability
	8 h	24 h	8 h	24 h	48 h
Control (0.1 % ethanol)	37.4 ± 2.4	41.3 ± 3.5	22.1 ± 1.2	20.9 ± 0.9	100
AA (100 μM)	40.2 ± 7.2	41.6 ± 3.8	22.3 ± 2.7	23.8 ± 2.1	112.1* ± 3.9
DGLA (100 μM)	43.6* ± 9.6	42.7 ± 2.3	29.4* ± 2.1	23.6 ± 1.6	109.1* ± 5.7

HCA-7 colony 29 cells treated with 0.1% ethanol, 100 μM AA or 100 μM DGLA. Data represent the mean ± SD derived from three separate experiments with triplicate wells per condition. Cell viability (%) was compared with the control group. Control cells were incubated with 0.1% ethanol (final concentration). (*) P<0.01, significantly different from control.

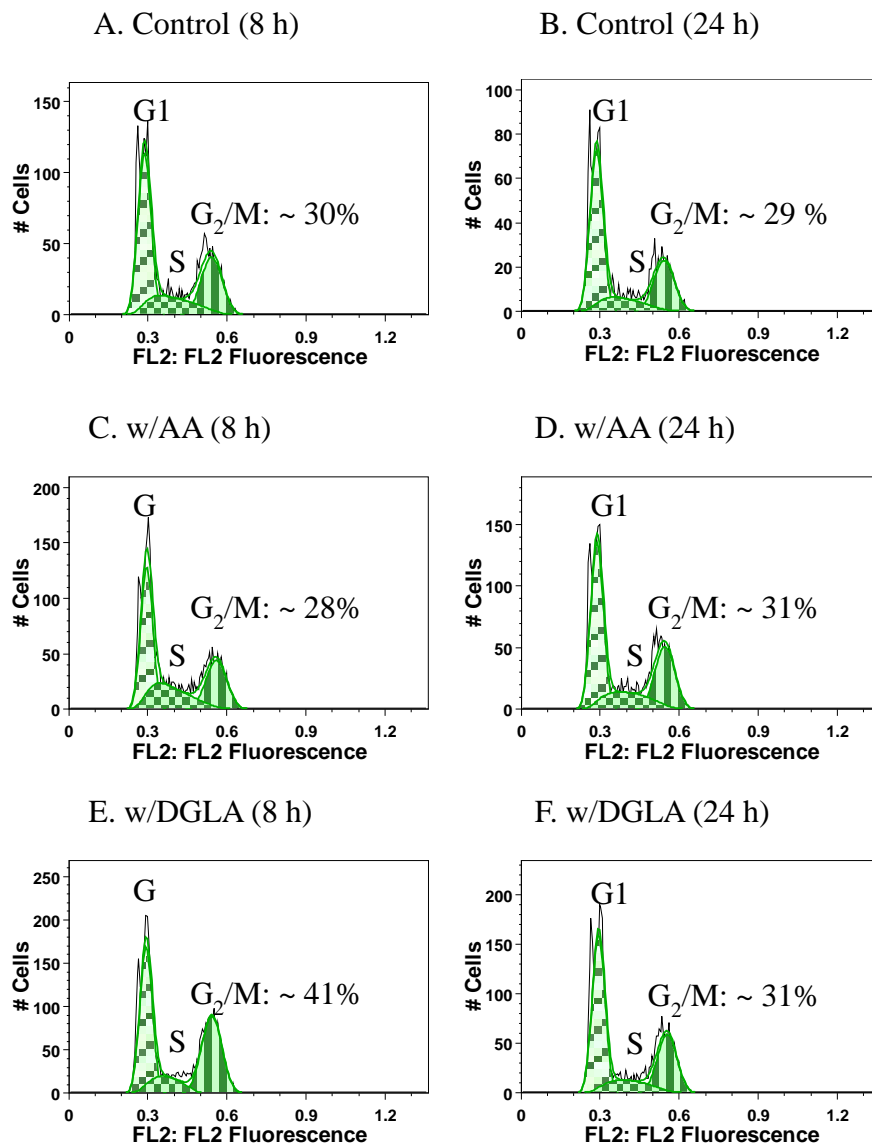


Fig. 15. Effect of PUFA on cell cycle distribution.

(A-B) HCA-7 colony 29 cells were treated with 0.1% ethanol for 8 and 24 h, respectively, (C-D) HCA-7 colony 29 cells were treated with 100 μ M AA for 8 and 24 h, respectively, (E-F) HCA-7 colony 29 cells were treated with 100 μ M DGLA for 8 and 24 h, respectively.

To further confirm our hypothesis, PI staining was performed to evaluate the effects of AA and DGLA on cell cycle distribution at 8 and 24 h (Table 3 and Fig. 15). At 8 h, when most of the DGLA was not converted to AA, cells treated with DGLA induced a significant cell G₂/M phase arrest (~ 40% compared to control and AA-treated cells ~ 30% Table 3). The DGLA mediated G₂/M phase cell cycle arrest was accompanied by a G₁ delay (Table 3). However, both

G₁ and G₂/M arrests were almost completely recovered at 24 h as AA accumulated in cells and competed with DGLA for the COX to form the pro-proliferative metabolites.

The G₂/M checkpoint is an important cell cycle checkpoint that insures that cells do not initiate mitosis before they have a chance to repair damaged DNA after replication. Several mechanisms have been reported whereby free radicals could cause various DNA damage, such as oxidized bases, abasic sites, DNA-DNA intrastrand adducts, DNA strand breaks and DNA-protein cross-links [197, 198]. In addition, substantial evidence suggests that the highly reactive free radicals could cause DNA lesions that up-regulate the apoptotic genes p53 and p21 to induce cell apoptosis [199, 200]. The increased p53 was correlated to the accumulation of G₂/M arrest in cells [201-203]. Thus a possible mechanism for the inhibitory effect of DGLA-derived free radical metabolites is through the activation of the tumor suppressor p53.

4.2.4. Comparison of effects of free radical metabolites and PGEs on cell growth

The effect of PGEs on cell growth was also evaluated since PGEs are the most studied COX metabolites, which are believed to be involved in regulating cancer cell growth through the down-stream signaling pathways. Cells were treated with PGE₂ and PGE₁ at the same concentration as that of the radical derivatives. However, as shown in Fig. 16, both PGE₂ and PGE₁ slightly increased cell proliferation compared to the control treatment, with little difference as the concentration increased. As the concentration of PGE₂ increased from 0.01 to 1 μM, the cell viability increased by ~8.4%, while for PGE₁, the cell viabilities were not significantly altered at any of the three concentrations (Fig. 16).

It was surprising that the PGE₁, which was considered to be the anti-inflammatory PGE, not only did not inhibit colon cancer cell growth as reported [70, 186], but on the contrary, promoted proliferation in HCA-7 colony 29 cells. PGE₁ has been used to treat chronic

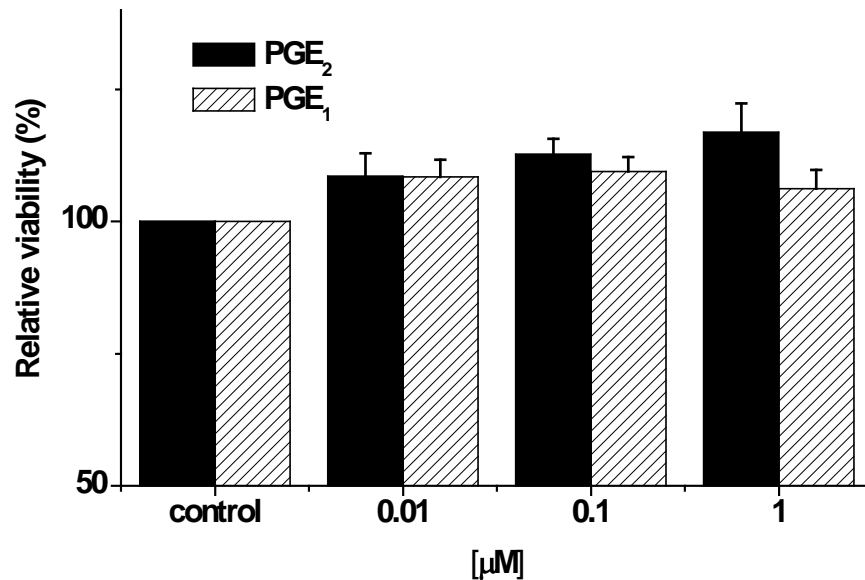


Fig. 16. Effect of PGEs on colon cancer cell growth.

HCA-7 colony 29 cells were treated with PGEs at concentrations of 0.01, 0.1 and 1 μM for 48 h. Data represent the mean ± SD derived from three separate experiments with triplicate wells per condition. Cell viability (%) was compared with a control group. Control cells were incubated with 0.1% ethanol (final concentration).

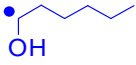
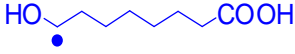
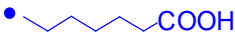
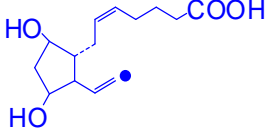
inflammatory diseases in vascular tissues. An increase in PGE₁ might contribute to the attenuation of the development of atherosclerosis *via* the inhibition of the adhesion molecules in vascular smooth muscle cells and endothelial cells [76]. Increasing evidence suggested that PGE₁ also possesses anti-cancer activity; it was able to inhibit cancer cell growth *in vitro*. A high dose of PGE₁ (30 μg/mL) inhibited the proliferation of HeLa cells [185]. The proliferative activity of murine B16-F10 melanoma cells was found to be particularly affected by PGE₁: B16-F10 cells' proliferation decreased by about 40% after 48 and 72 h of treatment with 10 μg/mL of PGE₁ [70]. PGE₁ only showed this inhibitory effect at a high concentration (more than 10 μg/mL), while a low dose of PGE₁ (3 μg/mL) may fail to alter cell proliferation or even increase cell growth [185]. That would explain why PGE₁ did not show an inhibitory effect on cell growth in HCA-7 colony 29 cells. According to our results in the cell proliferation assay, the highest dose of PGE₁ used to treat HCA-7 colony 29 cells was 1 μM, which equals ~0.35 μg/mL, much lower than the

effective concentration for inhibition. Our results were also consistent with the observations in [185] that a lower concentration of PGE₁ increased cell proliferation, although the underlying mechanism was not yet clear. However, under physiological conditions, the level of PGE₁ could never achieve a concentration as high as 1 μM. In our results (Fig. 14), the highest concentration of PGE₁ with a direct treatment of 100 μM of DGLA was only around 0.1 μM.

The same issues were raised in the research targeting the pro-proliferation effect of PGE₂. The elevated COX-2 expression observed in colon cancer cells resulted in a high concentration of AA-derived PGs, in particular PGE₂. PGE₂ has been shown to stimulate the growth of cancer cells. The growth of the colon cancer cells (HT-29) was stimulated by a range of PGE₂ concentrations (from 0.1 up to 10 μM), *e.g.*, PGE₂ (0.5 μM) increased cell yield by ~19% over control levels and cell numbers were ~45% greater than control levels with 10 μM PGE₂ [204]. The cell growth increased as the level of PGE₂ increased. In addition, the expression of vascular endothelial growth factor, one of the major regulators for angiogenesis, was induced by PGE₂ at a concentration of 0.5 μM in LS-174T cells [205], suggesting that PGE₂ signaling may exert pro-oncogenic actions that play a critical role in colorectal carcinogenesis. However, the concentration of PGE₂ that was used in those experiments was higher than what could be achieved under physiological conditions.

In order to detect a possible association between these novel free radical metabolites and the opposing bioactivity of AA *vs.* DGLA, the effects of free radical metabolites on the proliferation of HCA-7 colony 29 were evaluated *via* the MTS assay. Because PUFA-derived free radicals cannot be synthesized in order to test them on cells due to their very short lifetimes, various concentrations (from 0.01 to 1 μM) of the selected derivatives of free radicals (the corresponding alcohol form) were used to assess their effect on colon cancer cell proliferation.

Table 4. The tested free radical derivatives (metabolites).

Radical Derivatives	Radicals	Resources
1-Hexanol		C-15 oxygenation of COX/AA & COX/DGLA
8-Hydroxyoctanoic acid		C-8 oxygenation of COX/DGLA
Heptanoic acid		C-8 oxygenation of COX/DGLA
To be made and studied		C-15 oxygenation of COX/AA

The corresponding derivatives of $\bullet\text{C}_6\text{H}_{13}\text{O}$, $\bullet\text{C}_7\text{H}_{13}\text{O}_2$ and $\bullet\text{C}_8\text{H}_{15}\text{O}_3$ were hexanol, heptanoic acid and 8-hydroxyoctanoic acid, respectively (Table 4). The $\bullet\text{C}_6\text{H}_{13}\text{O}$ was the common free radical that was observed in both COX/AA and COX/DGLA peroxidation, and the corresponding spin adduct was m/z 296 (POBN/ $\bullet\text{C}_6\text{H}_{13}\text{O}$). Two more free radicals, $\bullet\text{C}_7\text{H}_{13}\text{O}_2$ and $\bullet\text{C}_8\text{H}_{15}\text{O}_3$, were exclusive free radical metabolites from COX/DGLA and corresponded to the spin adducts of m/z 324 (POBN/ $\bullet\text{C}_7\text{H}_{13}\text{O}_2$) and m/z 354 (POBN/ $\bullet\text{C}_8\text{H}_{15}\text{O}_3$). Among the three radical derivatives, both hexanol and 8-hydroxyoctanoic acid inhibited cell proliferation at concentrations from 0.01 to 1.0 μM , while 8-hydroxyoctanoic acid had the most inhibitory effect (decreasing the cell viability to $\sim 80\%$ compared to the control group) and the hexanol had a moderately inhibitory effect (Fig. 17). The heptanoic acid did not inhibit cell proliferation (Fig. 17).

Among the four types of free radicals that were characterized and profiled in both COX/AA and COX/DGLA peroxidation, the derivatives of $\bullet\text{C}_6\text{H}_{13}\text{O}$, $\bullet\text{C}_7\text{H}_{13}\text{O}_2$ and $\bullet\text{C}_8\text{H}_{15}\text{O}_3$ were tested on cell growth *via* the MTS assay (Fig. 17). The only one not tested was the exclusive radical $\bullet\text{C}=\text{C}$ ($\bullet\text{C}_{14}\text{H}_{21}\text{O}_4$) from COX/AA peroxidation. The $\bullet\text{C}_{14}\text{H}_{21}\text{O}_4$ radical does not have commercially available derivatives. We believed that this special radical should be

closely related to the pro-carcinogenic effect of AA. The radical derivative of $\bullet\text{C}_{14}\text{H}_{21}\text{O}_4$ will be synthesized and studied for its potential role on colon cancer cell growth in the future.

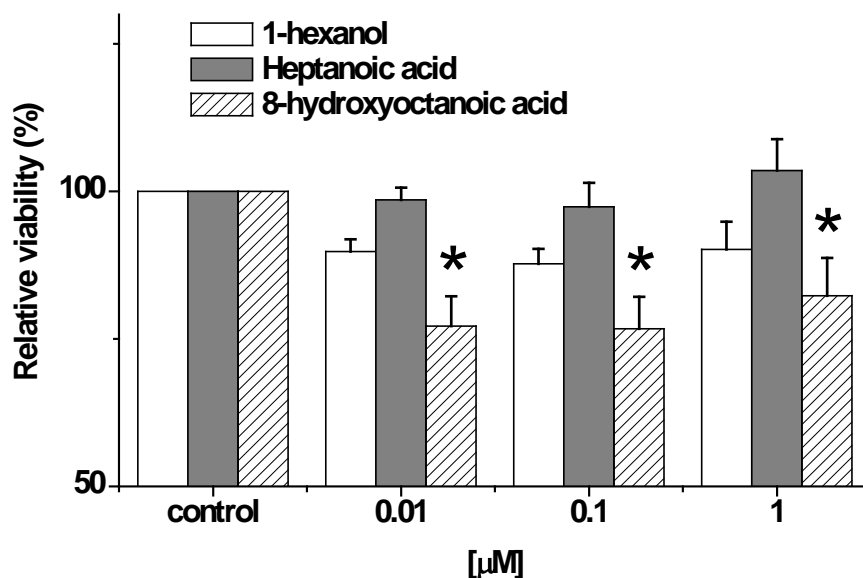


Fig. 17. Effect of free radical derivatives on colon cancer cell growth.

HCA-7 colony 29 cells were treated with free radical derivatives at concentrations of 0.01, 0.1 and 1.0 μM for 48 h. 1-hexanol was derived from $\bullet\text{C}_6\text{H}_{13}\text{O}$. Heptanoic acid was derived from $\bullet\text{C}_8\text{H}_{15}\text{O}_3$. 8-hydroxyoctanoic acid was derived from $\bullet\text{C}_7\text{H}_{13}\text{O}_2$. Data represent the mean \pm SD derived from three separate experiments with triplicate wells per condition. Cell viability (%) was compared with the control group. Control cells were incubated with 0.1% ethanol (final concentration). (*) $P < 0.01$, significantly different from control.

The exclusive free radicals generated from COX-catalyzed DGLA showed an inhibitory effect on colon cancer cell growth, while we believed that the exclusive free radicals ($\bullet\text{C}=\text{C}$) generated from COX-catalyzed AA should have the opposite effect. Because the effect of the $\bullet\text{C}=\text{C}$ on cell growth was not able to be tested due to the lack of corresponding derivatives, we tested the effect of the precursor instead. We had proved that the PUFA-derived free radical metabolites rather than PGEs were the critical player in the proliferation of colon cancer cell growth. Thus, if AA and DGLA exerted different effects on colon cancer cell growth, the difference should be attributed to their exclusive free radical metabolites.

Among the tested free radical derivatives, those from the exclusively DGLA-derived free radicals showed an inhibitory effect on HCA-7 colony 29's growth, while the PGE₁ did not. Taken together, our results suggest that these free radical metabolites may play a more important role in regulating colon cancer cell growth than PGEs.

4.2.5. Study of double doses of PUFA treatment

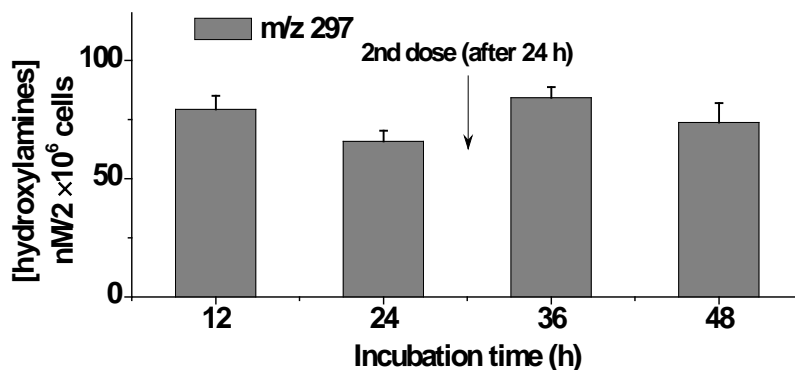
DGLA has a potential inhibitory effect on colon cancer cell growth *via* free radical metabolites through COX peroxidation. But the rapid conversion from DGLA to AA in cells decreased the DGLA levels while concurrently increasing AA levels, which abolished the inhibitory effect of DGLA on cell growth as shown in Table 3. We expected that the increased availability of DGLA in cells after a second dose would subsequently increase DGLA-derived radicals and restore the inhibitory effect of DGLA on cell growth.

In order to determine the formation of free radical products after the second dose of PUFA was introduced, radical formation with double doses of PUFA treatment was profiled, with the second dose administered 24 h after the first. The concentrations of hydroxylamines after the second dose were profiled at 36 and 48 h, which was equivalent to the time points of 12 and 24 h after the first dose.

Hydroxylamines in cells treated with double doses of DGLA: In cells treated with double doses of DGLA, the common ion of m/z 297 as the reduced adduct of POBN/[•]C₆H₁₃O and the exclusive ions of m/z 325 and m/z 355 from COX/DGLA as the reduced adducts of POBN/[•]C₇H₁₃O₂ and POBN/[•]C₈H₁₅O₃, respectively, all increased at 36 and 48 h after the introduction of the second dose compared to that at 12 and 24 h (Fig. 18). There was a small increase in the concentrations of the m/z 297 ions from ~ 79.2 nM at 12 h to 84.1 nM at 36 h and from 65.7 nM at 24 h to 73.6 nM at 48 h (Fig. 18A). The concentrations of the m/z 325 ions

increased by about 25 % from ~7.8 nM at 12 h to 9.8 nM at 36 h and by about 40% from 8.6 nM at 12 h to 12.2 nM at 24 h (Fig. 18B). The concentrations of the m/z 355 ions increased substantially, by around 83% from ~7.1 nM at 12 h to 13.0 nM at 36 h, but at 24 and 48 h the levels stayed about the same (12.4 and 13.8 nM, respectively, Fig. 18B).

A. Profile of common radical product w/ double doses of DGLA



B. Profile of exclusive radical products w/ double doses of DGLA

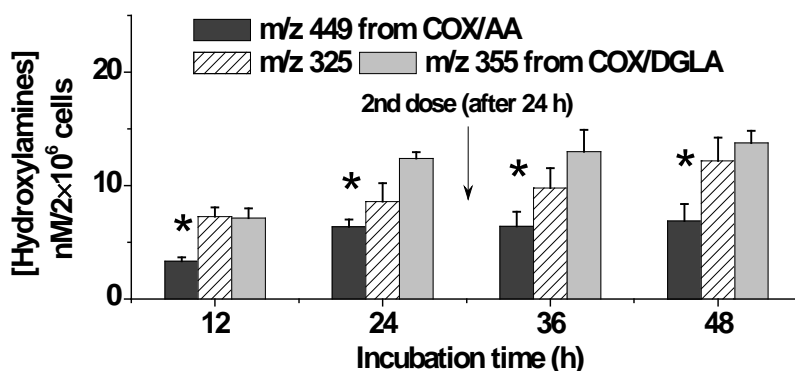


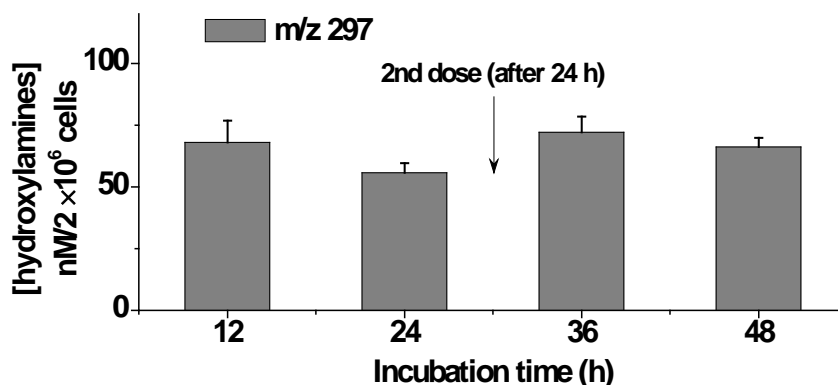
Fig. 18. Profile of hydroxylamines with double doses of DGLA treatment.

HCA-7 colony 29 cells were treated with 100 μ M of DGLA for 24 h and the second dose was added after another 24 h of incubation. The hydroxylamines were profiled at 12, 24, 36 and 48 h. (A) Profile of common radical product (m/z 297) in cells treated with DGLA. (B) Profile of exclusive radical products in cells treated with DGLA. The exclusive radical products in COX/DGLA peroxidation were m/z 325 and m/z 355. Hydroxylamines were quantified with d_9 -POBN. (*) m/z 449 was the hydroxylamine generated from COX/AA peroxidation. Data are expressed as means \pm SD from $n \geq 3$.

Hydroxylamines in cells treated with double doses of AA: In cells treated with double doses of AA, there was a slight increase in the hydroxylamine of the m/z 297 ion (the reduced

adduct of POBN/ \bullet C₆H₁₃O) at 36 and 48 h (~72.1 and 66.1 nM) as compared to those observed at 12 and 24 h (~68.0 and 55.8 nM) (Fig. 19A). The m/z 449 ion as the reduced adduct of POBN/ \bullet C₁₄H₂₁O₄ showed a slight increase at 36 h compared to 12 h (from ~7.0 to 8.0 nM) and had accumulated much more at 48 h (around a 50% increase) than at 24 h (from ~5.7 to 8.7 nM) (Fig. 19B).

A. Profile of common radical product w/ double doses of AA



B. Profile of exclusive radical product w/ double doses of AA

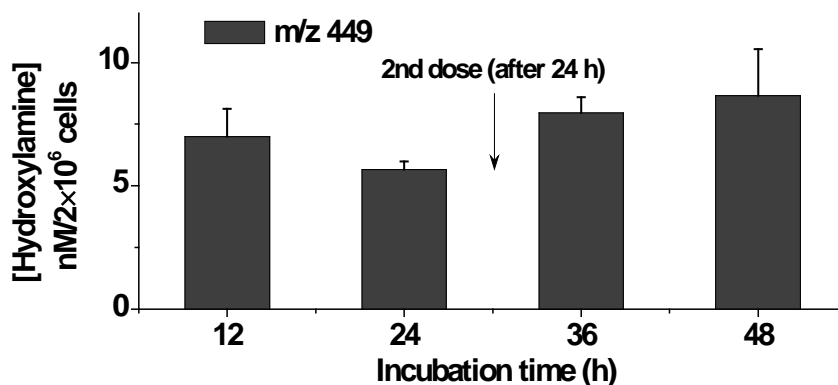


Fig. 19. Profile of hydroxylamines with double doses of AA treatment.

HCA-7 colony 29 cells were treated with 100 μ M of AA for 24 h and the second dose was added after 24 h incubation. The hydroxylamines were profiled at 12, 24, 36 and 48 h. (A) Profile of common radical product (m/z 297) in cells treated with AA. (B) Profile of exclusive radical product (m/z 449) in cells treated with AA. Data are expressed as means \pm SD from $n \geq 3$.

In cells treated with double doses of DGLA, the trend of the m/z 297 ion's formation was similar to that observed in cells treated with AA. Most interestingly, the exclusive free radical

product of m/z 449 from COX/AA peroxidation remained at the same level after the second dose of DGLA as compared to that at 12 and 24 h (Fig. 18B), suggesting that the increased DGLA in cells indeed competed with AA for COX and suppressed the formation of AA-derived pro-proliferation free radical metabolites, while at the same time it increased the formation of the DGLA-derived anti-proliferation free radical metabolites.

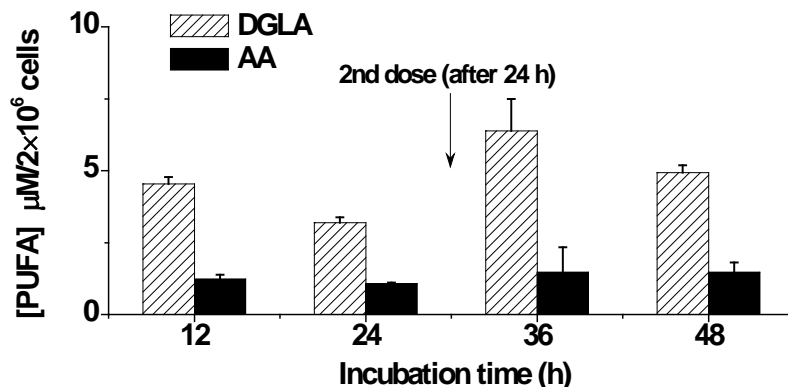
We have observed in the single dose PUFA treatments that both the formation of free radical metabolites and the PGEs decreased from 12 to 24 h (Figs. 11-14). These decreases were assumed to be due to the decreased pool of free fatty acids in cells. In the double dose PUFA treatment, it is worth noticing that at 36 and 48 h, equivalent to the time points of 12 and 24 h after the first dose, the free radical metabolites were increased rather than decreased. To address this interesting outcome, we profiled the PUFA and PGEs in the double dose treatment.

PUFAs and PGEs in cells treated with double doses of DGLA: After the second dose was introduced, the concentration of AA was a little bit higher at 36 h and 48 h compared to that at 12 h and 24 h (Fig. 20A). Due to the conversion from DGLA to AA, a very small increase in the concentration of AA was observed. Compared to the small increase of the concentration of PGE₂, the production of PGE₁ increased significantly after the second dose to ~ 123.4 nM at 48 h (Fig. 20B), which successfully brought the ratio of [PGE₁]:[PGE₂] up to around 3:1 from the 1:1 ratio we observed in the single dose treatment at 48 h (Fig. 20B).

AA and PGE₂ in cells treated with double doses of AA: The profiles of AA and PGE₂ in the cell culture medium with double doses of AA are shown in Fig. 21. When the second dose of AA was introduced to the cell culture 24 h after administration of the first dose, the uptake pattern of AA was similar to the one we observed in treatment with double doses of DGLA (Fig. 21A).

For the generation of PGE₂, the second dose of AA continued to increase the production of PGE₂ up to the peak concentration at ~ 144.8 nM after 48 h (Fig. 21B).

A. Profile of PUFAs from cells treated w/ double doses of DGLA



B. Profile of PGEs from cells treated w/ double doses of DGLA

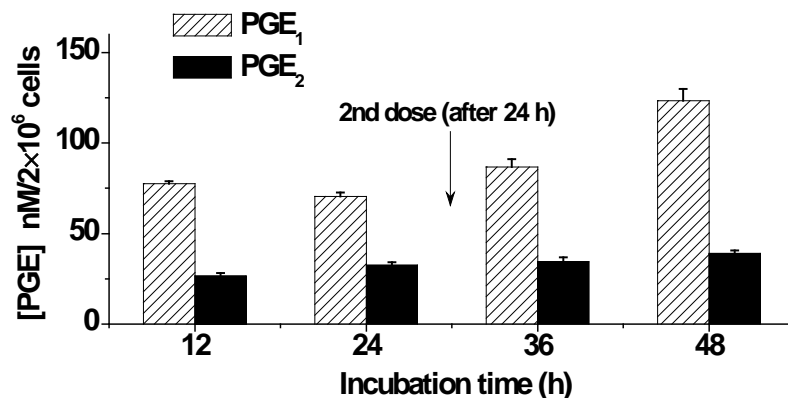
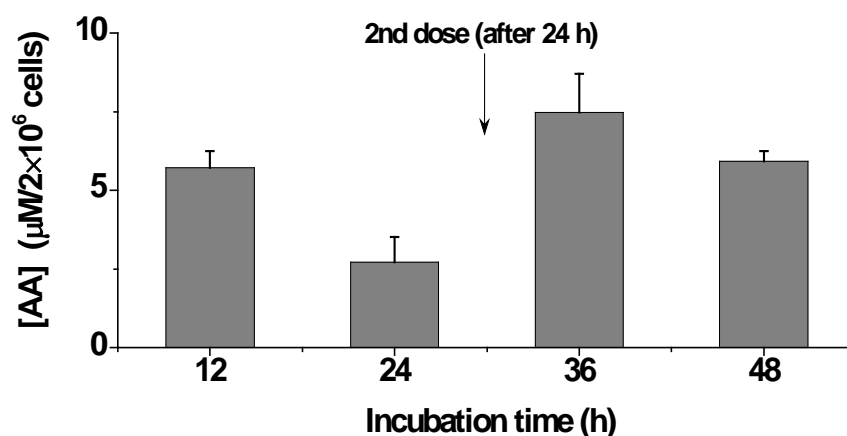


Fig. 20. Profile of DGLA, AA, PGE₁ and PGE₂ with double doses of DGLA treatment.

HCA-7 colony 29 cells were treated with 100 μM of DGLA for 24 h, with the second dose added after a 24 h incubation. The levels of AA and DGLA, as well as their metabolites PGE₁ and PGE₂, were evaluated after 12, 24, 36 and 48 h. (A) Profiles of DGLA and AA in cell culture medium, (B) Profiles of PGE₁ and PGE₂ in cell culture medium. DGLA, AA, PGE₁ and PGE₂ were quantified with the internal standards DGLA-d₆, AA-d₈, PGE₁-d₄ and PGE₂-d₉, respectively. Data are expressed as means ± SD from n≥3.

A. Profile of AA from cells treated w/ double doses of AA



B. Profile of PGE₂ from cells treated w/ double doses of AA

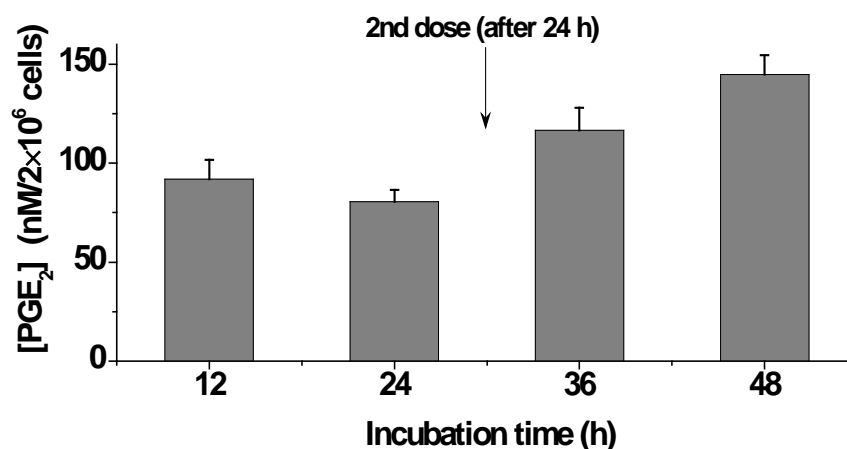


Fig. 21. Profiles of AA and PGE₂ with double doses of AA treatment.

HCA-7 colony 29 cells were treated with 100 μM of AA for 24 h and the second dose was added after a 24 h incubation. The levels of AA and PGE₂ were evaluated after 12, 24, 36 and 48 h. (A) The concentration of AA in cell culture medium; (B) The concentration of PGE₂ in cell culture medium. AA and PGE₂ were quantified with the internal standards AA-d₈ and PGE₂-d₉, respectively. Data are expressed as means \pm SD from $n \geq 3$.

The formation of PGEs verified the formation of the free radical metabolites in the double dose-PUFA treatment. In cells treated with double doses of AA, the peak concentrations of PGE₂ (Fig. 21B) and the exclusive free radical product of $\bullet\text{C}_{14}\text{H}_{21}\text{O}_4$ from COX/AA (Fig. 19B) were observed at 48 h. Similarly, the peak concentrations of PGE₁ (Fig. 20B) and the exclusive free radical products of $\bullet\text{C}_7\text{H}_{13}\text{O}_2$ and $\bullet\text{C}_8\text{H}_{15}\text{O}_3$ from COX/DGLA (Fig. 18B) were observed at

48 h in cells treated with double doses of DGLA. The large amount of available DGLA overwhelmed AA at the COX site in cells, thus increasing the DGLA-derived metabolites (including the anti-proliferation free radical metabolites and the non-radical PGE₁) and suppressing the formation of AA-derived metabolites (including the pro-proliferation free radical metabolites and PGE₂).

Comparison of effects of single dose vs. double doses of PUFA treatment on cell growth:

The effect of double doses of AA and DGLA was also evaluated *via* the MTS assay. DGLA showed an inhibitory effect on cell proliferation compared to AA (Fig. 22). Compared to the single dose treatment, double doses of DGLA decreased cell proliferation. The cell viability decreased from 109.0 % to 102.5 % (Fig. 22). On the other hand, double doses of AA significantly increased cell proliferation (the cell viability was increased from 112.4 % to 132.9 %, Fig. 22).

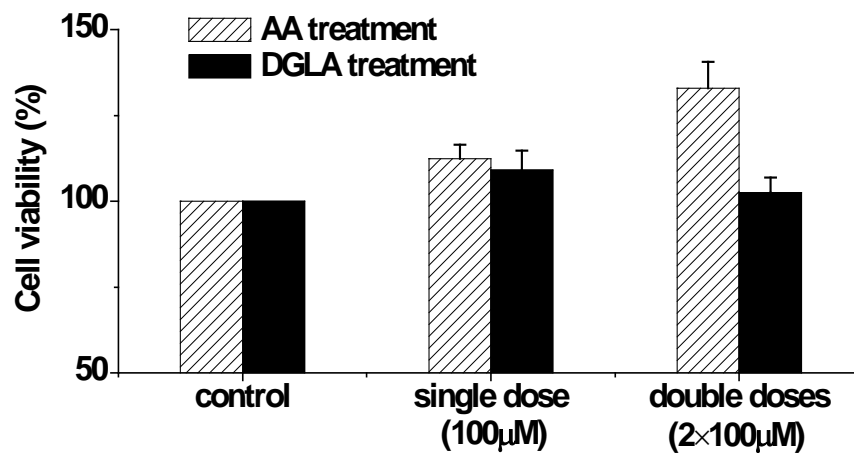


Fig. 22. Effects of single dose vs. double dose treatment of DGLA or AA on cell proliferation.

HCA-7 colony 29 cells were treated with a single dose (100 μM) or double doses (2 × 100 μM) of DGLA or AA for 48 h. Data represent the mean ± SD derived from three separate experiments with triplicate wells per condition.

It was the increased ratio between [DGLA-derived free radical metabolites] *vs.* [AA-derived free radical metabolites] that resulted in the anti-proliferation effect of the double doses

of DGLA compared to AA as observed in the MTS assay (Fig. 22). Our results suggest that the double dose DGLA treatment controlled the conversion of DGLA to AA. When DGLA was increased, cells benefited from the elevated ratio of [DGLA-derived free radical metabolites]/[AA-derived free radical metabolites], which exerted an anti-proliferation effect on HCA-7 colony 29 cells. However, this increased ratio was due only to the increase of DGLA-derived free radical metabolites (Fig. 18B), as the AA-derived free radical metabolites maintained the same level (Fig. 18B) after the second dose of DGLA was introduced.

In this chapter, common and exclusive free radicals as the reduced forms were profiled for up to 48 h in COX-catalyzed AA vs. DGLA peroxidation in cells. AA, DGLA, free radical derivatives and prostaglandins were tested for their effects on the cellular growth response. Among the tested compounds, rather than PGE₁, the derivative corresponding to a DGLA-derived exclusive free radical (8-hydroxyoctanoic acid) showed the most inhibitory effect on cell growth. Thus, the anti-proliferative effect of DGLA was associated with the DGLA-derived exclusive free radicals metabolites.

To increase the level of the anti-proliferative DGLA-derived free radical metabolites, double doses of DGLA were used to increase the level of DGLA in cells to compete with AA for COX. However, as shown in Fig. 22, although the double doses of DGLA treatment decreased cell proliferation compared to the single dose treatment, the cell growth was still not inhibited compared to the control group (0.1% ethanol). Thus, the approach of increasing the DGLA concentration in cells was not enough to fully restore the anti-proliferative effect of DGLA. Thus, other options that can reciprocally regulate the level of DGLA and AA in cells should be considered.

CHAPTER 5. INHIBITION OF THE CONVERSION FROM DGLA TO AA ATTENUATED CANCER CELL GROWTH AND ENHANCED THE EFFICACY OF A CHEMOTHERAPY DRUG

5.1. Introduction

Identification of factors that modulate tumorigenesis is crucial in cancer prevention and treatment. Most cancer drug discovery studies have tried to target cell proliferation, using cell-based screening systems to identify anti-cancer compounds. However, the translation of such discoveries into cancer therapy has had limited success [206, 207]. Current research shows that targeting lipid metabolism or related factors that modulate the tumor microenvironment may also be a promising approach for cancer therapy [208, 209].

AA is the major ω -6 PUFA in tissues and is converted from DGLA in our body by D5D (Scheme 1). It is generally accepted that of the COX metabolism products, AA-derived eicosanoids such as PGs₂ promote cancer growth by activating the down-stream pro-carcinogenic signaling pathways [181-183]. Given the importance of AA metabolites in cancer biology, many studies have focused on the biosynthesis and degradation enzymes to suppress the tumorigenic effects of AA-derived eicosanoids [210]. COX-2 has been considered to be a target enzyme in cancer therapy, and several COX inhibitors have been developed and used in treatments for colon cancer [211, 212]. Although some of these drugs targeting eicosanoid signaling, such as aspirin and celecoxib, have shown efficacy in suppressing cancer, they have also been associated with severe toxicity during the treatment of cancer [210, 213]; thus, other strategies must be identified to target AA metabolism. The role in tumorigenesis of endogenous AA production, which occurs upstream of the COX pathway (Scheme 1), remains unexplored.

One way of modulating PG biosynthesis and tumor development may be decreasing AA levels *via* inhibiting its biosynthesis from its upstream fatty acids (DGLA) .

D5D is one of the rate-limiting enzymes responsible for the synthesis of AA. Decreased D5D activity can lead to reduced AA production. For example, CP-24879 (p-isopentoxylaniline), an aniline derivative, was identified as a mixed D5D/D6D inhibitor during the screening of chemical and natural product libraries [214]. In mouse mastocytoma ABMC-7 cells cultured chronically with CP-24879, the desaturase activity was inhibited in a concentration-dependent manner that correlated with decreases in AA and its metabolite, LTC₄ [214]. In the livers of mice treated chronically with the maximally tolerated dose of CP-24879 (3.0 mg/kg, t.i.d.), the activities of D5D/D6D were inhibited by approximately 80%, and thus AA was depleted by nearly 50% compared to control [214]. These results suggest that D5D/D6D inhibitors may play a role in regulating an anti-inflammatory and anti-cancer response by decreasing the level of AA and the production of AA-derived metabolites. Sesamin and curcumin are potential D5D inhibitors which could interfere with the desaturation of PUFAs [215, 216]. Between sesamin and curcumin, the latter was more effective at increasing the ratio of DGLA to AA in cultured rat hepatocytes [215]. Kinetic studies of the inhibitory properties of sesamin and curcumin using rat liver microsome D5D showed that rat liver microsome D5D was noncompetitively inhibited by sesamin ($k_i=155 \mu\text{M}$) and curcumin ($k_i=36 \mu\text{M}$) [215, 216].

Our previous results (Chapter 4) have shown that the free radical metabolites generated from AA and DGLA peroxidation through COX might correspond to their contrasting bioactivities, *i.e.*, their pro- and anti-inflammatory effects. Increasing the anti-proliferative DGLA-derived exclusive free radical metabolites by increasing the level of DGLA in cells (*i.e.*,

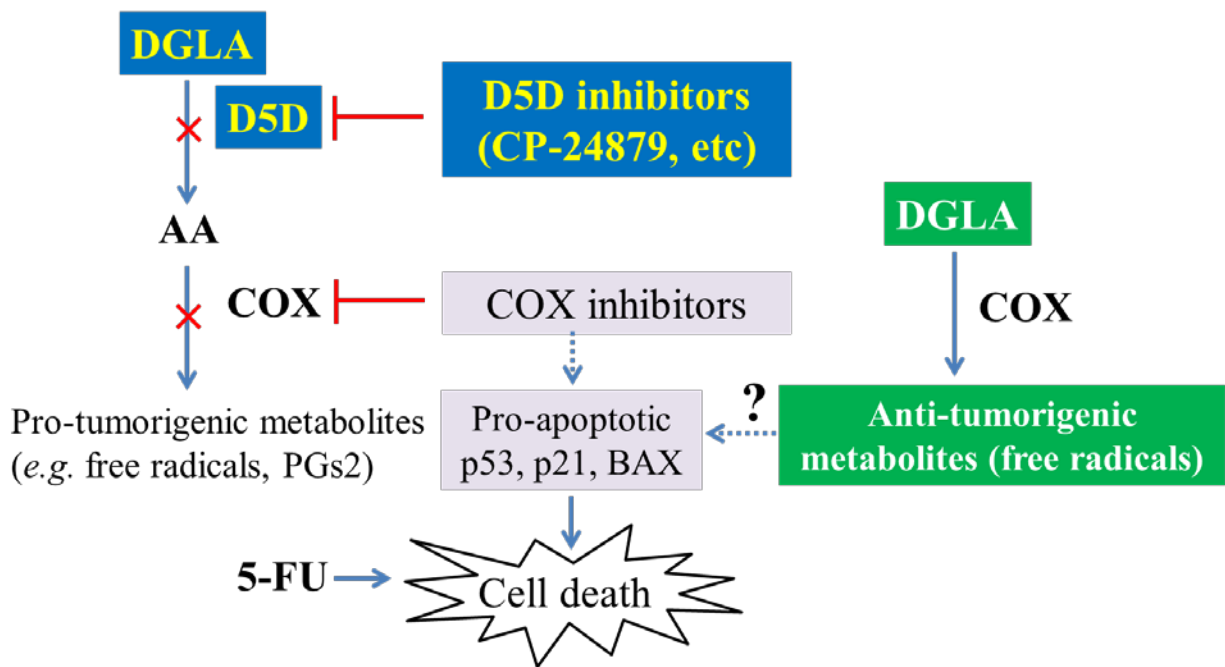
double doses of DGLA treatment *vs.* a single dose of DGLA treatment) was able to attenuate colon cancer cell growth.

We proposed that inhibiting the conversion from DGLA to AA could enhance the formation of DGLA-derived free radicals; while greatly limiting the formation of exclusive AA-derived free radicals may more effectively slow down the cancer cell growth. In this study, cells were co-treated with DGLA and D5D inhibitors. Hydroxylamines, PUFAs and PGEs were profiled and a cell proliferation assay was performed. Among the three tested D5D inhibitors, including CP-24879, sesamin and curcumin (Scheme 3), the most effective was CP-24879. Our results showed that CP-24879 partially suppressed the activity of D5D. The formation of exclusive AA-derived exclusive free radical metabolites and PGE₂ was significantly delayed and decreased after co-treatment with DGLA and CP-24879. However, these cells still exhibited some accumulation of AA-derived COX metabolites.

In order to completely block the conversion from DGLA to AA, HCA-7 colony 29 cells were also transfected with siRNA. D5D knockdown cells restored the anti-proliferative effect of DGLA. Decreased colon cancer cell growth was observed as decreasing the AA-derived free radical metabolites and simultaneously increasing the DGLA-derived free radical metabolites by D5D inhibition (CP-24879) or D5D knockdown (transfection with siRNA).

5-fluorouracil (5-FU), a fluorinated pyrimidine analog, has been used against cancer for more than 50 years. It is still one of the most widely applied drugs in the therapy of patients with colon cancer [217]. It is a suicide inhibitor of thymidylate synthase, acting through irreversible inhibition [217]. Since COX-2 was overexpressed in colon cancer, it was suggested that a combination treatment with a COX-2 inhibitor and anti-cancer agents such as 5-FU might result in synergistic apoptosis in colon cancer cells [217-219]. Increasing evidence showed that several

COX inhibitors, such as NSAIDs, increased the susceptibility of colon cancer cells to chemotherapy drugs, *e.g.* 5-FU, and influenced the mRNA expression of apoptosis-related genes p53, p21 and BAX [220-222]. This synergism was associated with decreased COX-2 expression and reduced formation of AA-derived eicosanoids [217].



Scheme 13. Proposed mechanism of the synergistic effect of DGLA and 5-FU.

We hypothesized that instead of interfering with the COX pathway, we could greatly enhance the cytotoxicity of 5-FU in colon cancer cells by targeting D5D (Scheme 13). Our results showed that targeting D5D could decrease the conversion from DGLA to AA, thus leading to decreased formation of AA-derived metabolites. In addition, the DGLA-derived metabolites, especially the exclusive free radical metabolites, could inhibit colon cancer cell growth. The cytotoxicity effect was evaluated *via* MTS assay. Our results showed that HCA-7 colony 29 is not sensitive to treatment with 5-FU ($IC_{50} > 1mM$). However, co-treatment with DGLA and CP-24879 sensitized HCA-7 colony 29 cells to 5-FU. In D5D knockdown cells, the

synergistic effect of DGLA and 5-FU on cell cytotoxicity was more significant. The increased susceptibility of colon cancer cells to 5-FU may be attributed to the DGLA-derived free radical metabolite-induced DNA damage.

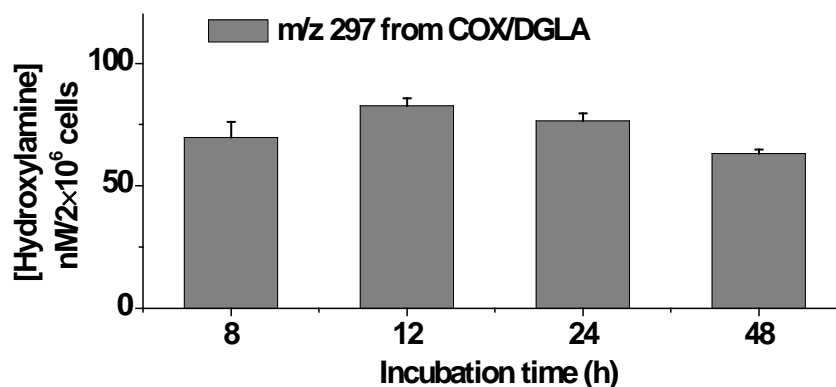
5.2. Results and Discussion

5.2.1. Hydroxylamines, PUFAs and PGEs in co-treatment with DGLA and CP-24879

Hydroxylamines in cells co-treated with DGLA and CP-24879: To investigate whether the D5D inhibitor CP-24879 could decrease the production of AA-derived free radical products by inhibiting the biosynthesis of AA, hydroxylamines (especially those that are exclusive in AA and DGLA) were profiled after a combined treatment with DGLA and CP-24879 at 8, 12, 24 and 48 h (Fig. 23). The production of the m/z 297 ion (the radical produced in common by AA and DGLA), as the reduced adduct of $\text{POBN}/\bullet\text{C}_6\text{H}_{13}\text{O}$, reached a peak concentration of ~82.7 nM at 12 h and then decreased to ~76.5 nM at 24 h and to ~63.1 nM 48 h (Fig. 23A).

The exclusive ions of m/z 325 and m/z 355 from COX/DGLA as the reduced adducts of $\text{POBN}/\bullet\text{C}_7\text{H}_{13}\text{O}_2$ and $\text{POBN}/\bullet\text{C}_8\text{H}_{15}\text{O}_3$, respectively, were observed in the combined treatment of DGLA and CP-24879 at 8, 12, 24 and 48 h (Fig. 23B). The concentrations of the m/z 325 ion were about 2.1 nM at 8 h, and increased to a peak of ~7.0 nM at 24 h followed by a decrease to 5.8 nM at 48 h (Fig. 23B). A similar trend was observed in the formation of the m/z 355 ion. The concentration was ~2.0 nM at 8 h, increasing to a peak of 10.5 nM at 24 h and maintaining the same level of 10.4 nM at 48 h (Fig. 23B). The exclusive AA-derived free radical product, the m/z 449 ion, as the reduced adduct of $\text{POBN}/\bullet\text{C}_{14}\text{H}_{21}\text{O}_4$, was not observed at 8 or 12 h, and the concentrations at 24 and 48 h were around 0.2 nM and 0.9 nM, respectively (Fig. 23B).

A. Profile of common radical product with DGLA+CP-24879



B. Profile of exclusive radical products with DGLA+CP-24879

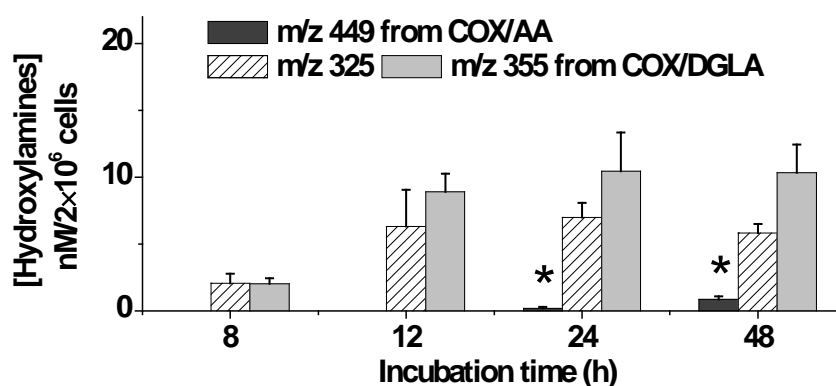


Fig. 23. Profiles of hydroxylamines with co-treatment of DGLA and CP-24879.

HCA-7 colony 29 cells were treated with 100 μ M DGLA and 5 μ M CP-24879, and the hydroxylamines were profiled at 12, 24, 36 and 48 h. (A) Profile of the common radical product (m/z 297) in cells treated with DGLA and CP-24879. (B) Profile of the exclusive radical products in cells treated with DGLA and CP-24879. The exclusive radical products in COX/DGLA peroxidation were m/z 325 and m/z 355. Hydroxylamines were quantified with d₉-POBN. (*) m/z 449 was the hydroxylamine generated from COX/AA peroxidation. Data are expressed as means \pm SD from n \geq 3.

The m/z 297 ion was the only hydroxylamine observed after co-treatment with DGLA and CP-24879 for 4 h. The concentration of the m/z 297 ion was at almost the same level as the one we observed in the DGLA treatment (data not shown). Compared to what we observed in cells treated with DGLA alone (Fig. 12), the concentrations of the m/z 297 ions were at about the same level at 12 h and 48 h; however, they increased by about 16% at 24 h. For the exclusively

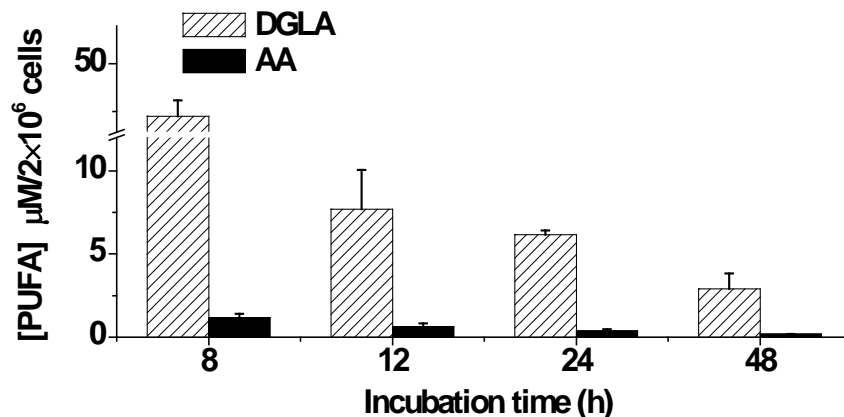
DGLA-derived free radical products, the m/z 325 and m/z 355 ion concentrations increased at all tested time points, and the most noticeable increase occurred at 8 h. In DGLA-treated cells, only trace amounts of both ions were observed (Fig. 12B); with the co-treatment with CP-24879 and DGLA, the concentrations of m/z 325 and m/z 355 increased to ~ 2.1 nM. On the other hand, the formation of the exclusive AA-derived free radical product, the m/z 449 ion, was significantly delayed as well as decreased in the co-treatment with DGLA and CP-24879. It was under the detection limit at 8 and 12 h, while a trace amount of the m/z 449 ion was detected at 24 h. The concentration at 48 h was decreased to 15% compared to that in the DGLA-only treatment (Fig. 12B).

The significant decrease in the accumulation of the AA-derived exclusive free radical product suggests that the biosynthesis of AA from DGLA in cells was inhibited by CP-34879. In the meantime, the increasing formation of free radical products, especially the m/z 325 and m/z 355 ions (e.g. DGLA-derived exclusive free radicals products) as shown in Fig. 23B, indicates that without AA as a competitor, the metabolism of DGLA through COX greatly increased. Because DGLA is the substrate for D5D, the inhibition of D5D also contributed to the increase of DGLA in cells.

PUFAs and PGEs in cells co-treated with DGLA and CP-24879: The formation of hydroxylamines showed that the biosynthesis of AA was inhibited by the co-treatment with CP-24879; we also measured PUFAs and PGEs to confirm these results. The profiles of PUFAs and PGEs in cell culture medium with the co-treatment with DGLA and CP-24879 are shown in Fig. 24. The concentrations of DGLA were ~36.2, 7.7, 6.2 and 2.9 μM at 8, 12, 24 and 48 h, respectively (Fig. 24A). The highest concentration of PGE₁ (~ 92 nM) was observed at 8 h and gradually decreased to 64.0 nM at 48 h (Fig. 24B).

Even when the D5D inhibitor CP-24879 was applied, AA and PGE₂ were also observed (Fig. 24). Within the tested time points, the peak concentration of AA (~ 1.2 μM) was observed at 8 h, followed by a decrease to 0.2 μM at 48 h (Fig. 24A). On the other hand, the production of PGE₂ increased from 8 h (~ 6.9 nM) to 48 h (14.4 nM) (Fig. 24B).

A. Profile of PUFAs from cells treated w/ DGLA+CP-24879



B. Profile of PGEs from cells treated w/ DGLA+CP-24879

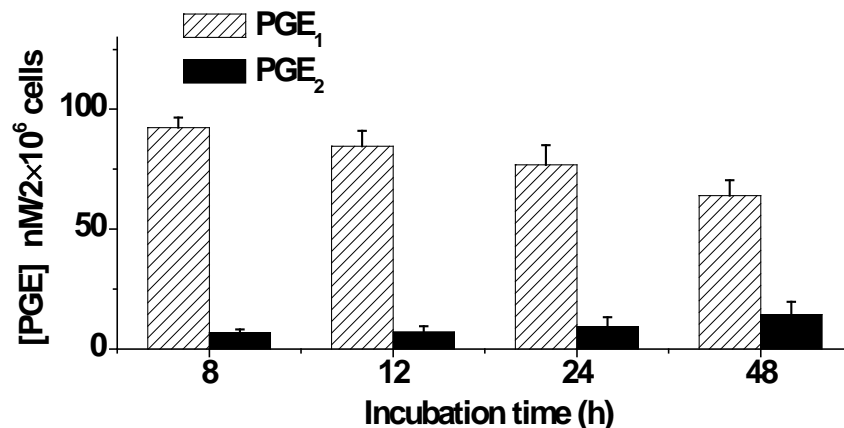


Fig. 24. Profiles of DGLA, AA, PGE₁ and PGE₂ with co-treatment of DGLA and CP-24879. HCA-7 colony 29 cells were cultured under normal cell growth conditions for 8, 12, 24 and 48 h with a supplement of 100 μM of DGLA and 5 μM of CP-24879. (A) Profiles of DGLA and AA in cell culture medium, (B) Profiles of PGE₁ and PGE₂ in cell culture medium. DGLA, AA, PGE₁ and PGE₂ were quantified with the internal standards DGLA-d₆, AA-d₈, PGE₁-d₄ and PGE₂-d₉, respectively. Data are expressed as means ± SD from n≥3.

Compared to treatment with DGLA alone, the concentration of DGLA in the cell culture medium increased in the co-treatment of DGLA with CP-24879. At 48 h, the ratio of the free DGLA to AA was around 4 to 1. At the same time, AA was significantly decreased in the presence of CP-24879; the concentration of AA was only 30% of what we had seen in the DGLA treatment at 8 h (Fig. 14A) and was less than 50% at 12, 24 and 48 h. The concentrations of PGE₁ at each time point increased in the co-treatment with DGLA and CP-24879 compared to the treatment with DGLA. Due to the decrease in its precursor AA, the concentration of PGE₂ dramatically dropped. The ratio of [PGE₁]:[PGE₂] increased from ~ 1:1 (DGLA treatment) to 4.4:1 (co-treatment of DGLA and CP-24879) at 48 h. Similarly, at 8, 12 and 24 h, the ratio was also increased.

The formation of PGEs was consistent with the formation of the free radical metabolites in the combined treatment with DGLA and CP-24879. The more PGE₁ was observed, the more of the exclusive free radical products of $\bullet\text{C}_7\text{H}_{13}\text{O}_2$ and $\bullet\text{C}_8\text{H}_{15}\text{O}_3$ from COX/DGLA were formed. On the other hand, when the concentration of PGE₂ was very low at 8 and 12 h, the free radical product of $\bullet\text{C}_{14}\text{H}_{21}\text{O}_4$ from COX/AA was not observed. As PGE₂ accumulated and its concentration increased, the free radical product of $\bullet\text{C}_{14}\text{H}_{21}\text{O}_4$ started to show up.

The profiles of the AA-derived exclusive free radical product (m/z 449 ion) and PGE₂ suggest that although CP-24879 delayed as well as decreased the formation of AA-derived metabolites, it did not completely block the biosynthesis of AA from DGLA. However, when we increased the concentration of the inhibitors in hope of achieving a more extensive suppression of the D5D activity, the COX activity was also affected in a dose-dependent manner. We observed that both PGE₁ and PGE₂ formation were significantly decreased when we increased the concentration of CP-24879 to a higher level (in the range of 10 to 50 μM) (data not shown).

Therefore, we concluded that to maintain the COX activity as well as to effectively control the formation of AA, a concentration of 5 μ M for CP-24879 is appropriate.

5.2.2. Effects of DGLA and CP-24879 on cell proliferation and cell cycle distribution

In order to study the effect of co-treatment with DGLA and CP-24879 on colon cancer cell growth, we performed the MTS assay and PI staining (Table 5). In cells co-treated with DGLA and CP-24879 for 48 h, cell viability was ~109.1% compared to ~98.3% in the DGLA treatment (Table 3). The cells in the G₂/M phase were ~26.3%, which was increased by more than 10% in both of these two treatments (DGLA+CP-24879 and DGLA) compared to the control group at 8 h (Table 5, Figs. 25A, 25C and 25E). The G₂/M phase cell cycle arrest was accompanied by an increase in G₁ phase cells (Table 5).

Table 5. Effect of DGLA and CP-24879 on cell cycle distribution and proliferation.

HCA-7 Colony 29 treated w/	Cell Cycle Distribution				Cell Proliferation
	% in G ₁ Phase		% in G ₂ /M Phase		% viability
	8 h	24 h	8 h	24 h	48 h
Control (0.1 % ethanol)	37.4 ± 2.4	22.1 ± 1.2	29.7 ± 2.3	20.9 ± 0.9	100
DGLA (100 μ M)	43.6 ± 9.6	29.4 ± 2.1	41.3* ± 2.5	23.6 ± 1.6	109.1* ± 5.7
DGLA w/ 5 μ M CP	42.8* ± 6.3	29.4 ± 3.0	42.4* ± 1.8	26.3* ± 1.8	98.3* ± 5.0

HCA-7 colony 29 cells treated with 100 μ M DGLA and a combined treatment of 100 μ M DGLA and 5 μ M CP-24879. Data represent the mean \pm SD derived from three separate experiments with triplicate wells per condition. (a) % cell viability was compared with control group. Note, control cells were incubated with 0.1% DMSO and 0.1% ethanol (final concentrations). (*) P<0.01, significantly different from control.

That no significant difference was observed between these two treatments is probably because at 8 h, DGLA was still the dominant fatty acid in the cells. As our data in Fig. 14 showed, the level of AA converted from DGLA through D5D in the cells was not high enough to compete with DGLA for COX. In other words, the DGLA-derived free radical metabolites

overwhelmed the AA-derived free radical metabolites and the anti-proliferative effect of DGLA was dominant at the 8 h time point.

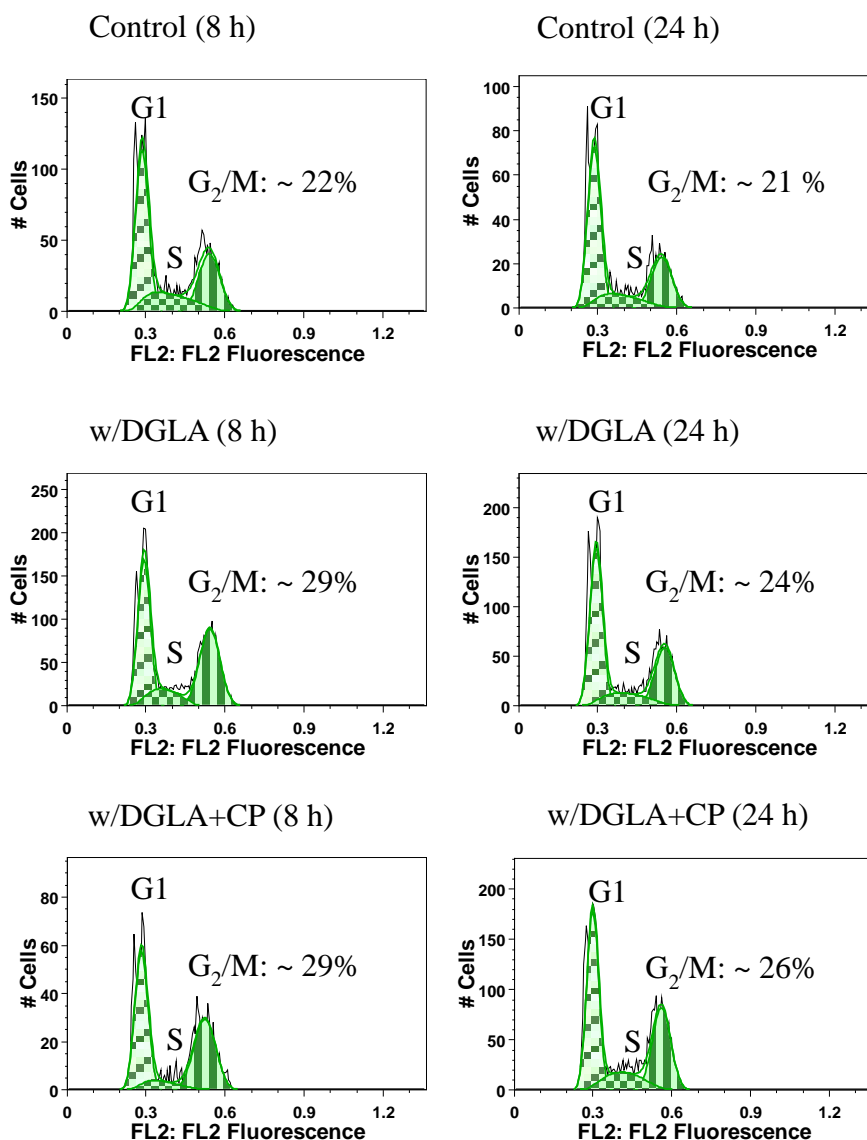


Fig. 25. Effects of co-treatment of DGLA and CP-24879 on cell cycle distribution.

(A-B) HCA-7 colony 29 cells were treated with 0.1% ethanol for 8 and 24 h, respectively, (C-D) HCA-7 colony 29 cells were treated with 100 μ M DGLA for 8 and 24 h, respectively, (A-B) HCA-7 colony 29 cells were co-treated with 100 μ M DGLA and 5 μ M CP-24879 for 8 and 24 h, respectively.

When the incubation time was increased to 24 h, as the formation of AA and its derived free radical metabolites increased, the anti-proliferative effect of DGLA was abolished. The

percentage of cells in the G₂ phase was similar to that in the control group (Table 5, Figs. 25B and 25D). The DGLA-induced cell G₂/M arrest was attenuated by the action of CP-24879 at 24 h. In the co-treatment with DGLA and CP-24879, the percentage of cells in the G₂/M phase was ~26.3%, which was 10% more than in the control and DGLA groups (Table 5, Figs. 25D and 25F). However, CP-24879 did not completely restore the anti-proliferative effect of DGLA. This failure may be due to the partial but not complete suppression of D5D, which was shown by the increasing formation of AA-derived free radical metabolites and PGE₂ as the incubation time increased (Figs. 22B and 23B).

Compared to the single dose and double dose DGLA treatments (Table 5 and Fig. 22), the co-treatment with CP-24879 significantly decreased cell proliferation. Our data suggested that DGLA indeed has a potentially inhibitory effect on the growth of HCA-7 colony 29 cells if its conversion to AA is limited. Targeting D5D is a promising approach to manifesting an anti-inflammatory and anti-cancer response by simultaneously increasing the anti-proliferative DGLA-derived free radical metabolites and decreasing the ensuing production of AA-derived pro-proliferation metabolites.

5.2.3. Possible inhibition mechanism of CP-24879

CP-24879 was identified as a mixed D5D/D6D inhibitor during the screening of chemical and natural product libraries [214]. However, the inhibitory mechanism was still unknown. In order to gain more insight into the inhibitory action of CP-24879, we used Western blot analysis to check the expression of D5D with different treatments. Cells were treated with 100 μM of DGLA alone, 5 μM CP-24879 alone, and 100 μM DGLA with 5 μM CP-24879. No significant difference in expression of D5D was observed (Fig. 26) between the different treatments.

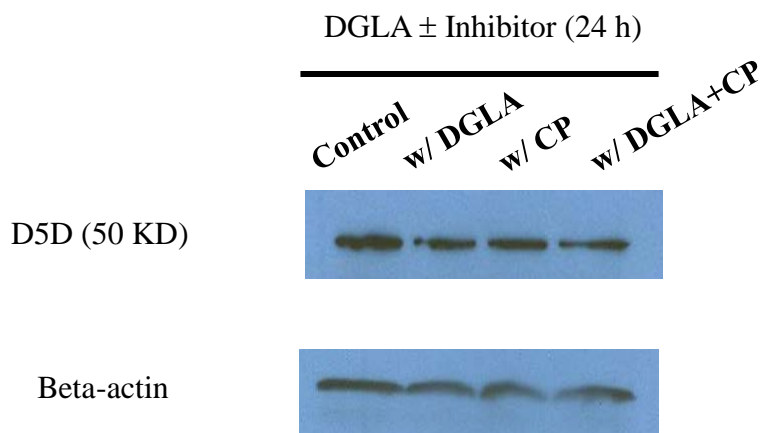


Fig. 26. Western blot analysis of D5D expression with co-treatment of DGLA and CP-24879.

Cells were treated with DGLA \pm CP-24879 for 24 h. Forty micrograms of protein per sample was separated by SDS-PAGE, transferred to PVDF membrane, and immunoblotted using a D5D-specific antibody. Beta-actin served as the loading control.

Our data suggest that CP-24879 inhibits the enzymatic activity of D5D without affecting its protein expression. Thus, CP-24879 did not inhibit D5D *via* regulating gene expression.

Although D5D has been cloned and expressed in cells [14], the crystal structure of D5D remains unsolved. Thus, the exact inhibitory mechanism is not clear at this stage. In general, the competitive enzyme inhibitor is a compound whose structure and molecular geometry closely resemble that of the substrate. It is possible that CP-24879 inhibits D5D through uncompetitive or noncompetitive action, because CP-24879 is not structurally close to a fatty acid (Scheme 3). The details of the inhibitory mechanism need to be further investigated.

5.2.4. Study of other D5D inhibitors

Our previous data showed that CP-24879 suppressed D5D activity and attenuated the conversion from DGLA to AA. However, the exclusive AA-derived free radical product (the m/z 449 ion) as well as PGE₂ was still observed after 48 h (Figs. 23B and 24B). Although the combined treatment of DGLA and CP-24879 has an anti-proliferative effect compared to the DGLA treatment, the cell growth was not inhibited compared to the control group. Therefore, we

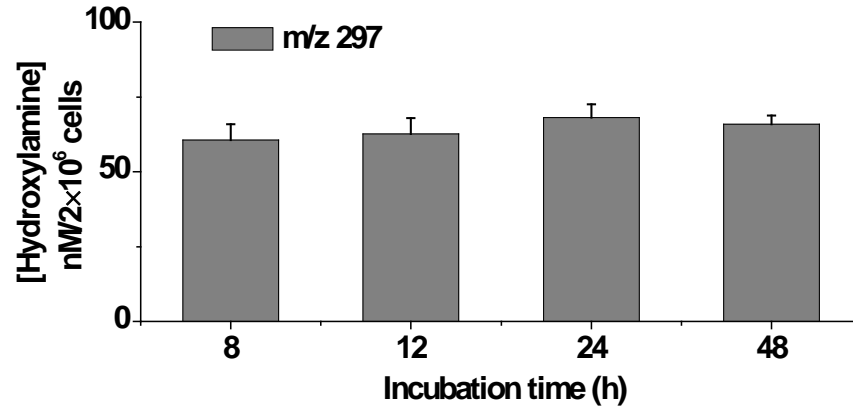
also tested the other commercial available D5D inhibitors. Besides the synthetic CP-24879, it has been reported that sesamin and curcumin obtained from natural sources are also potential D5D inhibitors [214, 215].

Co-treatment with sesamin and DGLA: hydroxylamine, PUFA and PGEs: First of all, we tested the effect of sesamin as the D5D inhibitor. Hydroxylamines were measured at 8, 12, 24 and 48 h after co-treatment with DGLA and sesamin (Fig. 27). For the common free radical product, m/z 297 as the reduced adduct of POBN/ \bullet C₆H₁₃O, the peak concentration of ~8.1 nM was observed at 24 h (Fig. 27A). The concentrations from 12 h to 48 h were within the range of 60.7 to 68.1 nM.

The exclusive ions of m/z 325 and m/z 355 from COX/DGLA as the reduced adducts of POBN/ \bullet C₇H₁₃O₂ and POBN/ \bullet C₈H₁₅O₃, respectively, were observed in the combined treatment with DGLA and sesamin at 8, 12, 24 and 48 h (Fig. 27B). Trace levels of both ions (~0.2 nM) were detected at 8 h. The concentrations of the m/z 325 ion were around 6.4 nM at 12 h and 6.2 nM at 24 h, followed by a decrease to 5.5 nM at 48 h. For the formation of the m/z 355 ion, the concentration was ~6.7 nM at 12 h, increasing to ~7.6 nM at 24 h and maintaining a similar level (~7.3 nM) up to 48 h. The exclusive AA-derived free radical product, the m/z 449 ion as the reduced product of POBN/ \bullet C₁₄H₂₁O₄, was also observed. It was detected at 8, 12 and 48 h, with concentrations of 3.5, 6.0 and 4.4 nM, respectively (Fig 27B).

The profiles of all the free radical products in the combined treatment of DGLA with sesamin were similar to those we observed in the DGLA-alone treatment (Fig. 12). In particular, the high concentration of the AA-derived free radical product m/z 449 ion suggests that sesamin did not inhibit the conversion from DGLA to AA. This may be due to the poor solubility of sesamin in the cell culture medium. It was reported that sesamin inhibits the conversion of

A. Profile of common radical product with DGLA+sesamin



B. Profile of exclusive radical products with DGLA+sesamin

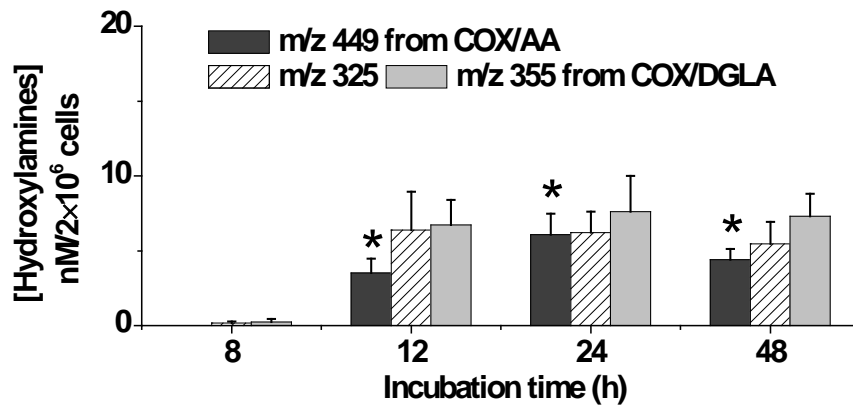
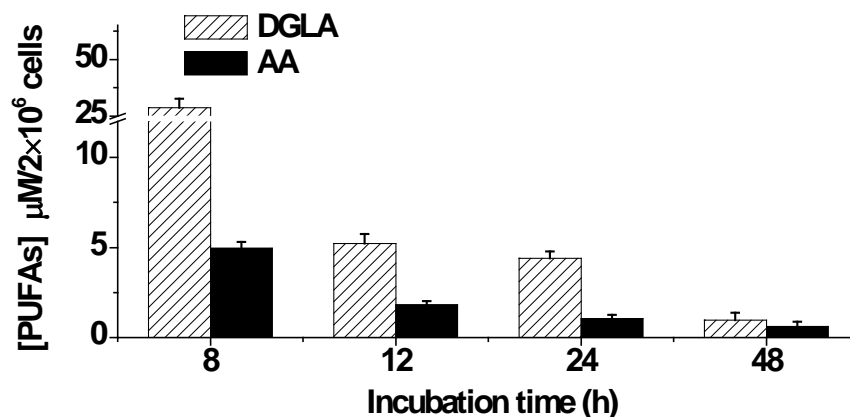


Fig. 27. Profiles of hydroxylamines with co-treatment of DGLA and sesamin.

HCA-7 colony 29 cells were co-treated with 100 μ M DGLA and 100 μ M sesamin in the presence of 20 mM POBN, and the hydroxylamines were profiled at 12, 24, 36 and 48 h. (A) Profile of common radical product (m/z 297) in cells treated with DGLA and sesamin. (B) Profiles of exclusive radical products in cells treated with DGLA and sesamin. The exclusive radical products in COX/DGLA peroxidation were m/z 325 and m/z 355, Hydroxylamines were quantified with d₉-POBN. (*) m/z 449 was the hydroxylamine generated from COX/AA peroxidation. Data are expressed as means \pm SD from n \geq 3.

A. Profile of PUFAs from cells treated w/ DGLA+sesamin



B. Profile of PGEs from cells treated w/ DGLA+sesamin

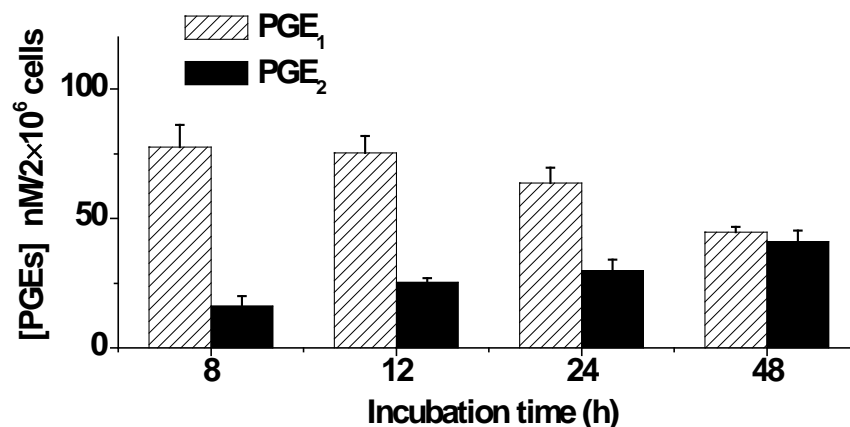


Fig. 28. Profiles of DGLA, AA, PGE₁ and PGE₂ with co-treatment of DGLA and sesamin.

HCA-7 colony 29 cells were co-treated with 100 μM DGLA and 100 μM sesamin. PUFAs and PGEs were profiled at 12, 24, 36 and 48 h. (A) Profiles of DGLA and AA in cell culture medium, (B) Profiles of PGE₁ and PGE₂ in cell culture medium. DGLA, AA, PGE₁ and PGE₂ were quantified with the internal standards DGLA-d₆, AA-d₈, PGE₁-d₄ and PGE₂-d₉, respectively. Data are expressed as means ± SD from n≥3.

DGLA to AA with a K_i value of 155 μM in rat liver microsomes [216]. However, the highest final concentration that sesamin was able to achieve in the cell culture medium was 100 μM. Higher concentrations, *e.g.*, 150 and 200 μM, were also tested; however, the excess sesamin formed crystals in the medium.

PUFA and PGE formation in co-treatment with DGLA and sesamin was also measured at 8, 12, 24 and 48 h (Fig. 28). The results were also similar to what we observed in the DGLA-

only treatment (Fig. 14). As the DGLA continuously converted to AA, the ratio between [DGLA] and [AA] decreased (Fig. 28A). It was clearer in the profile of PGEs: the concentration of PGE₁:PGE₂ increased to about 1:1 at 48 h (Fig. 28B). The results confirmed that sesamin at the concentration of 100 μM did not exert an inhibitory effect on D5D activity.

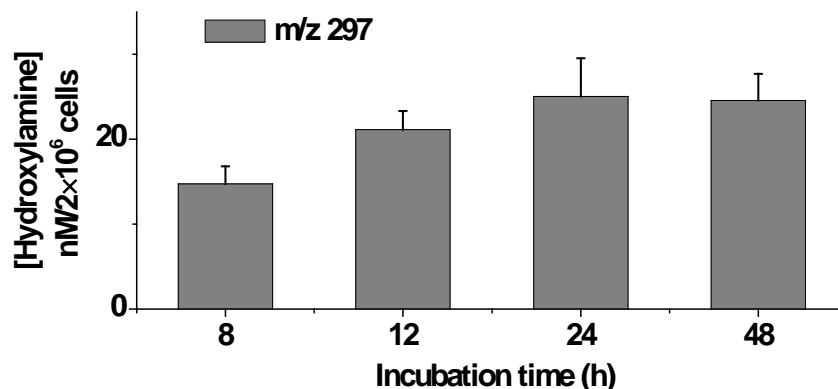
Co-treatment with curcumin and DGLA: Hydroxylamine, PUFA and PGEs: Another reported D5D inhibitor we tested was curcumin. The formation of hydroxylamines was profiled at 8, 12, 24 and 48 h (Fig. 29). For the common radical product, the m/z 297 ion as the reduced adduct of POBN/•C₆H₁₃O, the peak concentration of ~ 25.1 nM was observed at 24 h (Fig. 29A). The concentrations at 8, 24 and 48 h were ~14.8, 21.1 and 24.6 nM, respectively.

The exclusive ions of m/z 325 and m/z 355 from COX/DGLA as the reduced adducts of POBN/•C₇H₁₃O₂ and POBN/•C₈H₁₅O₃, respectively, were observed in the combined treatment with DGLA and curcumin at 12, 24 and 48 h (Fig. 29B). The concentrations of the m/z 325 ion were ~ 1.5, 2.7 and 2.0 nM at 12, 24 and 48 h; the concentrations of m/z 355 were about 2.9, 3.3 and 3.0 at 12, 24 and 48 h. The exclusive AA-derived free radical product, the m/z 449 ion as the reduced product of POBN/•C₁₄H₂₁O₄, was also observed. It was detected at 8, 12 and 48 h, with concentrations of 0.5, 1.0 and 0.8 nM, respectively (Fig. 29B).

The formation of all the free radical products (including the common and exclusive free radical products) in the combined treatment of DGLA with curcumin was significantly decreased (more than a 60% decrease) compared to that in the DGLA alone treatment (Fig. 12). Because both the AA-derived exclusive free radical products and the DGLA-derived exclusive free radical products decreased at the same time, it was hard to tell whether the curcumin inhibited the conversion from DGLA to AA from the profiles of AA and DGLA. However, the decreased

formation of the free radical products suggests that curcumin significantly decreases the activity of COX.

A. Profile of common radical product with DGLA+curcumin



B. Profile of exclusive radical products with DGLA+curcumin

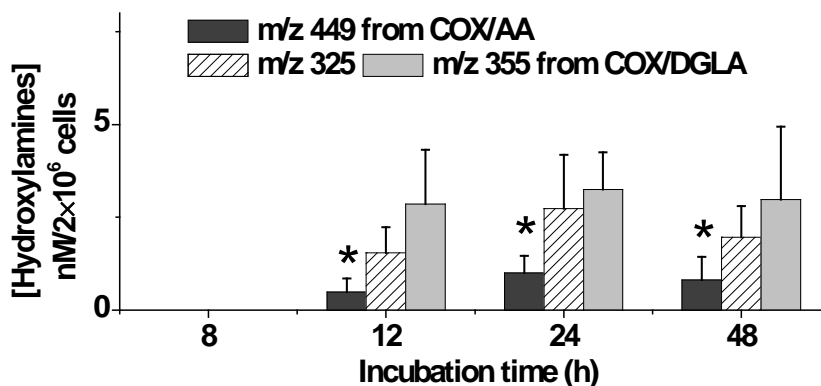


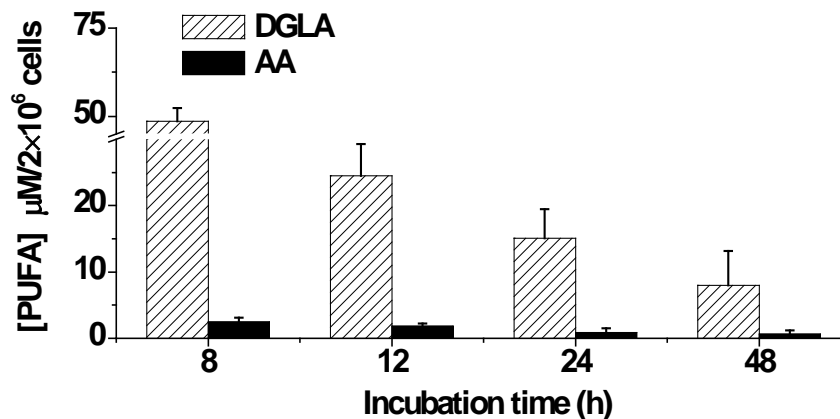
Fig. 29. Profiles of hydroxylamines with co-treatment of DGLA and curcumin.

HCA-7 colony 29 cells were co-treated with 100 μ M DGLA and 20 μ M curcumin in the presence of 20 mM POBN, and the hydroxylamines were profiled at 12, 24, 36 and 48 h. (A) Profile of common radical product (m/z 297) in cells treated with DGLA and curcumin. (B) Profile of exclusive radical products in cells treated with DGLA and curcumin. The exclusive radical products in COX/DGLA peroxidation were m/z 325 and m/z 355. Hydroxylamines were quantified with d₉-POBN. (*) m/z 449 was the hydroxylamine generated from COX/AA peroxidation. Data are expressed as means \pm SD from n \geq 3.

PUFAs and PGEs produced in the co-treatment with DGLA and curcumin were profiled at 8, 12, 24 and 48 h. As shown in Fig. 30, the level of DGLA in the cell medium was \sim 48.6 μ M at 8 h and decreased to 24.5 μ M at 12 h, 15.1 μ M at 24 h and 8.0 μ M at 48 h (Fig. 30A). The

highest concentration of PGE₁ (~ 33.1 nM) was observed at 8 h, after which it decreased to 26.4, 25.0 and 23.7 nM at 12, 24 and 48 h, respectively (Fig. 30B).

A. Profile of PUFAs from cells treated w/ DGLA+curcumin



B. Profile of PGEs from cells treated w/ DGLA+curcumin

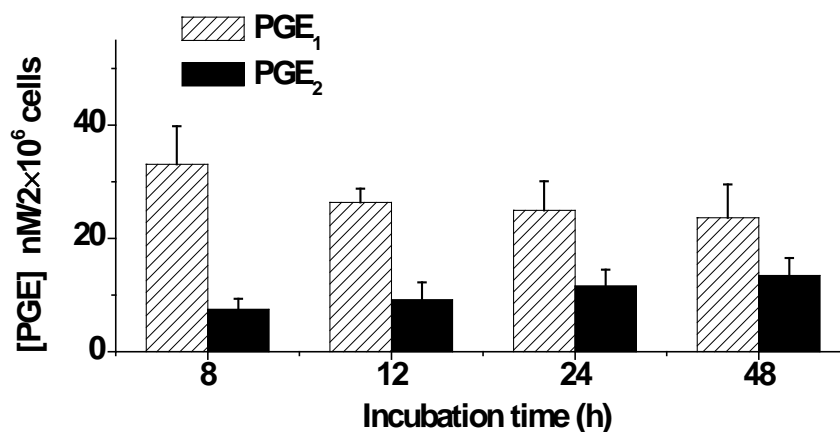


Fig. 30. Profiles of DGLA, AA, PGE₁ and PGE₂ with co-treatment of DGLA and curcumin. HCA-7 colony 29 cells were co-treated with 100 μM DGLA and 20 μM curcumin. PUFAs and PGEs were profiled at 12, 24, 36 and 48 h. (A) Profiles of DGLA and AA in cell culture medium, (B) Profiles of PGE₁ and PGE₂ in cell culture medium. DGLA, AA, PGE₁ and PGE₂ were quantified with the internal standards DGLA-d₆, AA-d₈, PGE₁-d₄ and PGE₂-d₉, respectively. Data are expressed as means ± SD from n≥3.

The profiles of PUFA and PGEs in the co-treatment with DGLA and curcumin were consistent with the results from the free radical products. Compared to the treatment with DGLA alone (Fig. 14), the concentration of DGLA significantly increased at all tested time points for

the co-treatment with DGLA and curcumin. For example, the level of DGLA at 8 h increased by 70%. Conversely, the formation of PGEs significantly decreased at all tested time points (more than a 50% decrease). The ratio of [DGLA] to [AA], and especially [PGE₁] vs. [PGE₂], suggests that curcumin inhibits the D5D activity to some extent. The ratio of [PGE₁]:[PGE₂] was close to 1:2.

When the concentration of curcumin was varied from 5 to 50 μ M in the curcumin-DGLA treatment, the lowest tested concentration (5 μ M) did not affect D5D activity in cells, while it did inhibit PGE biosynthesis (data not shown). These results suggest that curcumin is not a specific inhibitor for D5D.

Cell proliferation study of D5D inhibitors: The effects of sesamin and curcumin together with DGLA on cell proliferation were evaluated *via* the MTS assay (Fig. 31). As expected, sesamin failed to restore the anti-proliferative effect of DGLA, and co-treatment with DGLA and sesamin promoted cell growth compared to the control group, which showed an effect similar to the ones for the DGLA-alone treatment (Fig. 31). On the other hand, curcumin with DGLA exerted a significant anti-proliferative effect, which decreased cell proliferation by ~24% compared to the control group (Fig. 31). However, this anti-proliferative effect was induced by curcumin rather than DGLA, because treatment with curcumin alone, without DGLA, showed a similar effect (data not shown). Curcumin is the principal curcuminoid of the popular Indian spice turmeric, which is a member of the ginger family. Increasing evidence has shown that curcumin has multiple roles in the treatment of cancer; *e.g.*, it exerts a potential anti-inflammatory and anti-cancer effect by down-regulating the oncogene Mdm2 [223], down-regulating the peroxidizing enzymes COX and LOX [224], and scavenging free radicals as an antioxidant [224].

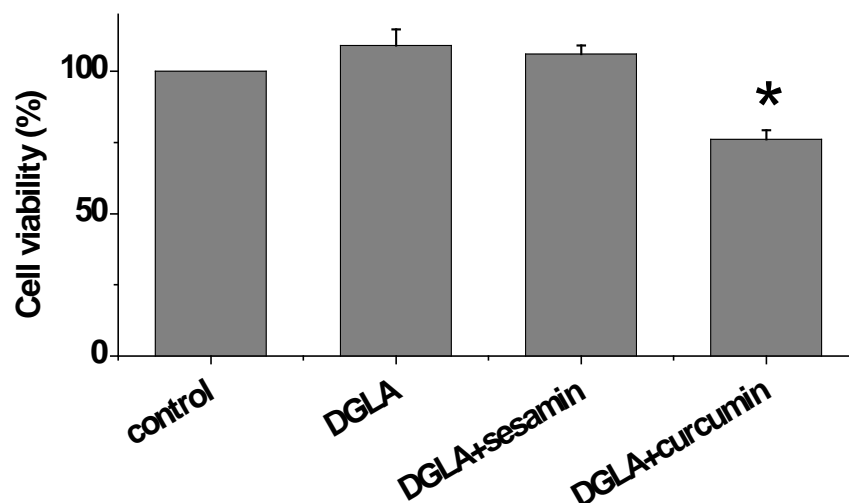


Fig. 31. Effect of DGLA with sesamin or curcumin on cell proliferation.

HCA-7 colony 29 cells were treated with 100 μ M DGLA or a combined treatment of 100 μ M DGLA with 100 μ M sesamin or 100 μ M DGLA with 20 μ M curcumin. Data represent the mean \pm SD derived from three separate experiments with triplicate wells per condition. Note, % cell viability was compared with the control group. Control cells were incubated with 0.1% dimethylsulfoxide and 0.1% ethanol (final concentration). (*) $P < 0.01$, significantly different from control.

By far, among all the tested inhibitors, CP-24879 was the most effective; it exerts the greatest inhibitory effect on the biosynthesis of AA by suppressing D5D activity while not affecting the activity of COX. The combined treatment of DGLA and CP-24879 delayed and decreased the formation of AA-derived free radical metabolites, while concurrently increasing the formation of DGLA-derived free radical metabolites, which resulted in the partial restoration of the anti-proliferative effect of DGLA.

5.2.5. DGLA enhanced the efficacy of the chemotherapy drug 5-FU

5-FU, a fluorinated pyrimidine analog, is one of the most widely applied drugs in the therapy of patients with colon cancer. Due to the high expression of COX-2 in colon cancer, research has shown that COX inhibitors sensitize colon cancer cells to chemotherapy drugs [210, 213]. This synergism was linked with decreased expression of COX-2 and reduced formation of AA-derived eicosanoids [210, 213].

Targeting D5D to decrease the biosynthesis of AA from DGLA could also reduce the formation of AA-derived eicosanoids. In addition, our previous data suggested that the exclusive free radical metabolites derived from DGLA could inhibit cell growth, and DGLA could induce cell arrest at the G₂/M phase. Here, for the first time, we have investigated whether DGLA could increase the susceptibility of HCA-7 colony 29 (with a high expression of COX-2) to 5-FU.

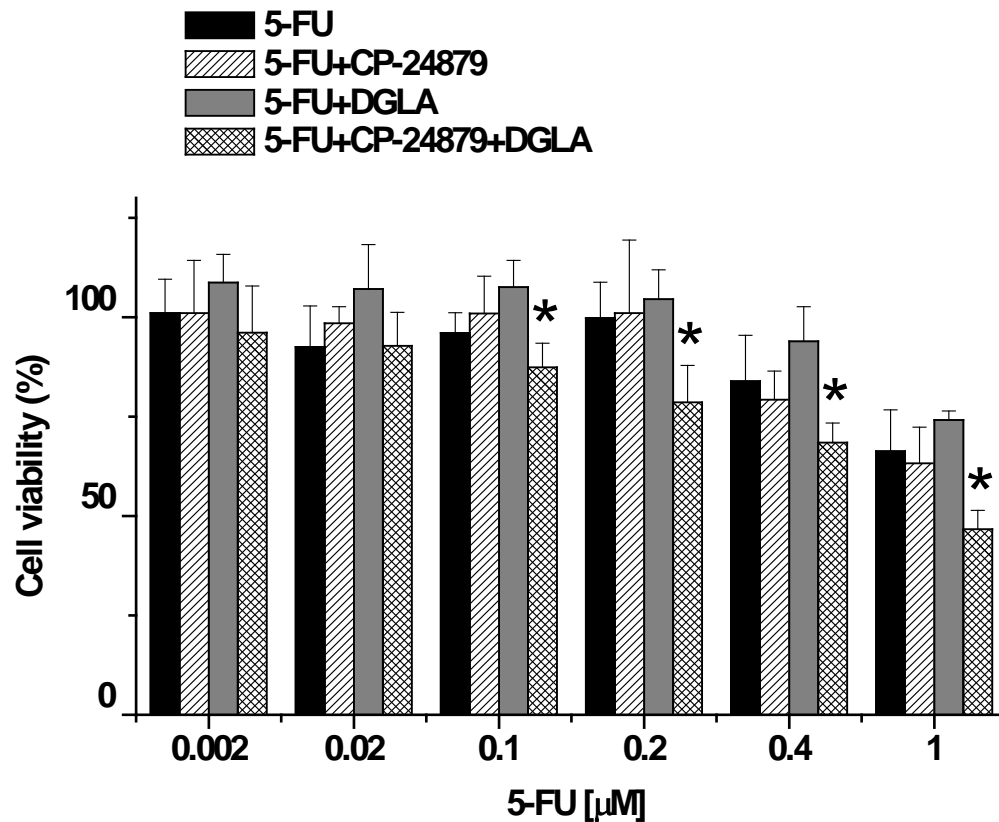


Fig. 32. Co-treatment of DGLA and CP-24879 enhanced the efficacy of 5-FU.

HCA-7 colony 29 cells were treated with various concentrations of 5-FU, 5-FU with 5 μM CP-24879, 5-FU with 100 μM DGLA, and the combined treatment of 5-FU and 100 μM DGLA with 5 μM CP-24879. Data represent the mean ± SD derived from three separate experiments with triplicate wells per condition. Note that % cell viability was compared with the control group. Control cells were incubated with 0.1% dimethylsulfoxide and 0.1% ethanol (final concentration). (*) P<0.01, significantly different from control.

Four different treatments, including 5-FU, 5-FU+CP-24879, 5-FU+DGLA, and 5-FU+CP-24879+DGLA, were designed, and for each group, a series of concentrations of 5-FU (ranging from 0.02 to 1 mM) were applied. Cell proliferation after a 48 h treatment was

measured *via* the MTS assay as shown in Fig. 32. HCA-7 colony 29 was not sensitive to low concentrations of 5-FU alone ($IC_{50} > 1\text{mM}$). 5-FU only inhibited colon cancer cell growth at concentrations higher than 0.4 mM (Fig. 32). CP-24879 did not alter the effect of 5-FU on cell growth. DGLA decreased the sensitivity of HCA-7 colony 29 cells to 5-FU; the cell proliferation increased compared to the 5-FU-only treatment. With the addition of both DGLA and CP-24879, the sensitivity of cells to 5-FU increased. The cell viability decreased by more than 10% with 0.4 mM 5-FU and decreased by more than 15% with 1 mM 5-FU (Fig. 32).

When cells were co-treated with DGLA and 5-FU, the increase in cell proliferation was expected due to the rapid conversion from DGLA to AA through D5D. As shown in Fig. 14B, after 48 h, the formation of PGE_1 was almost equal to PGE_2 , indicating that AA was competing with DGLA for COX. And this competition also resulted in the formation of excess AA-derived free radical metabolites (Fig. 12B). The presence of AA-derived free radical metabolites may abolish the anti-proliferative effect of DGLA-derived free radical metabolites. In this case, it protects the cells from undergoing apoptosis. When the D5D inhibitor was introduced, formation of the AA-derived free radical metabolites was delayed and reduced (Fig. 23B), thus the DGLA-derived free radical metabolites exhibited anti-proliferation effects that synergized the apoptosis induced by 5-FU in colon cancer cells.

5-FU induced anti-cancer effects and toxicity, including blocking DNA synthesis, inducing translational errors, and regulating the pro-apoptosis genes p53, p21 and BAX [220-222]. Treatment with both CP-24879 and DGLA restored the anti-proliferative effect of DGLA, enhancing the DGLA-derived free radical metabolites that may have an anti-carcinogenic effect through causing DNA lesions and activating tumor suppressors such as p53. Thus, the

synergistic effect of DGLA with 5-FU might be due to their co-effect in causing DNA damage and activating pro-apoptosis genes.

5.2.6. Effect of DGLA in D5D knockdown cells

Although the CP-24879 was able to partially restore DGLA's anti-carcinogenic effect, nevertheless, the inhibition of D5D activity was not complete. As we observed from Table 5, DGLA with CP-24879 decreased cell proliferation compared to DGLA treatment, but was not significantly different than the control treatment. Another approach to inhibiting the conversion from DGLA to AA was to use RNA interference to suppress D5D gene expression. D5D was silenced in HCA-7 colony 29 cells *via* siRNA transfection.

D5D expression was measured after transfecting HCA-7 colony 29 with negative control siRNA or the D5D siRNA for 48 h by Western blot analysis (Fig. 33). The expression of D5D decreased as the siRNA concentration increased. D5D expression was completely silenced with 150 nM D5D siRNA (Fig. 33).

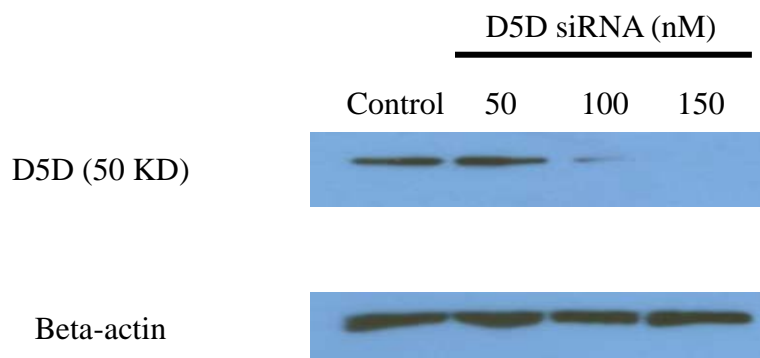


Fig. 33. Western blot analysis of D5D knockdown.

Cells were transfected with negative control siRNA (150 nM) and D5D siRNA (50 to 150 nM). Western blot analysis was performed after 48 h. Forty micrograms of protein per sample was separated by SDS-PAGE, transferred to PVDF membrane, and immunoblotted using a D5D-specific antibody. Beta-actin served as the loading control.

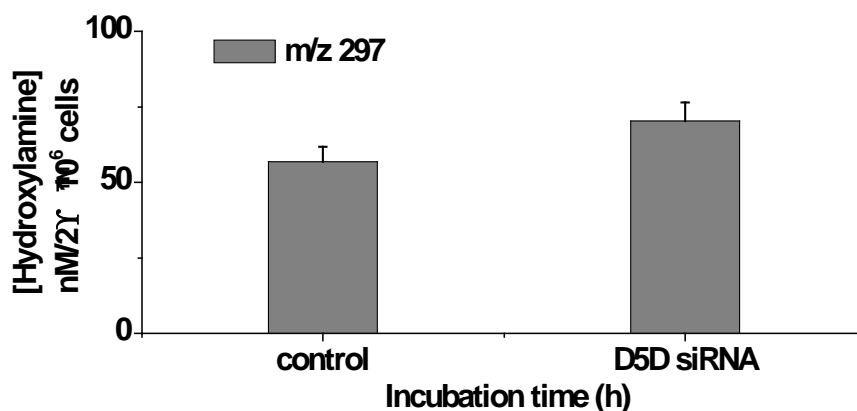
After D5D was successfully knocked down in HCA-7 colony 29 cells, the formation of hydroxylamines was profiled after treating the cells with DGLA for 48 h (Fig. 34). The

concentration of the m/z 297 ion (common radical product) as the reduced adduct of POBN/ \bullet C₆H₁₃O was ~56.8 nM in the control cells (transfected with negative control siRNA) and ~70.3 nM in the D5D knockdown cells (Fig. 34A). The exclusive ions of m/z 325 and m/z 355 from COX/DGLA, as the reduced adducts of POBN/ \bullet C₇H₁₃O₂ and POBN/ \bullet C₈H₁₅O₃, respectively, were observed after 48 h (Fig. 34B). The concentrations of the m/z 325 ion were ~4.9 nM in the control cells and ~9.2 nM in the D5D knockdown cells (Fig. 34B). For the m/z 355 ion, the concentration was ~8.9 nM in control cells and ~12.5 nM in the D5D knockdown cells (Fig. 34B). The exclusive AA-derived free radical product, the m/z 449 ion as the reduced adduct of POBN/ \bullet C₁₄H₂₁O₄, was not observed at 8 or 12 h, and the concentrations at 24 and 48 h were around 4.0 nM in the control and not detectable in the D5D knockdown cells.

Compared to the control cells, the formation of all the free radical products, including the m/z 297, m/z 325 and m/z 355 ions, increased in the D5D knockdown cells, especially the DGLA-derived exclusive free radical products (Fig. 34). The concentration of the m/z 325 ion increased by ~80% and that of the m/z 355 ion increased by ~40%. Conversely, due to the silencing of D5D expression, the exclusive AA-derived free radical product, the m/z 449 ion, was not observed. Compared to the formation of hydroxylamines in the cells co-treated with CP-24879 and DGLA at 48 h (Fig. 23B), the concentrations of m/z 325 and m/z 355 increased and the formation of the exclusive AA-derived free radical product, the m/z 449 ion, decreased.

PUFAs and PGEs in the cell culture medium were also measured after 48 h and the results were consistent with the formation of hydroxylamines (Fig. 35). The concentration of DGLA in the control cells was ~1.3 μ M and in the D5D knockdown cells was ~3.1 μ M (Fig. 35A). PGE₁ in the control cells was ~42.0 nM and in D5D knockdown cells it was ~85.2 nM (Fig. 35B).

A. Profile of common radical product w/ DGLA



B. Profile of exclusive radical products w/ DGLA

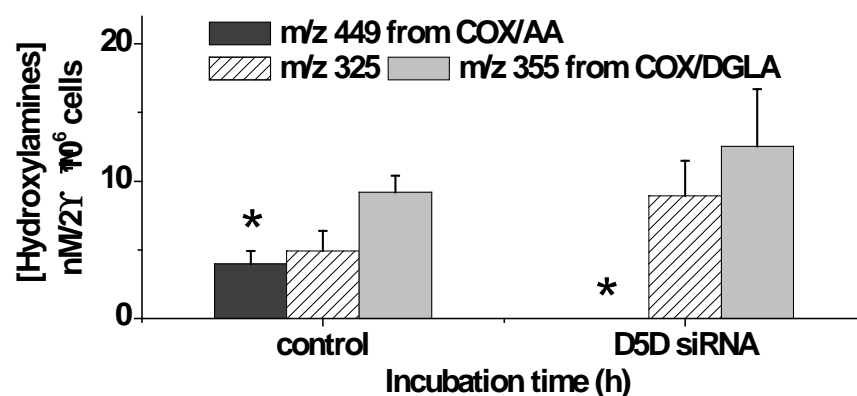
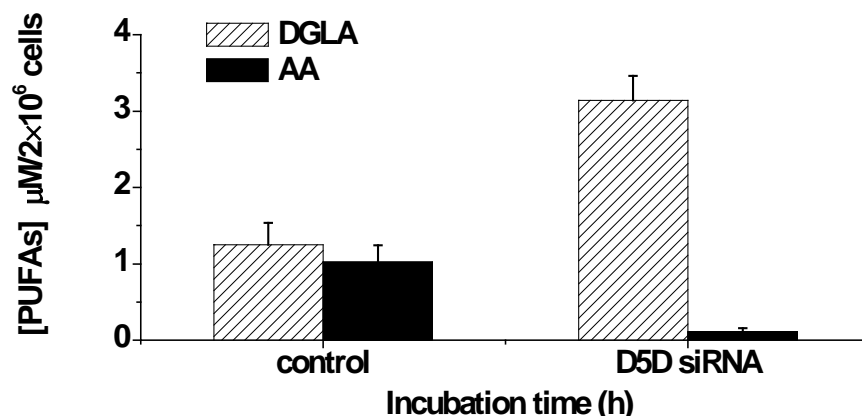


Fig. 34. Profiles of hydroxylamines in D5D knockdown cells with DGLA treatment.

HCA-7 colony 29 cells were transfected with 150 nM of control siRNA or D5D siRNA, and then treated with 100 μ M of DGLA for 48 h. (A) Profile of the common radical product (m/z 297) in cells treated with DGLA. (B) Profiles of exclusive radical products in cells treated with DGLA. The exclusive radical products in COX/DGLA peroxidation were m/z 325 and m/z 355. Hydroxylamines were quantified with d_9 -POBN. (*) m/z 449 was the hydroxylamine generated from COX/AA peroxidation. Data are expressed as means \pm SD from $n \geq 3$.

A. Profile of PUFA from transfected cells treated w/ DGLA



B. Profile of PGEs from transfected cells treated w/ DGLA

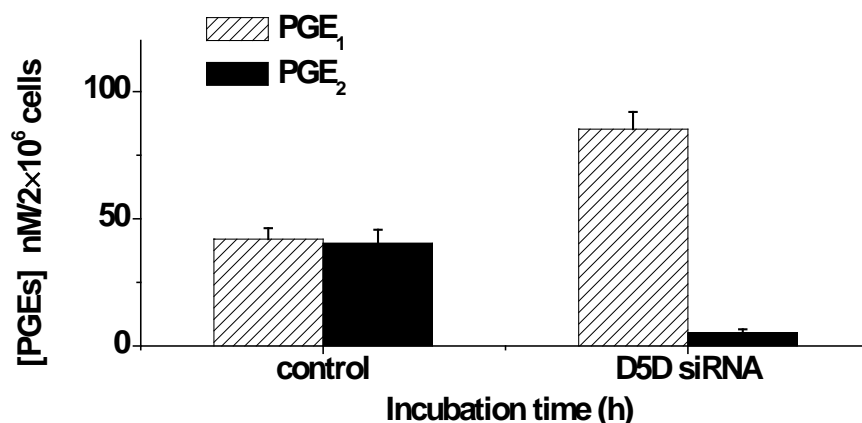


Fig. 35. Profiles of DGLA, AA, PGE₁ and PGE₂ in D5D knockdown cells with DGLA treatment.

HCA-7 colony 29 cells were transfected with 150 nM of control siRNA or D5D siRNA, and then treated with 100 μM of DGLA for 48 h. (A) Profiles of DGLA and AA in cell culture medium, (B) Profiles of PGE₁ and PGE₂ in cell culture medium. DGLA, AA, PGE₁ and PGE₂ were quantified with the internal standards DGLA-d₆, AA-d₈, PGE₁-d₄ and PGE₂-d₉, respectively. Data are expressed as means \pm SD from $n \geq 3$.

Without the inhibition of D5D expression, in control cells the ratios of both DGLA vs. AA and PGE₁ vs. PGE₂ were close to 1 after 48 h (Fig. 14). In the D5D knockdown cells, the amounts of both AA and PGE₂ were very low, close to the level that was measured in the cells without exogenous DGLA added (data not shown). Compared to the co-treatment with DGLA

and CP-24879, the formation of PGE₁ was significantly increased and PGE₂ was significantly decreased in the D5D knockdown cells.

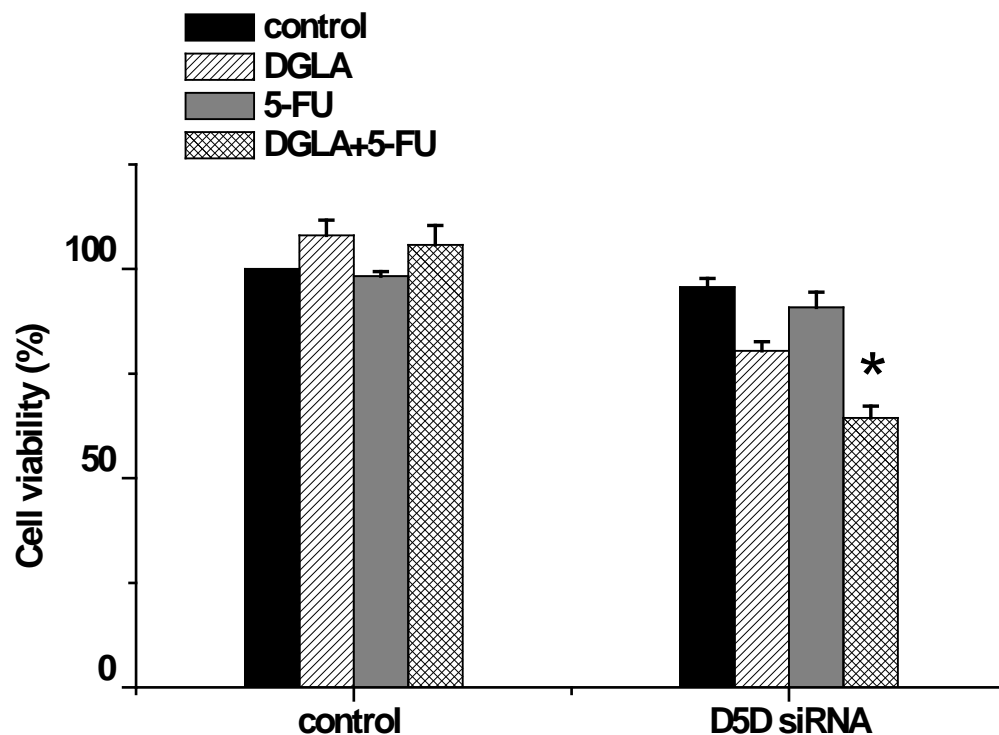


Fig. 36. Cell proliferation assays in D5D knockdown cells.

Cells were transfected with 150 nM of control siRNA and D5D siRNA, respectively, and then treated with 100 μ M DGLA, 0.2 μ M 5-FU and 100 μ M DGLA+0.2 μ M 5-FU for 48 h. Data represent the mean \pm SD derived from three separate experiments with triplicate wells per condition. Note that % cell viability was compared with the control group. The transfection procedure was described in Materials and Methods. (*) $P < 0.01$, significantly different from control.

The synergistic effect of DGLA and 5-FU on cytotoxicity in D5D knockdown cells was also evaluated (Fig. 36). The transfected cells were treated with DGLA, 5-FU, or DGLA+5-FU for 48 h and the cell proliferation was examined *via* the MTS assay. In D5D knockdown cells, DGLA alone was able to exert significant inhibition on cell growth, and it increased the cytotoxicity of 5-FU in the combined treatment (Fig. 36). No inhibitory effect was observed in the control cells. The concentration of 5-FU used in this study was 0.2 mM. The combination of

5-FU and DGLA in D5D knockdown cells decreased cell viability more than the combined treatment of DGLA, CP-24879 and 5-FU at the same concentrations (Fig. 32).

In D5D knockdown cells, the biosynthesis of AA was completely blocked. AA-derived free radical metabolites were not detectable, and the DGLA-derived free radical metabolites increased significantly. Compared to the results showed in Fig. 32, siRNA transfection was better at suppressing the expression of D5D, which resulted in the anti-proliferative effect of DGLA.

In summary, when the conversion from DGLA to AA was inhibited, DGLA exhibited an anti-proliferative effect which was associated with the enhancement of the formation of DGLA-derived free radicals and reduction of the formation of AA-derived free radicals. Thus, targeting D5D instead of COX-2 is a new approach which could be used in the control of colon cancer growth and progression.

CHAPTER 6. SUMMARY, DICUSSION AND FUTURE DIRECTIONS

6.1. Introduction

The typical western diet enriched in ω -6 PUFAs (mainly LA) is associated with an increased risk of cancer and other inflammation-related diseases. LA in the diet is converted to DGLA and then AA through a series of desaturation and elongation actions in the body (Scheme 1). As the most abundant ω -6 PUFA in mammalian cells, AA is metabolized to the pro-inflammatory PGE₂ through COX. DGLA, the upstream fatty acid of AA, is also a substrate for COX and is converted to the anti-inflammatory PGE₁ (Scheme 2). PGE₂ and PGE₁ are well-known lipid signaling molecules that participate in various physiological and pathological actions by activating the PKA signaling pathway through EP receptors. In general, PGE₂ and PGE₁ were believed to be corresponded to the opposing effects of AA *vs.* DGLA. However, the structures of PGE₂ and PGE₁ are similar (PGE₁ only missing one double bond in the structure). Thus, it could be problematic for them to exert opposing activities if they bind to the same receptor(s).

COX catalyzes PUFA peroxidation through a series of free radical reactions. In COX-catalyzed PUFA peroxidation, in addition to PGEs and other type of PGs, several free radicals, the most reactive intermediate metabolites, were also formed. However, due to their highly reactive nature, AA and DGLA derived individual free radicals had not been characterized in cells, therefore, their possible role in cancer progression and prevention still remained a mystery. In order to understand the possible association between those free radicals and colon cancer growth, for the first time we successfully characterized free radicals formed from cellular COX-catalyzed AA and DGLA peroxidation *via* refined LC/MS method along with SPE using the human colon cancer cell line HCA-7 colony 29, a cell line with high COX-2 expression. This

new technique allowed us to profile free radicals (as hydroxylamines) for the first time to characterize free radicals in cells under normal growth conditions in which other biological parameter could also be assessed.

6.2. Summary of Research Data

6.2.1. Summary of chapter 3: detection and characterization of free radicals from COX/AA and COX/DGLA in cells

Common and exclusive free radicals as the reduced forms were identified and characterized in COX-catalyzed AA vs. DGLA peroxidation in cells (Table 6). The $\bullet\text{C}_6\text{H}_{13}\text{O}$ radical was the free radical generated in common from both COX/AA and COX/DGLA peroxidation. The $\bullet\text{C}_{14}\text{H}_{21}\text{O}_4$ radical was the exclusive free radical from COX/AA, and the $\bullet\text{C}_7\text{H}_{13}\text{O}_2$ and $\bullet\text{C}_8\text{H}_{14}\text{O}_3$ radicals were the exclusive free radicals from COX/DGLA.

Table 6. Common and exclusive free radicals in COX/AA vs. COX/DGLA

	Common Radicals	Exclusive Radicals
COX/AA	$\bullet\text{C}_6\text{H}_{13}\text{O}$	$\bullet\text{C}_{14}\text{H}_{21}\text{O}_4$
COX/DGLA	$\bullet\text{C}_6\text{H}_{13}\text{O}$	$\bullet\text{C}_7\text{H}_{13}\text{O}_2$ and $\bullet\text{C}_8\text{H}_{14}\text{O}_3$

6.2.2. Summary of chapter 4: assessment of the association between AA-/DGLA-derived free radicals and colon cancer cell growth

According to our data (Table 3 and Fig. 22), AA clearly promoted the growth of HCA-7 colony 29 cells, while DGLA may have the opposite effect depend on the way to treat cells. However, due to the rapid conversion from DGLA to AA by D5D in cells, the anti-proliferative effect of DGLA could be abolished, and the generated AA (from DGLA) exerts pro-tumorigenic effect. A close correlation between free radicals and cell growth was revealed for the first time with our refined method.

Because PUFA-derived free radicals cannot be synthesized to test them on cells due to their very short lifetimes, the related free radical derivatives (Table 4) were selected and used to test for individual bioactivity. Among the tested free radical derivatives, the derivatives corresponding to the DGLA-derived exclusive free radical (8-hydroxyoctanoic acid) showed the most inhibitory effect on cell growth comparing with those effects from other tested radical derivatives and PGEs. PGE₁ did not show an anti-proliferative effect on cell growth at the tested concentration. Thus, the anti-proliferative effect of DGLA may associate with the DGLA-derived exclusive free radicals metabolites.

Due to the lack of commercially available derivatives, the exclusive radical $\bullet\text{C}=\text{C}$ ($\bullet\text{C}_{14}\text{H}_{21}\text{O}_4$) from COX/AA peroxidation was not yet to be tested for the effect on cell growth. We anticipate that this special radical may be closely corresponded to the pro-carcinogenic effect of AA and future studies will be conducted.

6.2.3. Summary of chapter 4: double dose of DGLA attenuates colon cancer cell growth

In order to increase the level of the anti-proliferative DGLA-derived free radical metabolites, double doses of DGLA were used to raise the level of DGLA in cells to compete with its downstream fatty acid, AA, for COX. Double doses of DGLA inhibited cell proliferation compared to the cells treated with a single dose of DGLA after 48 h (Fig. 22).

However, no significant difference was observed compared to the control treatment (0.01% ethanol, Fig. 22), probably due to the presence of the AA-derived exclusive free radical metabolites. In addition, although in double doses of DGLA treatment the ratio between DGLA-derived exclusive free radical metabolites vs. AA-derived exclusive free radical metabolites decreased compared to the single dose DGLA treatment, the decrease of AA-derived radical was

not enough to fully restore the anti-proliferative effect of DGLA. Thus, other options that could reciprocally regulate the level of DGLA and AA in cells should be considered.

6.2.4. Summary of chapter 5: blocking D5D activity inhibits cell proliferation and sensitizes cells to chemotherapy drugs

To raise the ratio between the anti-proliferative DGLA- vs. pro-proliferative AA-derived free radical metabolites, we also inhibit the biosynthesis of AA from DGLA treatment, including decreasing D5D activity with enzyme inhibitors and silencing D5D gene expression by siRNA transfection. Among the tested D5D inhibitors, *e.g.* sesamin, curcumin and CP-24879, CP-24879 was the most effective: 1) it decreased the AA-derived free radical metabolites and concurrently increased the DGLA-derived free radical metabolites; 2) DGLA combined with CP-24879 decreased cell proliferation compared to the DGLA alone and double dose-DGLA treatments; and 3) however, CP-24879 did not completely block the biosynthesis of AA, although it delayed and decreased the production of AA-derived free radical.

Transfecting HCA-7 colony 29 with siRNA diminished the expression of D5D, which resulted in the full recovery of the anti-proliferative effect of DGLA. In D5D knockdown cells, the biosynthesis of AA was completely blocked. AA-derived free radical metabolites were not detectable, and the DGLA-derived free radical metabolites increased significantly.

Targeting D5D was able to decrease the pro-proliferative AA-derived free radical metabolites and simultaneously increased anti-proliferative DGLA-derived free radical metabolites. The combined treatment with DGLA and D5D inhibitors also increased the susceptibility of colon cancer cells to the chemotherapy drug 5-FU. In the D5D knockdown cells, the synergistic effects of DGLA and 5-FU are more significant for cell growth inhibition and cytotoxicity probably through the activation of the pro-apoptosis signaling pathway, *e.g.* p53.

In conclusion, our refined spin-trapping, LC/MS method along with SPE allowed us to detect and profile the free radicals in the same experimental setting in which the cell proliferation and cell cycle distribution could also be assessed. The opposite effects of DGLA and AA were associated with their exclusive free radical metabolites, rather than the PGEs. Suppressing D5D activity with D5D inhibitors or silencing the D5D expression by siRNA knockdown increased the content of DGLA-derived metabolites *vs.* AA-derived metabolites, thus inhibiting cell proliferation. Our data could be used to guide that DGLA is a beneficial ω -6 fatty acid, and an appropriate dietary intervention with a balanced ratio of cellular DGLA *vs.* AA could control colon cancer growth and progression.

6.3. Discussion

In order to investigate the association between cancer cell growth and free radicals generated from COX-catalyzed AA *vs.* DGLA peroxidation, we have for the first time characterized free radicals formed from HCA-7 colony 29 cells under normal growing conditions. Unlike the cell-PBS system (Figs. 2 and 3), in which large doses of POBN and PUFAs must be introduced to generate enough free radicals to be trapped and measured, our refined spin-trapping experiment grew cells in a normal culture medium with a much lower concentration of POBN and PUFAs. In addition, instead of measuring ESR-active radical adducts, we actually measured a reduced form (hydroxylamines, Scheme 12) of the POBN adducts using LC/MS and LC/MS², since hydroxylamines are much more stable redox forms of spin adducts than ESR-active POBN adducts, especially in cell culture media.

Our data suggested that in both COX-catalyzed DGLA and AA systems, 8 h and 12 h incubation seem to be the critical time points for free radical formation. The overall radical production in both peroxidation systems accumulated and approached a peak at about 12 h (Figs.

11 and 12). Considering POBN's decreased trapping ability in culture media, in reality the radical production would be at a plateau after 12 h. The exclusive radical products, *i.e.*, the m/z 449 hydroxylamine as the reduced product of POBN/ \bullet C₁₄H₂₁O₄, and the m/z 355 and m/z 325 hydroxylamines as reduced products of POBN/ \bullet C₈H₁₅O₃ and POBN/ \bullet C₇H₁₃O₂, generated from COX-catalyzed AA and DGLA, respectively, started to show up at 8 h. The appearance of the hydroxylamine of m/z 449 (referring to \bullet C₁₄H₂₁O₄) was much delayed (with much less produced as well) compared to the hydroxylamine of m/z 297 (referring to \bullet C₆H₁₃O). These two free radicals were expected to form at the same time points and in similar quantities since they are two co-metabolites fragmenting from the same product through β' -scission of PGF₂-alkoxyl radicals as proposed elsewhere ([171], Scheme 10). The delayed appearance of m/z 449 suggested that β' -scission could also occur on alkoxyl radicals derived from other types of PGs (PGH₂ *etc.*) during COX-catalyzed AA peroxidation, instead of taking place at the PGF₂ stage [171] in which the \bullet C=C radical, whose adduct was reduced to the m/z 449 hydroxylamine, was formed at the same time as the hydroxylamine of m/z 297. Again, β' -scission of a PGH₁-type alkoxyl radical did not result in a \bullet C=C radical from DGLA ([173], Scheme 11) that could form \bullet C₁₄H₂₁O₄ as in AA peroxidation.

In addition, the formation of a similar amount of the hydroxylamine of m/z 449 (asterisked in Fig. 12B), as the hydroxylamines of m/z 355 and m/z 325 during COX-catalyzed peroxidation in cells treated by DGLA (12 h to 48 h), suggested that once formed (converted from DGLA by D5D), AA is a more favored substrate than DGLA for COX peroxidation. The formation peak of AA (from DGLA) was found at 8 h, although the concentration of DGLA was still much higher than AA (~5-6 fold, Fig. 14A). DGLA can be very effectively converted to AA; in turn both fatty acids competitively compete with each other for COX peroxidation. When cells

were incubated with AA, neither DGLA nor the DGLA-exclusive hydroxylamines of m/z 355 and m/z 325 were detected. However, a considerable amount of m/z 449 was detected as early as 8 h (Fig. 12B).

The formation of the hydroxylamine of m/z 449 was generally associated with cell growth promotion. The sustained G₂ phase cell cycle arrests were observed at the time points and the treatments in which the hydroxylamine of m/z 449 was barely measurable. For example, treatment of DGLA ~ 8 h was correlated with sustained G₂ phase cell cycle arrest, while the combined treatment with DGLA and CP-24879 was correlated with sustained G₂ phase cell cycle arrest within one day. The considerable abundance of the hydroxylamine of m/z 449 formed in cells after treatment with AA (8 h to 24 h, Fig. 11B) and the one-day DGLA treatment was correlated with a lack of any difference in G₂ phase cell cycle distribution *vs.* the control.

The two series of prostaglandins, PGs1 and PGs2, are well-known bioactive metabolites. Unlike PGs2s, which are generally viewed as pro-inflammatory and pro-carcinogenic PGs, PGs1s may possess anti-inflammatory and anti-cancer activity. However, some research studies of PGs on cell growth were considered somewhat unrealistic since much higher concentrations of PGs (particularly PGE₁) were used than the concentrations that could form under normal cell culture conditions with fatty acid supplementation. It was reported that no more than 13 nM of PGEs could form from cultured cells without a fatty acid supplement [225-228]. The colon cancer cell (HT-29) growth could be stimulated by up to 45% by PGE₂ at a range of concentrations from 0.5 μM to 10 μM [204]. At a similar concentration, PGE₂ could also induce the expression of vascular endothelial growth factor, one of the major regulators for LS-174T cell angiogenesis, thus exerting pro-oncogenic actions in colorectal carcinogenesis [205]. On the other hand, a dose of PGE₁ (30 μg/mL) was reported to inhibit the proliferation of HeLa cells

[185] and B16-F10 cells [70]. However, at lower doses (3.0 $\mu\text{g/mL}$), PGE_1 could not inhibit cell proliferation, and even increased cell growth [185].

In our experiments, no more than 0.12 μM of PGEs (2×10^6 cells, Figs. 13 and 14) could actually be detected from the 100 μM PUFA treatments. However, when a range of 0.01 μM to 1.0 μM PGE (~ 40 to 4000 fold higher than the PGEs per number of cells actually formed and measured in our experiments) was used to directly treat an HCA-7 colony with 29 cells (5×10^3 cells) in our study, neither PGE_1 nor PGE_2 showed much effect on cell proliferation (Fig. 16). The inconsistent cell growth responses from the PUFA treatment (Table 3) and the PGEs used to directly treat cells (Fig. 16) suggested that rather than PGEs, free radicals and derivatives should be considered for their possible bioactivities. Interestingly, inhibited cell proliferation effects were observed from some of the tested free radical derivatives (Fig. 17) at the same concentrations as the PGEs in Fig. 16. The 8-hydroxyoctanoic acid (a derivative of $\bullet\text{C}_8\text{H}_{15}\text{O}_3$ as an exclusive product from 8-C oxygenation in COX catalyzed DGLA peroxidation) showed some anti-proliferation effects, while another exclusive radical ($\bullet\text{C}_7\text{H}_{13}\text{O}_2$), a derivative from the 8-C oxygenation of DGLA (heptanoic acid), did not affect cell proliferation. However, as the common and major product from 15-C oxygenation of both AA and DGLA, 1-hexanol (a derivative of $\bullet\text{C}_6\text{H}_{13}\text{O}$) was also correlated with inhibition of cell proliferation.

Although no mechanism has so far been defined for the tested exclusive free radical derivatives, our results suggest that the radical metabolites derived from C-8 oxygenation of DGLA had an inhibitory effect on colon cancer cell growth. In addition, based on the time course of $\bullet\text{C}=\text{C}$ radical generation and the related cell growth response (Fig. 11B and Table 3), it is logical to propose that $\bullet\text{C}_{14}\text{H}_{21}\text{O}_4$ or its derivative corresponds with AA-promoted cell growth. A future goal is to study the effect of the $\bullet\text{C}_{14}\text{H}_{21}\text{O}_4$ radical on cell growth by selecting or

synthesizing similar compounds and their derivatives to further explore COX peroxidation and AA bioactivity. Finally, the data in this study indicate that the novel free radicals as well as the related radical derivatives formed from COX peroxidation should be the new targets to be tested for their promoting or inhibiting effect on cancer cell growth. Understanding these radicals and their related radical reactions may allow us to advance our knowledge of the mechanisms of PUFA's bioactivity in cancer biology.

Three D5D inhibitors, *e.g.* sesamin, curcumin and CP-24879, were tested for their effect on suppressing D5D activity. Our data suggested that sesamin did not inhibit the conversion from DGLA to AA (Fig. 31), due to the poor solubility of sesamin in the cell culture medium. It was reported that sesamin inhibits the conversion of DGLA to AA with a K_i value of 155 μM in rat liver microsomes [215]. However, the highest final concentration that sesamin was able to achieve in the cell culture medium was 100 μM . were also tested; however, the excess sesamin formed crystals in the medium, *e.g.*, 150 and 200 μM .

In the case of curcumin, when the concentration of curcumin was varied from 5 to 50 μM in the curcumin-DGLA treatment, the lowest tested concentration (5 μM) did not affect D5D activity in cells, while it did inhibit PGEs biosynthesis (data not shown). These results suggest that curcumin is not a specific inhibitor for D5D.

HCA-7 colony 29 was not sensitive to the chemotherapy drug 5-FU which is widely used in the treatment of colon cancer (Fig. 32). 5-FU induced anti-cancer effects and toxicity, including blocking DNA synthesis, inducing translational errors, and regulating the pro-apoptosis genes p53, p21 and BAX [220-222]. Treatment with both CP-24879 and DGLA restored the anti-proliferative effect of DGLA, enhancing the DGLA-derived free radical metabolites that may have an anti-carcinogenic effect through causing DNA lesions and

activating tumor suppressors such as p53. Thus, the synergistic effects of DGLA with 5-FU might be due to their co-effect in causing DNA damage and activating pro-apoptosis genes.

6.4. Future Directions

6.4.1. Study of the association between the AA-derived exclusive free radical and colon cancer cell growth

Among the four free radicals detected in cellular COX-catalyzed AA and DGLA peroxidation, the corresponding derivatives (in alcohol form) of $\bullet\text{C}_6\text{H}_{13}\text{O}$ (the common free radical generated from both COX/AA and COX/DGLA peroxidation), $\bullet\text{C}_7\text{H}_{13}\text{O}_2$ and $\bullet\text{C}_8\text{H}_{14}\text{O}_3$ (two exclusive free radicals from COX/DGLA) were used to test the effects of the parent free radicals on the growth of HCA-7 colony 29. Our results (Fig. 17) showed that the derivatives corresponding to one DGLA-derived exclusive free radical (8-hydroxyoctanoic acid) had the most inhibitory effect on cell growth. We also expected that the AA-derived exclusive free radical ($\bullet\text{C}_{14}\text{H}_{21}\text{O}_4$) should have a pro-proliferative effect. However, the derivative of this particular free radical was not commercially available, thus its role in regulating colon cancer cell growth is not yet clear. In the future, we will synthesis a compound structurally close to $\bullet\text{C}_{14}\text{H}_{21}\text{O}_4$ and test its effect on cell growth. The results will help us get a better understanding of the pro-tumorigenic role of AA in cancer biology.

6.4.2. Study of the roles of AA-and DGLA-derived free radicals' metabolism in signal transduction

AA and DGLA have opposing effects on colon cancer cell growth. AA promotes cell proliferation while DGLA inhibits cell growth. Since our results showed that the PGEs at physiological concentration were not responsible for the contrasting effects of AA vs. DGLA, we concluded that that was associated with their exclusive free radical metabolites. The role of free

radicals in carcinogenesis is complex. Most cancer types have increased generation of free radicals, which can react with DNA, proteins and lipids in the body and cause extensive oxidative damage. The increased free radicals can lead to DNA strand breaks, point mutations and aberrant DNA crossing-linking, contributing to carcinogenesis by mutating proto-oncogenes and suppress tumor suppressor genes.

We proposed that the newly characterized lipid mediators, AA-derived exclusive free radical metabolites and DGLA-derived exclusive free radical metabolites, may act through different mechanisms. AA-derived free radical metabolites may provoke the pro-tumorigenic pathway by activate the oncogene, *e.g.* epidermal growth factor receptor (EGFR) and Human Epidermal Growth Factor Receptor 2 (HER2); while DGLA-derived free radical metabolites may induce the pro-apoptotic pathway activate the apoptotic genes such as p53, p21 and BAX. The underlying mechanism will be further studied using the free radical derivatives. The results will make a clear association between the exclusive free radical metabolites from COX/AA and COX/DGLA and the contrasting bioactivities of AA *vs.* DGLA, and ultimately reveal the full role of COX/DGLA in cancer biology.

6.4.3. Study of the inhibitory mechanism of D5D and search for new inhibitors

D5D is the rate-limiting enzyme responsible for the biosynthesis of AA from DGLA. Suppressing D5D expression was seen to decrease cell proliferation. Accordingly, the content of AA and AA-derived pro-proliferative metabolites significantly decreased. In the meantime, DGLA and DGLA-derived anti-proliferative metabolites increased. Our results indicated that D5D is a potentially critical factor for tumorigenesis, and that targeting this enzyme could be effective in suppressing tumor growth. So far, there have been only very limited studies targeting D5D, and only a few inhibitors have been identified. None of them are very specific inhibitors

and the inhibitory mechanism was not clear. There is an increasing need for developing new D5D inhibitors and elucidating the mechanism of their action. An effective D5D inhibitor has a potential use as an anti-cancer drug to reduce cancer growth.

6.4.4. Investigation of the effect of normal diet in a D5D knockout mouse model

LA is the most abundant ω -6 PUFA in normal diet which was enriched with corn oil. LA was converted to DGLA first, and then convert to AA *via* D5D in our body. We found that inhibit the conversion form DGLA to AA in cells could attenuate colon cancer cell growth. Thus, the use of D5D inhibitors or D5D knockdown may be useful for study the role of DGLA in cancer development. An animal model could be used to investigate whether a supplement of ω -6 rich diet with D5D inhibitors could control tumor growth. Furthermore, a novel D5D knockout mouse model has recently been generated and characterized [229]. The D5D knockout resulted in the depletion of AA and massive enhancement of DGLA, which is consisted with the reduction in intestinal crypt proliferation [229]. Hence, in future studies, this AA-deficient mouse model will be used to investigate the mechanism of the protective and therapeutic role of DGLA in cancer development.

REFERENCES

- [1] Calder, P. C. Polyunsaturated fatty acids and inflammation. *Biochemical Society transactions* **33**:423-427; 2005.
- [2] Schmitz, G.; Ecker, J. The opposing effects of n-3 and n-6 fatty acids. *Progress in lipid research* **47**:147-155; 2008.
- [3] Das, U. N. Essential Fatty acids - a review. *Curr Pharm Biotechnol* **7**:467-482; 2006.
- [4] Das, U. N. Biological significance of essential fatty acids. *The Journal of the Association of Physicians of India* **54**:309-319; 2006.
- [5] Das, U. N. Essential fatty acids: biochemistry, physiology and pathology. *Biotechnology journal* **1**:420-439; 2006.
- [6] Ollis, T. E.; Meyer, B. J.; Howe, P. R. Australian food sources and intakes of omega-6 and omega-3 polyunsaturated fatty acids. *Annals of nutrition & metabolism* **43**:346-355; 1999.
- [7] Horrobin, D. F. The regulation of prostaglandin biosynthesis by the manipulation of essential fatty acid metabolism. *Reviews in pure & applied pharmacological sciences* **4**:339-383; 1983.
- [8] Bezdard, J.; Blond, J. P.; Bernard, A.; Clouet, P. The metabolism and availability of essential fatty acids in animal and human tissues. *Reproduction, nutrition, development* **34**:539-568; 1994.
- [9] Zhou, L.; Nilsson, A. Sources of eicosanoid precursor fatty acid pools in tissues. *Journal of lipid research* **42**:1521-1542; 2001.
- [10] Sargent, J. R. Fish oils and human diet. *The British journal of nutrition* **78 Suppl 1**:S5-13; 1997.
- [11] Larsson, S. C.; Kumlin, M.; Ingelman-Sundberg, M.; Wolk, A. Dietary long-chain n-3 fatty acids for the prevention of cancer: a review of potential mechanisms. *The American journal of clinical nutrition* **79**:935-945; 2004.
- [12] Mozaffarian, D.; Ascherio, A.; Hu, F. B.; Stampfer, M. J.; Willett, W. C.; Siscovick, D. S.; Rimm, E. B. Interplay between different polyunsaturated fatty acids and risk of coronary heart disease in men. *Circulation* **111**:157-164; 2005.
- [13] Melin, T.; Nilsson, A. Delta-6-desaturase and delta-5-desaturase in human Hep G2 cells are both fatty acid interconversion rate limiting and are unregulated under essential fatty acid deficient conditions. *Prostag Leukotr Ess* **56**:437-442; 1997.
- [14] Cho, H. P.; Nakamura, M.; Clarke, S. D. Cloning, expression, and fatty acid regulation of the human delta-5 desaturase. *The Journal of biological chemistry* **274**:37335-37339; 1999.
- [15] Rouzer, C. A.; Marnett, L. J. Endocannabinoid oxygenation by cyclooxygenases, lipoxygenases, and cytochromes P450: cross-talk between the eicosanoid and endocannabinoid signaling pathways. *Chemical reviews* **111**:5899-5921; 2011.
- [16] Buczynski, M. W.; Dumlao, D. S.; Dennis, E. A. Thematic Review Series: Proteomics. An integrated omics analysis of eicosanoid biology. *Journal of lipid research* **50**:1015-1038; 2009.
- [17] Fan, Y. Y.; Chapkin, R. S. Importance of dietary gamma-linolenic acid in human health and nutrition. *The Journal of nutrition* **128**:1411-1414; 1998.
- [18] Robinson, J. G.; Ijioma, N.; Harris, W. Omega-3 fatty acids and cognitive function in women. *Womens Health (Lond Engl)* **6**:119-134; 2010.
- [19] Funk, C. D. Prostaglandins and leukotrienes: advances in eicosanoid biology. *Science* **294**:1871-1875; 2001.

- [20] Patterson, E.; Wall, R.; Fitzgerald, G. F.; Ross, R. P.; Stanton, C. Health implications of high dietary omega-6 polyunsaturated Fatty acids. *Journal of nutrition and metabolism* **2012**:539426; 2012.
- [21] Simopoulos, A. P. The importance of the ratio of omega-6/omega-3 essential fatty acids. *Biomedicine & pharmacotherapy = Biomedecine & pharmacotherapie* **56**:365-379; 2002.
- [22] Calder, P. C.; Yaqoob, P. Omega-3 polyunsaturated fatty acids and human health outcomes. *Biofactors* **35**:266-272; 2009.
- [23] Woutersen, R. A.; Appel, M. J.; van Garderen-Hoetmer, A.; Wijnands, M. V. Dietary fat and carcinogenesis. *Mutation research* **443**:111-127; 1999.
- [24] Calder, P. C. Dietary modification of inflammation with lipids. *P Nutr Soc* **61**:345-358; 2002.
- [25] Simopoulos, A. P.; Leaf, A.; Salem, N., Jr. Essentiality of and recommended dietary intakes for omega-6 and omega-3 fatty acids. *Annals of nutrition & metabolism* **43**:127-130; 1999.
- [26] Simopoulos, A. P.; Leaf, A.; Salem, N., Jr. Workshop on the Essentiality of and Recommended Dietary Intakes for Omega-6 and Omega-3 Fatty Acids. *Journal of the American College of Nutrition* **18**:487-489; 1999.
- [27] Simopoulos, A. P. The importance of the omega-6/omega-3 fatty acid ratio in cardiovascular disease and other chronic diseases. *Exp Biol Med* **233**:674-688; 2008.
- [28] Kremmyda, L. S.; Tvrzicka, E.; Stankova, B.; Zak, A. Fatty acids as biocompounds: their role in human metabolism, health and disease: a review. part 2: fatty acid physiological roles and applications in human health and disease. *Biomedical papers of the Medical Faculty of the University Palacky, Olomouc, Czechoslovakia* **155**:195-218; 2011.
- [29] Simopoulos, A. P. Omega-3 fatty acids in inflammation and autoimmune diseases. *Journal of the American College of Nutrition* **21**:495-505; 2002.
- [30] Berquin, I. M.; Edwards, I. J.; Chen, Y. Q. Multi-targeted therapy of cancer by omega-3 fatty acids. *Cancer letters* **269**:363-377; 2008.
- [31] Kelly, F. J. The metabolic role of n-3 polyunsaturated fatty acids: relationship to human disease. *Comparative biochemistry and physiology. A, Comparative physiology* **98**:581-585; 1991.
- [32] Takai, S.; Jin, D.; Kawashima, H.; Kimura, M.; Shiraishi-Tateishi, A.; Tanaka, T.; Kakutani, S.; Tanaka, K.; Kiso, Y.; Miyazaki, M. Anti-atherosclerotic effects of dihomo-gamma-linolenic acid in ApoE-deficient mice. *Journal of atherosclerosis and thrombosis* **16**:480-489; 2009.
- [33] Kapoor, R.; Huang, Y. S. Gamma linolenic acid: An antiinflammatory omega-6 fatty acid. *Curr Pharm Biotechno* **7**:531-534; 2006.
- [34] Madhavi, N.; Das, U. N. Effect of N-6 and N-3 Fatty-Acids on the Survival of Vincristine Sensitive and Resistant Human Cervical-Carcinoma Cells in-Vitro. *Cancer letters* **84**:31-41; 1994.
- [35] Itzkowitz, S. H.; Yio, X. Inflammation and cancer IV. Colorectal cancer in inflammatory bowel disease: the role of inflammation. *American journal of physiology. Gastrointestinal and liver physiology* **287**:G7-17; 2004.
- [36] Ullman, T. A.; Itzkowitz, S. H. Intestinal inflammation and cancer. *Gastroenterology* **140**:1807-1816; 2011.

- [37] De Marzo, A. M.; Platz, E. A.; Sutcliffe, S.; Xu, J.; Gronberg, H.; Drake, C. G.; Nakai, Y.; Isaacs, W. B.; Nelson, W. G. Inflammation in prostate carcinogenesis. *Nature reviews. Cancer* **7**:256-269; 2007.
- [38] Mantovani, A.; Allavena, P.; Sica, A.; Balkwill, F. Cancer-related inflammation. *Nature* **454**:436-444; 2008.
- [39] Whitcomb, D. C. Inflammation and cancer - V. Chronic pancreatitis and pancreatic cancer. *Am J Physiol-Gastr L* **287**:G315-G319; 2004.
- [40] Shen, H. M.; Tergaonkar, V. NF kappa B signaling in carcinogenesis and as a potential molecular target for cancer therapy. *Apoptosis* **14**:348-363; 2009.
- [41] Helbig, G.; Christopherson, K. W.; Bhat-Nakshatri, P.; Kumar, S.; Kishimoto, H.; Miller, K. D.; Broxmeyer, H. E.; Nakshatri, H. NF-kappa B promotes breast cancer cell migration and metastasis by inducing the expression of the chemokine receptor CXCR4. *Journal of Biological Chemistry* **278**:21631-21638; 2003.
- [42] Pikarsky, E.; Porat, R. M.; Stein, I.; Abramovitch, R.; Amit, S.; Kasem, S.; Gutkovich-Pyest, E.; Urieli-Shoval, S.; Galun, E.; Ben-Neriah, Y. NF-kappa B functions as a tumour promoter in inflammation-associated cancer. *Nature* **431**:461-466; 2004.
- [43] Greten, F. R.; Eckmann, L.; Greten, T. F.; Park, J. M.; Li, Z. W.; Egan, L. J.; Kagnoff, M. F.; Karin, M. IKKbeta links inflammation and tumorigenesis in a mouse model of colitis-associated cancer. *Cell* **118**:285-296; 2004.
- [44] Liu, W.; Reinmuth, N.; Stoeltzing, O.; Parikh, A. A.; Tellez, C.; Williams, S.; Jung, Y. D.; Fan, F.; Takeda, A.; Akagi, M.; Bar-Eli, M.; Gallick, G. E.; Ellis, L. M. Cyclooxygenase-2 is up-regulated by interleukin-1 beta in human colorectal cancer cells via multiple signaling pathways. *Cancer research* **63**:3632-3636; 2003.
- [45] Mifflin, R. C.; Saada, J. I.; Di Mari, J. F.; Adegboyega, P. A.; Valentich, J. D.; Powell, D. W. Regulation of COX-2 expression in human intestinal myofibroblasts: mechanisms of IL-1-mediated induction. *American journal of physiology. Cell physiology* **282**:C824-834; 2002.
- [46] Newton, R.; Kuitert, L. M.; Bergmann, M.; Adcock, I. M.; Barnes, P. J. Evidence for involvement of NF-kappaB in the transcriptional control of COX-2 gene expression by IL-1beta. *Biochemical and biophysical research communications* **237**:28-32; 1997.
- [47] Prosperi, J. R.; Mallery, S. R.; Kigerl, K. A.; Erfurt, A. A.; Robertson, F. M. Invasive and angiogenic phenotype of MCF-7 human breast tumor cells expressing human cyclooxygenase-2. *Prostaglandins & other lipid mediators* **73**:249-264; 2004.
- [48] Cha, Y. I.; DuBois, R. N. NSAIDs and cancer prevention: targets downstream of COX-2. *Annu Rev Med* **58**:239-252; 2007.
- [49] Ding, Y. F.; Tong, M.; Liu, S. Q.; Moscow, J. A.; Tai, H. H. NAD(+)-linked 15-hydroxyprostaglandin dehydrogenase (15-PGDH) behaves as a tumor suppressor in lung cancer. *Carcinogenesis* **26**:65-72; 2005.
- [50] Wolf, I.; O'Kelly, J.; Rubinek, T.; Tong, M.; Nguyen, A.; Lin, B. T.; Tai, H. H.; Karlan, B. Y.; Koeffler, H. P. 15-hydroxyprostaglandin dehydrogenase is a tumor suppressor of human breast cancer. *Cancer research* **66**:7818-7823; 2006.
- [51] Backlund, M. G.; Mann, J. R.; Holla, V. R.; Buchanan, F. G.; Tai, H. H.; Musiek, E. S.; Milne, G. L.; Katkuri, S.; DuBois, R. N. 15-hydroxyprostaglandin dehydrogenase is down-regulated in colorectal cancer. *Journal of Biological Chemistry* **280**:3217-3223; 2005.
- [52] Hata, A. N.; Breyer, R. M. Pharmacology and signaling of prostaglandin receptors: multiple roles in inflammation and immune modulation. *Pharmacology & therapeutics* **103**:147-166; 2004.

- [53] Gupta, R. A.; Tan, J.; Krause, W. F.; Geraci, M. W.; Willson, T. M.; Dey, S. K.; DuBois, R. N. Prostacyclin-mediated activation of peroxisome proliferator-activated receptor delta in colorectal cancer. *Proceedings of the National Academy of Sciences of the United States of America* **97**:13275-13280; 2000.
- [54] Sugimoto, Y.; Narumiya, S. Prostaglandin E receptors. *The Journal of biological chemistry* **282**:11613-11617; 2007.
- [55] Mutoh, M.; Watanabe, K.; Kitamura, T.; Shoji, Y.; Takahashi, M.; Kawamori, T.; Tani, K.; Kobayashi, M.; Maruyama, T.; Kobayashi, K.; Ohuchida, S.; Sugimoto, Y.; Narumiya, S.; Sugimura, T.; Wakabayashi, K. Involvement of prostaglandin E receptor subtype EP(4) in colon carcinogenesis. *Cancer research* **62**:28-32; 2002.
- [56] Sonoshita, M.; Takaku, K.; Sasaki, N.; Sugimoto, Y.; Ushikubi, F.; Narumiya, S.; Oshima, M.; Taketo, M. M. Acceleration of intestinal polyposis through prostaglandin receptor EP2 in Apc(Delta 716) knockout mice. *Nat Med* **7**:1048-1051; 2001.
- [57] Regan, J. W. EP2 and EP4 prostanoid receptor signaling. *Life sciences* **74**:143-153; 2003.
- [58] Fujino, H.; West, K. A.; Regan, J. W. Phosphorylation of glycogen synthase kinase-3 and stimulation of T-cell factor signaling following activation of EP2 and EP4 prostanoid receptors by prostaglandin E2. *The Journal of biological chemistry* **277**:2614-2619; 2002.
- [59] Fujino, H.; Xu, W.; Regan, J. W. Prostaglandin E2 induced functional expression of early growth response factor-1 by EP4, but not EP2, prostanoid receptors via the phosphatidylinositol 3-kinase and extracellular signal-regulated kinases. *The Journal of biological chemistry* **278**:12151-12156; 2003.
- [60] Buchanan, F. G.; Wang, D.; Bargiacchi, F.; DuBois, R. N. Prostaglandin E2 regulates cell migration via the intracellular activation of the epidermal growth factor receptor. *The Journal of biological chemistry* **278**:35451-35457; 2003.
- [61] Han, S.; Roman, J. Suppression of prostaglandin E2 receptor subtype EP2 by PPARgamma ligands inhibits human lung carcinoma cell growth. *Biochemical and biophysical research communications* **314**:1093-1099; 2004.
- [62] Baron, J. A. Aspirin and NSAIDs for the prevention of colorectal cancer. *Recent results in cancer research. Fortschritte der Krebsforschung. Progres dans les recherches sur le cancer* **181**:223-229; 2009.
- [63] Iwama, T. NSAIDs and colorectal cancer prevention. *Journal of gastroenterology* **44 Suppl 19**:72-76; 2009.
- [64] Olsen, J. H.; Friis, S.; Poulsen, A. H.; Fryzek, J.; Harving, H.; Tjonneland, A.; Sorensen, H. T.; Blot, W. Use of NSAIDs, smoking and lung cancer risk. *British journal of cancer* **98**:232-237; 2008.
- [65] Zhao, Y. S.; Zhu, S.; Li, X. W.; Wang, F.; Hu, F. L.; Li, D. D.; Zhang, W. C.; Li, X. Association between NSAIDs use and breast cancer risk: a systematic review and meta-analysis. *Breast Cancer Res Tr* **117**:141-150; 2009.
- [66] Watkins, G.; Martin, T. A.; Bryce, R.; Mansel, R. E.; Jiang, W. G. gamma-Linolenic acid regulates the expression and secretion of SPARC in human cancer cells. *Prostag Leukotr Ess* **72**:273-278; 2005.
- [67] Jiang, W. G.; Singhrao, S. K.; Hiscox, S.; Hallett, M. B.; Bryce, R. P.; Horrobin, D. F.; Puntis, M. C. A.; Mansel, R. E. Regulation of desmosomal cell adhesion in human tumour cells by polyunsaturated fatty acids. *Clin Exp Metastas* **15**:593-602; 1997.

- [68] Menendez, J. A.; Roper, S.; del Mar Barbacid, M.; Montero, S.; Solanas, M.; Escrich, E.; Cortes-Funes, H.; Colomer, R. Synergistic interaction between vinorelbine and gamma-linolenic acid in breast cancer cells. *Breast Cancer Res Tr* **72**:203-219; 2002.
- [69] Johnson, M. M.; Swan, D. D.; Surette, M. E.; Stegner, J.; Chilton, T.; Fonteh, A. N.; Chilton, F. H. Dietary supplementation with gamma-linolenic acid alters fatty acid content and eicosanoid production in healthy humans. *Journal of Nutrition* **127**:1435-1444; 1997.
- [70] Tabolacci, C.; Lentini, A.; Provenzano, B.; Gismondi, A.; Rossi, S.; Beninati, S. Similar antineoplastic effects of nimesulide, a selective COX-2 inhibitor, and prostaglandin E1 on B16-F10 murine melanoma cells. *Melanoma research* **20**:273-279; 2010.
- [71] Skuladottir, G. V.; Heidarsdottir, R.; Arnar, D. O.; Torfason, B.; Edvardsson, V.; Gottskalksson, G.; Palsson, R.; Indridason, O. S. Plasma n-3 and n-6 fatty acids and the incidence of atrial fibrillation following coronary artery bypass graft surgery. *European journal of clinical investigation* **41**:995-1003; 2011.
- [72] Williams, C. D.; Whitley, B. M.; Hoyo, C.; Grant, D. J.; Iraggi, J. D.; Newman, K. A.; Gerber, L.; Taylor, L. A.; McKeever, M. G.; Freedland, S. J. A high ratio of dietary n-6/n-3 polyunsaturated fatty acids is associated with increased risk of prostate cancer. *Nutr Res* **31**:1-8; 2011.
- [73] Hofmanova, J.; Vaculova, A.; Kozubik, A. Polyunsaturated fatty acids sensitize human colon adenocarcinoma HT-29 cells to death receptor-mediated apoptosis. *Cancer letters* **218**:33-41; 2005.
- [74] Levin, G.; Duffin, K. L.; Obukowicz, M. G.; Hummert, S. L.; Fujiwara, H.; Needleman, P.; Raz, A. Differential metabolism of dihomo-gamma-linolenic acid and arachidonic acid by cyclo-oxygenase-1 and cyclo-oxygenase-2: implications for cellular synthesis of prostaglandin E1 and prostaglandin E2. *The Biochemical journal* **365**:489-496; 2002.
- [75] Negishi, M.; Sugimoto, Y.; Ichikawa, A. Prostanoid Receptors and Their Biological Actions. *Progress in lipid research* **32**:417-434; 1993.
- [76] Fan, Y. Y.; Ramos, K. S.; Chapkin, R. S. Cell cycle related inhibition of mouse vascular smooth muscle cell proliferation by prostaglandin E1: relationship between prostaglandin E1 and intracellular cAMP levels. *Prostaglandins, leukotrienes, and essential fatty acids* **54**:101-107; 1996.
- [77] Sassone-Corsi, P. Transcription factors responsive to cAMP. *Annual review of cell and developmental biology* **11**:355-377; 1995.
- [78] Das, U. N. Essential fatty acids and their metabolites could function as endogenous HMG-CoA reductase and ACE enzyme inhibitors, anti-arrhythmic, anti-hypertensive, anti-atherosclerotic, anti-inflammatory, cytoprotective, and cardioprotective molecules. *Lipids in health and disease* **7**; 2008.
- [79] Iyu, D.; Juttner, M.; Glenn, J. R.; White, A. E.; Johnson, A. J.; Fox, S. C.; Heptinstall, S. PGE(1) and PGE(2) modify platelet function through different prostanoid receptors. *Prostaglandins & other lipid mediators* **94**:9-16; 2011.
- [80] Sawamura, H.; Hayashi, H.; Onozaki, K. Differential effects of prostaglandin E1 and prostaglandin E2 on growth and differentiation of murine myeloid leukemic cell line, M1. *Microbiology and immunology* **39**:809-815; 1995.
- [81] Noguchi, K.; Shitashige, M.; Endo, H.; Kondo, H.; Ishikawa, I. Binary regulation of interleukin (IL)-6 production by EP1 and EP2/EP4 subtypes of PGE2 receptors in IL-1beta-stimulated human gingival fibroblasts. *Journal of periodontal research* **37**:29-36; 2002.

- [82] Fedyk, E. R.; Phipps, R. P. Prostaglandin E2 receptors of the EP2 and EP4 subtypes regulate activation and differentiation of mouse B lymphocytes to IgE-secreting cells. *Proceedings of the National Academy of Sciences of the United States of America* **93**:10978-10983; 1996.
- [83] Kapoor, R.; Huang, Y. S. Gamma linolenic acid: an antiinflammatory omega-6 fatty acid. *Curr Pharm Biotechnol* **7**:531-534; 2006.
- [84] Ziboh, V. A.; Naguwa, S.; Vang, K.; Wineinger, J.; Morrissey, B. M.; Watnik, M.; Gershwin, M. E. Suppression of leukotriene B4 generation by ex-vivo neutrophils isolated from asthma patients on dietary supplementation with gammalinolenic acid-containing borage oil: possible implication in asthma. *Clinical & developmental immunology* **11**:13-21; 2004.
- [85] Celotti, F.; Durand, T. The metabolic effects of inhibitors of 5-lipoxygenase and of cyclooxygenase 1 and 2 are an advancement in the efficacy and safety of anti-inflammatory therapy. *Prostaglandins & other lipid mediators* **71**:147-162; 2003.
- [86] Rubin, D.; Laposata, M. Cellular Interactions between N-6 and N-3 Fatty-Acids - a Mass Analysis of Fatty-Acid Elongation/Desaturation, Distribution among Complex Lipids, and Conversion to Eicosanoids. *Journal of lipid research* **33**:1431-1440; 1992.
- [87] Fujimoto, A.; Shingai, Y.; Oyama, T. B.; Kawanai, T.; Hashimoto, E.; Koizumi, K.; Kimura, K.; Masuda, T.; Oyama, Y. Apoptosis-inducing action of two products from oxidation of sesamol, an antioxidative constituent of sesame oil: a possible cytotoxicity of oxidized antioxidant. *Toxicology in vitro : an international journal published in association with BIBRA* **24**:1720-1726; 2010.
- [88] Lee, C. C.; Liu, K. J.; Wu, Y. C.; Lin, S. J.; Chang, C. C.; Huang, T. S. Sesamin inhibits macrophage-induced vascular endothelial growth factor and matrix metalloproteinase-9 expression and proangiogenic activity in breast cancer cells. *Inflammation* **34**:209-221; 2011.
- [89] Rubin, D.; Laposata, M. Regulation of agonist-induced prostaglandin E1 versus prostaglandin E2 production. A mass analysis. *The Journal of biological chemistry* **266**:23618-23623; 1991.
- [90] Kikawa, K. D.; Herrick, J. S.; Tateo, R. E.; Mouradian, M.; Tay, J. S.; Pardini, R. S. Induced Oxidative Stress and Cell Death in the A549 Lung Adenocarcinoma Cell Line by Ionizing Radiation Is Enhanced by Supplementation With Docosahexaenoic Acid. *Nutrition and Cancer-an International Journal* **62**:1017-1024; 2010.
- [91] Rise, P.; Ghezzi, S.; Levati, M. G.; Mirtini, R.; Colombo, C.; Galli, C. Pharmacological modulation of fatty acid desaturation and of cholesterol biosynthesis in THP-1 cells. *Lipids* **38**:841-846; 2003.
- [92] Shen, X.; Dannenberger, D.; Nuernberg, K.; Nuernberg, G.; Zhao, R. Trans-18:1 and CLA isomers in rumen and duodenal digesta of bulls fed n-3 and n-6 PUFA-based diets. *Lipids* **46**:831-841; 2011.
- [93] Girotti, A. W. Mechanisms of lipid peroxidation. *Journal of free radicals in biology & medicine* **1**:87-95; 1985.
- [94] Smith, W. L.; DeWitt, D. L.; Garavito, R. M. Cyclooxygenases: structural, cellular, and molecular biology. *Annual review of biochemistry* **69**:145-182; 2000.
- [95] Yamamoto, S. Mammalian lipoxygenases: molecular structures and functions. *Biochimica et biophysica acta* **1128**:117-131; 1992.
- [96] Das, U. N. Nutrients, essential fatty acids and prostaglandins interact to augment immune responses and prevent genetic damage and cancer. *Nutrition* **5**:106-110; 1989.

- [97] Lee, L. M.; Pan, C. C.; Cheng, C. J.; Chi, C. W.; Liu, T. Y. Expression of cyclooxygenase-2 in prostate adenocarcinoma and benign prostatic hyperplasia. *Anticancer research* **21**:1291-1294; 2001.
- [98] Rouzer, C. A.; Marnett, L. J. Structural and functional differences between cyclooxygenases: Fatty acid oxygenases with a critical role in cell signaling. *Biochemical and biophysical research communications* **338**:34-44; 2005.
- [99] Pidgeon, G. P.; Lysaght, J.; Krishnamoorthy, S.; Reynolds, J. V.; O'Byrne, K.; Nie, D.; Honn, K. V. Lipoxygenase metabolism: roles in tumor progression and survival. *Cancer Metast Rev* **26**:503-524; 2007.
- [100] Gardner, H. W. Oxygen radical chemistry of polyunsaturated fatty acids. *Free radical biology & medicine* **7**:65-86; 1989.
- [101] Wagner, B. A.; Buettner, G. R.; Burns, C. P. Free Radical-Mediated Lipid-Peroxidation in Cells - Oxidizability Is a Function of Cell Lipid Bis-Allylic Hydrogen Content. *Biochemistry* **33**:4449-4453; 1994.
- [102] Qian, S. Y.; Wang, H. P.; Schafer, F. Q.; Buettner, G. R. EPR detection of lipid-derived free radicals from PUFA, LDL, and cell oxidations. *Free radical biology & medicine* **29**:568-579; 2000.
- [103] Voulgaridou, G. P.; Anestopoulos, I.; Franco, R.; Panayiotidis, M. I.; Pappa, A. DNA damage induced by endogenous aldehydes: current state of knowledge. *Mutation research* **711**:13-27; 2011.
- [104] Koh, Y. H.; Park, Y. S.; Takahashi, M.; Suzuki, K.; Taniguchi, N. Aldehyde reductase gene expression by lipid peroxidation end products, MDA and HNE. *Free radical research* **33**:739-746; 2000.
- [105] Zhou, J.; Cai, B.; Jang, Y. P.; Pachydaki, S.; Schmidt, A. M.; Sparrow, J. R. Mechanisms for the induction of HNE- MDA- and AGE-adducts, RAGE and VEGF in retinal pigment epithelial cells. *Experimental eye research* **80**:567-580; 2005.
- [106] Barrera, G.; Pizzimenti, S.; Dianzani, M. U. Lipid peroxidation: control of cell proliferation, cell differentiation and cell death. *Molecular aspects of medicine* **29**:1-8; 2008.
- [107] Hussain, S. P.; Hofseth, L. J.; Harris, C. C. Radical causes of cancer. *Nature reviews. Cancer* **3**:276-285; 2003.
- [108] Marinari, U. M.; Nitti, M.; Pronzato, M. A.; Domenicotti, C. Role of PKC-dependent pathways in HNE-induced cell protein transport and secretion. *Molecular aspects of medicine* **24**:205-211; 2003.
- [109] Van Nieuwenhove, C. P.; Cano, P. G.; Perez-Chaia, A. B.; Gonzalez, S. N. Effect of Functional Buffalo Cheese on Fatty Acid Profile and Oxidative Status of Liver and Intestine of Mice. *J Med Food* **14**:420-427; 2011.
- [110] Arguelles, S.; Machado, A.; Ayala, A. Adduct formation of 4-hydroxynonenal and malondialdehyde with elongation factor-2 in vitro and in vivo. *Free Radical Bio Med* **47**:324-330; 2009.
- [111] Liu, X.; Wang, J. M. Anti-inflammatory effects of iridoid glycosides fraction of Folium syringae leaves on TNBS-induced colitis in rats. *J Ethnopharmacol* **133**:780-787; 2011.
- [112] Fekecs, T.; Kadar, Z.; Battyani, Z.; Kalmar-Nagy, K.; Szakaly, P.; Horvath, O. P.; Weber, G.; Ferencz, A. Changes in Oxidative Stress in Patients Screened for Skin Cancer After Solid-Organ Transplantation. *Transplantation proceedings* **42**:2336-2338; 2010.

- [113] Chandramathi, S.; Suresh, K.; Anita, Z. B.; Kuppusamy, U. R. Comparative assessment of urinary oxidative indices in breast and colorectal cancer patients. *J Cancer Res Clin* **135**:319-323; 2009.
- [114] Leung, E. Y. L.; Crozier, J. E. M.; Talwar, D.; O'Reilly, D. S. J.; Mckee, R. F.; Horgan, P. G.; McMillan, D. C. Vitamin antioxidants, lipid peroxidation, tumour stage, the systemic inflammatory response and survival in patients with colorectal cancer. *International Journal of Cancer* **123**:2460-2464; 2008.
- [115] Surinenaite, B.; Prasmickiene, G.; Milasiene, V.; Stratilatovas, E.; Didziapetriene, J. The influence of surgical treatment and red blood cell transfusion on changes in antioxidative and immune system parameters in colorectal cancer patients. *Med Lith* **45**:785-791; 2009.
- [116] Lu, X. F.; He, G. Q.; Yu, H. N.; Ma, Q.; Shen, S. R.; Das, U. N. Colorectal cancer cell growth inhibition by linoleic acid is related to fatty acid composition changes. *J Zhejiang Univ-Sc B* **11**:923-930; 2010.
- [117] Das, U. N.; Madhavi, N. Effect of polyunsaturated fatty acids on drug-sensitive and resistant tumor cells in vitro. *Lipids in health and disease* **10**:159; 2011.
- [118] Berquin, I. M.; Edwards, I. J.; Kridel, S. J.; Chen, Y. Q. Polyunsaturated fatty acid metabolism in prostate cancer. *Cancer metastasis reviews* **30**:295-309; 2011.
- [119] Ge, H. T.; Kong, X. Q.; Shi, L. M.; Hou, L. J.; Liu, Z. L.; Li, P. Gamma-linolenic acid induces apoptosis and lipid peroxidation in human chronic myelogenous leukemia K562 cells. *Cell biology international* **33**:402-410; 2009.
- [120] Menendez, J. A.; Ropero, S.; Mehmi, I.; Atlas, E.; Colomer, R.; Lupu, R. Overexpression and hyperactivity of breast cancer-associated fatty acid synthase (oncogenic antigen-519) is insensitive to normal arachidonic fatty acid-induced suppression in lipogenic tissues but it is selectively inhibited by tumoricidal alpha-linolenic and gamma-linolenic fatty acids: A novel mechanism by which dietary fat can alter mammary tumorigenesis. *Int J Oncol* **24**:1369-1383; 2004.
- [121] Watkins, G.; Martin, T. A.; Bryce, R.; Mansel, R. E.; Jiang, W. G. Gamma-Linolenic acid regulates the expression and secretion of SPARC in human cancer cells. *Prostaglandins, leukotrienes, and essential fatty acids* **72**:273-278; 2005.
- [122] deAntueno, R.; Elliot, M.; Ells, G.; Quiroga, P.; Jenkins, K.; Horrobin, D. In vivo and in vitro biotransformation of the lithium salt of gamma-linolenic acid by three human carcinomas. *British journal of cancer* **75**:1812-1818; 1997.
- [123] Menendez, J. A.; Ropero, S.; Lupu, R.; Colomer, R. Omega-6 polyunsaturated fatty acid gamma-linolenic acid (18:3n-6) enhances docetaxel (Taxotere) cytotoxicity in human breast carcinoma cells: Relationship to lipid peroxidation and HER-2/neu expression. *Oncology reports* **11**:1241-1252; 2004.
- [124] deKock, M.; Lottering, M. L.; Grobler, C. J. S.; Viljoen, T. C.; leRoux, M.; Seegers, J. C. The induction of apoptosis in human cervical carcinoma (HeLa) cells by gamma-linolenic acid. *Prostag Leukotr Ess* **55**:403-411; 1996.
- [125] Sagar, P. S.; Das, U. N.; Koratkar, R.; Ramesh, G.; Padma, M.; Kumar, G. S. Cytotoxic Action of Cis-Unsaturated Fatty-Acids on Human Cervical-Carcinoma (Hela) Cells - Relationship to Free-Radicals and Lipid-Peroxidation and Its Modulation by Calmodulin Antagonists. *Cancer letters* **63**:189-198; 1992.
- [126] Sagar, P. S.; Das, U. N. Cytotoxic Action of Cis-Unsaturated Fatty-Acids on Human Cervical-Carcinoma (Hela) Cells in-Vitro. *Prostag Leukotr Ess* **53**:287-299; 1995.

- [127] Kernoff, P. B. A.; Willis, A. L.; Stone, K. J.; Davies, J. A.; Mcnicol, G. P. Antithrombotic Potential of Dihomo-Gamma-Linolenic Acid in Man. *Brit Med J* **2**:1441-1444; 1977.
- [128] Garavito, R. M.; DeWitt, D. L. The cyclooxygenase isoforms: structural insights into the conversion of arachidonic acid to prostaglandins. *Biochimica et biophysica acta* **1441**:278-287; 1999.
- [129] Smith, W. L. Nutritionally essential fatty acids and biologically indispensable cyclooxygenases. *Trends in biochemical sciences* **33**:27-37; 2008.
- [130] Baron, J. A.; Sandler, R. S. Nonsteroidal anti-inflammatory drugs and cancer prevention. *Annu Rev Med* **51**:511-523; 2000.
- [131] Rostom, A.; Dube, C.; Lewin, G.; Tsertsvadze, A.; Barrowman, N.; Code, C.; Sampson, M.; Moher, D. Nonsteroidal anti-inflammatory drugs and cyclooxygenase-2 inhibitors for primary prevention of colorectal cancer: a systematic review prepared for the U.S. Preventive Services Task Force. *Annals of internal medicine* **146**:376-389; 2007.
- [132] Asano, T. K.; McLeod, R. S. Nonsteroidal anti-inflammatory drugs and aspirin for the prevention of colorectal adenomas and cancer: a systematic review. *Diseases of the colon and rectum* **47**:665-673; 2004.
- [133] Dempke, W.; Rie, C.; Grothey, A.; Schmoll, H. J. Cyclooxygenase-2: a novel target for cancer chemotherapy? *J Cancer Res Clin Oncol* **127**:411-417; 2001.
- [134] Rouzer, C. A.; Marnett, L. J. Mechanism of free radical oxygenation of polyunsaturated fatty acids by cyclooxygenases. *Chemical reviews* **103**:2239-2304; 2003.
- [135] Garavito, R. M.; Mulichak, A. M. The structure of mammalian cyclooxygenases. *Annu Rev Bioph Biom* **32**:183-206; 2003.
- [136] Smith, W. L.; Song, I. The enzymology of prostaglandin endoperoxide H synthases-1 and -2. *Prostaglandins & other lipid mediators* **68-69**:115-128; 2002.
- [137] Smith, W. L.; Garavito, R. M.; DeWitt, D. L. Prostaglandin endoperoxide H synthases (cyclooxygenases)-1 and -2. *The Journal of biological chemistry* **271**:33157-33160; 1996.
- [138] Xiao, G.; Chen, W.; Kulmacz, R. J. Comparison of structural stabilities of prostaglandin H synthase-1 and -2. *The Journal of biological chemistry* **273**:6801-6811; 1998.
- [139] Malkowski, M. G.; Ginell, S. L.; Smith, W. L.; Garavito, R. M. The productive conformation of arachidonic acid bound to prostaglandin synthase. *Science* **289**:1933-1937; 2000.
- [140] Thuresson, E. D.; Malkowski, M. G.; Lakkides, K. M.; Rieke, C. J.; Mulichak, A. M.; Ginell, S. L.; Garavito, R. M.; Smith, W. L. Mutational and X-ray crystallographic analysis of the interaction of dihomogamma-linolenic acid with prostaglandin endoperoxide H synthases. *The Journal of biological chemistry* **276**:10358-10365; 2001.
- [141] Thuresson, E. D.; Lakkides, K. M.; Rieke, C. J.; Smith, W. L. Enzyme-substrate interactions in the cyclooxygenase active site of ovine prostaglandin endoperoxide H synthase-1. *Faseb Journal* **14**:A1449-A1449; 2000.
- [142] Thuresson, E. D.; Lakkides, K. M.; Smith, W. L. Different catalytically competent arrangements of arachidonic acid within the cyclooxygenase active site of prostaglandin endoperoxide H synthase-1 lead to the formation of different oxygenated products. *Journal of Biological Chemistry* **275**:8501-8507; 2000.
- [143] Vecchio, A. J.; Simmons, D. M.; Malkowski, M. G. Structural basis of fatty acid substrate binding to cyclooxygenase-2. *The Journal of biological chemistry* **285**:22152-22163; 2010.

- [144] Mason, R. P.; Hanna, P. M.; Burkitt, M. J.; Kadiiska, M. B. Detection of Oxygen-Derived Radicals in Biological-Systems Using Electron-Spin-Resonance. *Environmental health perspectives* **102**:33-36; 1994.
- [145] Janzen, E. G.; Blackburn, B. J. Detection and Identification of Short-Lived Free Radicals by Electron Spin Resonance Trapping Techniques (Spin Trapping) - Photolysis of Organolead, -Tin, and -Mercury Compounds. *Journal of the American Chemical Society* **91**:4481-4486; 1969.
- [146] Janzen, E. G. Spin Trapping. *Accounts Chem Res* **4**:31-36; 1971.
- [147] Lagercrantz, C. Spin Trapping of Some Short-Lived Radicals by Nitroxide Method. *J Phys Chem-US* **75**:3466-3471; 1971.
- [148] North, J. A.; Spector, A. A.; Buettner, G. R. Detection of Lipid Radicals by Electron-Paramagnetic Resonance Spin Trapping Using Intact-Cells Enriched with Polyunsaturated Fatty-Acid. *Journal of Biological Chemistry* **267**:5743-5746; 1992.
- [149] Mak, I. T.; Arroyo, C. M.; Weglicki, W. B. Inhibition of Sarcolemmal Carbon-Centered Free-Radical Formation by Propranolol. *Circ Res* **65**:1151-1156; 1989.
- [150] Dikalova, A. E.; Kadiiska, M. B.; Mason, R. P. An in vivo ESR spin-trapping study: Free radical generation in rats from formate intoxication - role of the Fenton reaction. *Proceedings of the National Academy of Sciences of the United States of America* **98**:13549-13553; 2001.
- [151] Pazos, M.; Andersen, M. L.; Skibsted, L. H. Heme-Mediated Production of Free Radicals via Preformed Lipid Hydroperoxide Fragmentation. *Journal of agricultural and food chemistry* **56**:11478-11484; 2008.
- [152] Zhang, J. J.; Zhao, Y.; Zhao, B. L. Scavenging Effects of Dexrazoxane on Free Radicals. *J Clin Biochem Nutr* **47**:238-245; 2010.
- [153] Spulber, M.; Schlick, S. Using Cyclodextrins to Encapsulate Oxygen-Centered and Carbon-Centered Radical Adducts: The Case of DMPO, PBN, and MNP Spin Traps. *J Phys Chem A* **114**:6217-6225; 2010.
- [154] Guo, Q.; Qian, S. Y.; Mason, R. P. Separation and identification of DMPO adducts of oxygen-centered radicals formed from organic hydroperoxides by HPLC-ESR, ESI-MS and MS/MS. *Journal of the American Society for Mass Spectrometry* **14**:862-871; 2003.
- [155] Zhao, B. L.; Wang, J. C.; Hou, J. W.; Xin, W. J. Studies on nitric oxide free radicals generated from polymorphonuclear leukocytes (PMN) stimulated by phorbol myristate acetate (PMA). *Cell biology international* **20**:343-350; 1996.
- [156] Qian, S. Y.; Chen, Y. R.; Deterding, L. J.; Fann, Y. C.; Chignell, C. F.; Tomer, K. B.; Mason, R. P. Identification of protein-derived tyrosyl radical in the reaction of cytochrome c and hydrogen peroxide: characterization by ESR spin-trapping, HPLC and MS. *Biochemical Journal* **363**:281-288; 2002.
- [157] Gunther, M. R.; Tschirret-Guth, R. A.; Witkowska, H. E.; Fann, Y. C.; Barr, D. P.; de Montellano, P. R. O.; Mason, R. P. Site-specific spin trapping of tyrosine radicals in the oxidation of metmyoglobin by hydrogen peroxide. *Biochemical Journal* **330**:1293-1299; 1998.
- [158] Barr, D. P.; Gunther, M. R.; Deterding, L. J.; Tomer, K. B.; Mason, R. P. ESR spin-trapping of a protein-derived tyrosyl radical from the reaction of cytochrome c with hydrogen peroxide. *Journal of Biological Chemistry* **271**:15498-15503; 1996.
- [159] Chatterjee, S.; Lardinois, O.; Bhattacharjee, S.; Tucker, J.; Corbett, J.; Deterding, L.; Ehrenshaft, M.; Bonini, M. G.; Mason, R. P. Oxidative stress induces protein and DNA radical formation in follicular dendritic cells of the germinal center and modulates its cell death patterns in late sepsis. *Free Radical Bio Med* **50**:988-999; 2011.

- [160] Buettner, G. R.; Kelley, E. E.; Burns, C. P. Membrane Lipid-Free Radicals Produced from L1210 Murine Leukemia-Cells by Photofrin Photosensitization - an Electron-Paramagnetic-Resonance Spin-Trapping Study. *Cancer research* **53**:3670-3673; 1993.
- [161] Kadiiska, M. B.; Hanna, P. M.; Jordan, S. J.; Mason, R. P. Electron-Spin-Resonance Evidence for Free-Radical Generation in Copper-Treated Vitamin-E-Deficient and Selenium-Deficient Rats - in-Vivo Spin-Trapping Investigation. *Mol Pharmacol* **44**:222-227; 1993.
- [162] Kadiiska, M. B.; Mason, R. P.; Dreher, K. L.; Costa, D. L.; Ghio, A. J. In vivo evidence of free radical formation in the rat lung after exposure to an emission source air pollution particle. *Chemical research in toxicology* **10**:1104-1108; 1997.
- [163] Iwahashi, H.; Parker, C. E.; Mason, R. P.; Tomer, K. B. Radical Adducts of Nitrosobenzene and 2-Methyl-2-Nitrosopropane with 12,13-Epoxylinoleic Acid Radical, 12,13-Epoxylinolenic Acid Radical and 14,15-Epoxyarachidonic Acid Radical - Identification by Hplc Epr and Liquid-Chromatography Thermospray Ms. *Biochemical Journal* **276**:447-453; 1991.
- [164] Iwahashi, H.; Deterding, L. J.; Parker, C. E.; Mason, R. P.; Tomer, K. B. Identification of radical adducts formed in the reactions of unsaturated fatty acids with soybean lipoxygenase using continuous flow fast atom bombardment with tandem mass spectrometry. *Free radical research* **25**:255-274; 1996.
- [165] Qian, S. Y.; Yue, G. H.; Tomer, K. B.; Mason, R. P. Identification of all classes of spin-trapped carbon-centered radicals in soybean lipoxygenase-dependent lipid peroxidations of omega-6 polyunsaturated fatty acids via LC/ESR, LC/MS, and tandem MS. *Free Radical Bio Med* **34**:1017-1028; 2003.
- [166] Qian, S. Y.; Guo, Q.; Mason, R. P. Identification of spin trapped carbon-centered radicals in soybean lipoxygenase-dependent peroxidations of omega-3 polyunsaturated fatty acids by LC/ESR, LC/MS, and tandem MS. *Free Radical Bio Med* **35**:33-44; 2003.
- [167] Yue Qian, S.; Tomer, K. B.; Yue, G. H.; Guo, Q.; Kadiiska, M. B.; Mason, R. P. Characterization of the initial carbon-centered pentadienyl radical and subsequent radicals in lipid peroxidation: identification via on-line high performance liquid chromatography/electron spin resonance and mass spectrometry. *Free radical biology & medicine* **33**:998-1009; 2002.
- [168] Qian, S. Y.; Kadiiska, M. B.; Guo, Q. O.; Mason, R. P. A novel protocol to identify and quantify all spin trapped free radicals from in vitro/in vivo interaction of HO and DMDO: LC/ESR, LC/MS, and dual spin trapping combinations. *Free Radical Bio Med* **38**:125-135; 2005.
- [169] Yu, Q. F.; Shan, M.; Ni, K.; Qian, S. Y. LC/ESR/MS study of spin trapped carbon-centred radicals formed from in vitro lipoxygenase-catalysed peroxidation of gamma-linolenic acid. *Free radical research* **42**:442-455; 2008.
- [170] Shan, Z.; Yu, Q. F.; Purwaha, P.; Guo, B.; Qian, S. Y. A combination study of spin-trapping, LC/ESR and LC/MS on carbon-centred radicals formed from lipoxygenase-catalysed peroxidation of eicosapentaenoic acid. *Free radical research* **43**:13-27; 2009.
- [171] Yu, Q. F.; Purwaha, P.; Ni, K. Y.; Sun, C. W.; Mallik, S.; Qian, S. Y. Characterization of novel radicals from COX-catalyzed arachidonic acid peroxidation. *Free Radical Bio Med* **47**:568-576; 2009.
- [172] Purwaha, P.; Gu, Y.; Kelavkar, U.; Kang, J. X.; Law, B.; Wu, E. X.; Qian, S. Y. LC/ESR/MS study of pH-dependent radical generation from 15-LOX-catalyzed DPA peroxidation. *Free Radical Bio Med* **51**:1461-1470; 2011.
- [173] Xiao, Y.; Gu, Y.; Purwaha, P.; Ni, K. Y.; Law, B.; Mallik, S.; Qian, S. Y. Characterization of free radicals formed from COX-catalyzed DGLA peroxidation. *Free Radical Bio Med* **50**:1163-1170; 2011.

- [174] Qian, S. Y.; Buettner, G. R. Iron and dioxygen chemistry is an important route to initiation of biological free radical oxidations: an electron paramagnetic resonance spin trapping study. *Free radical biology & medicine* **26**:1447-1456; 1999.
- [175] Bergmann, C.; Strauss, L.; Zeidler, R.; Lang, S.; Whiteside, T. L. Expansion of human T regulatory type 1 cells in the microenvironment of cyclooxygenase 2 overexpressing head and neck squamous cell carcinoma. *Cancer research* **67**:8865-8873; 2007.
- [176] Zhang, Y.; Xu, X.; He, P. Tubeimoside-1 inhibits proliferation and induces apoptosis by increasing the Bax to Bcl-2 ratio and decreasing COX-2 expression in lung cancer A549 cells. *Molecular medicine reports* **4**:25-29; 2011.
- [177] Thiel, A.; Narko, K.; Heinonen, M.; Hemmes, A.; Tomasetto, C.; Rio, M. C.; Haglund, C.; Makela, T. P.; Ristimaki, A. Inhibition of cyclooxygenase-2 causes regression of gastric adenomas in trefoil factor 1 deficient mice. *International journal of cancer. Journal international du cancer* **131**:1032-1041; 2012.
- [178] Hammes, L. S.; Tekmal, R. R.; Naud, P.; Edelweiss, M. I.; Kirma, N.; Valente, P. T.; Syrjanen, K. J.; Cunha-Filho, J. S. Up-regulation of VEGF, c-fms and COX-2 expression correlates with severity of cervical cancer precursor (CIN) lesions and invasive disease. *Gynecologic oncology* **110**:445-451; 2008.
- [179] Eberhart, C. E.; Coffey, R. J.; Radhika, A.; Giardiello, F. M.; Ferrenbach, S.; DuBois, R. N. Up-regulation of cyclooxygenase 2 gene expression in human colorectal adenomas and adenocarcinomas. *Gastroenterology* **107**:1183-1188; 1994.
- [180] Sinicrope, F. A.; Lemoine, M.; Xi, L.; Lynch, P. M.; Cleary, K. R.; Shen, Y.; Frazier, M. L. Reduced expression of cyclooxygenase 2 proteins in hereditary nonpolyposis colorectal cancers relative to sporadic cancers. *Gastroenterology* **117**:350-358; 1999.
- [181] Pozzi, A.; Yan, X. X.; Macias-Perez, I.; Wei, S. Z.; Hata, A. N.; Breyer, R. M.; Morrow, J. D.; Capdevila, J. H. Colon carcinoma cell growth is associated with prostaglandin E2/EP4 receptor-evoked ERK activation. *Journal of Biological Chemistry* **279**:29797-29804; 2004.
- [182] Leone, V.; di Palma, A.; Ricchi, P.; Acquaviva, F.; Giannouli, M.; Di Prisco, A. M.; Iuliano, F.; Acquaviva, A. M. PGE2 inhibits apoptosis in human adenocarcinoma Caco-2 cell line through Ras-PI3K association and cAMP-dependent kinase A activation. *American journal of physiology. Gastrointestinal and liver physiology* **293**:G673-681; 2007.
- [183] Pai, R.; Soreghan, B.; Szabo, I. L.; Pavelka, M.; Baatar, D.; Tarnawski, A. S. Prostaglandin E2 transactivates EGF receptor: a novel mechanism for promoting colon cancer growth and gastrointestinal hypertrophy. *Nat Med* **8**:289-293; 2002.
- [184] Gianetti, J.; De Caterina, M.; De Cristofaro, T.; Ungaro, B.; Guercio, R. D.; De Caterina, R. Intravenous prostaglandin E1 reduces soluble vascular cell adhesion molecule-1 in peripheral arterial obstructive disease. *American heart journal* **142**:733-739; 2001.
- [185] Sagar, P. S.; Das, U. N. Cytotoxic action of cis-unsaturated fatty acids on human cervical carcinoma (HeLa) cells in vitro. *Prostaglandins, leukotrienes, and essential fatty acids* **53**:287-299; 1995.
- [186] Mengeaud, V.; Nano, J. L.; Fournel, S.; Rampal, P. Effects of eicosapentaenoic acid, gamma-linolenic acid and prostaglandin E1 on three human colon carcinoma cell lines. *Prostaglandins, leukotrienes, and essential fatty acids* **47**:313-319; 1992.
- [187] Bamba, H.; Ota, S.; Kato, A.; Kawamoto, C.; Matsuzaki, F. Effect of prostaglandin E1 on vascular endothelial growth factor production by human macrophages and colon cancer cells. *Journal of experimental & clinical cancer research : CR* **19**:219-223; 2000.

- [188] Thuresson, E. D.; Malkowski, M. G.; Lakkides, K. M.; Rieke, C. J.; Mulichak, A. M.; Ginell, S. L.; Garavito, R. M.; Smith, W. L. Mutational and X-ray crystallographic analysis of the interaction of dihomogamma-linolenic acid with prostaglandin endoperoxide H synthases. *Journal of Biological Chemistry* **276**:10358-10365; 2001.
- [189] Towner, R. A.; Qian, S. Y.; Kadiiska, M. B.; Mason, R. P. In vivo identification of aflatoxin-induced free radicals in rat bile. *Free Radical Bio Med* **35**:1330-1340; 2003.
- [190] Arthur, J. R. The glutathione peroxidases. *Cellular and molecular life sciences : CMLS* **57**:1825-1835; 2000.
- [191] Blair, I. A. Analysis of endogenous glutathione-adducts and their metabolites. *Biomed Chromatogr* **24**:29-38; 2010.
- [192] Thiebaut, A. C.; Chajes, V.; Gerber, M.; Boutron-Ruault, M. C.; Joulin, V.; Lenoir, G.; Berrino, F.; Riboli, E.; Benichou, J.; Clavel-Chapelon, F. Dietary intakes of omega-6 and omega-3 polyunsaturated fatty acids and the risk of breast cancer. *International journal of cancer. Journal international du cancer* **124**:924-931; 2009.
- [193] Brown, M. D.; Hart, C.; Gazi, E.; Gardner, P.; Lockyer, N.; Clarke, N. Influence of omega-6 PUFA arachidonic acid and bone marrow adipocytes on metastatic spread from prostate cancer. *British journal of cancer* **102**:403-413; 2010.
- [194] Pot, G. K.; Geelen, A.; van Heijningen, E. M. B.; Siezen, C. L. E.; van Kranen, H. J.; Kampman, E. Opposing associations of serum n-3 and n-6 polyunsaturated fatty acids with colorectal adenoma risk: An endoscopy-based case-control study. *International Journal of Cancer* **123**:1974-1977; 2008.
- [195] Sauer, L. A.; Blask, D. E.; Dauchy, R. T. Dietary factors and growth and metabolism in experimental tumors. *Journal of Nutritional Biochemistry* **18**:637-649; 2007.
- [196] Kimura, Y.; Kono, S.; Toyomura, K.; Nagano, J.; Mizoue, T.; Moore, M. A.; Mibu, R.; Tanaka, M.; Kakeji, Y.; Maehara, Y.; Okamura, T.; Ikejiri, K.; Futami, K.; Yasunami, Y.; Maekawa, T.; Takenaka, K.; Ichimiya, H.; Imaizumi, N. Meat, fish and fat intake in relation to subsite-specific risk of colorectal cancer: The Fukuoka Colorectal Cancer Study. *Cancer science* **98**:590-597; 2007.
- [197] Lloyd, D. R.; Phillips, D. H.; Carmichael, P. L. Generation of putative intrastrand cross-links and strand breaks in DNA by transition metal ion-mediated oxygen radical attack. *Chemical research in toxicology* **10**:393-400; 1997.
- [198] Cadet, J. DNA damage caused by oxidation, deamination, ultraviolet radiation and photoexcited psoralens. *IARC scientific publications*:245-276; 1994.
- [199] Parman, T.; Wiley, M. J.; Wells, P. G. Free radical-mediated oxidative DNA damage in the mechanism of thalidomide teratogenicity. *Nat Med* **5**:582-585; 1999.
- [200] Cooke, M. S.; Evans, M. D.; Dizdaroglu, M.; Lunec, J. Oxidative DNA damage: mechanisms, mutation, and disease. *FASEB journal : official publication of the Federation of American Societies for Experimental Biology* **17**:1195-1214; 2003.
- [201] Goodman, J. E.; Hofseth, L. J.; Hussain, S. P.; Harris, C. C. Nitric oxide and p53 in cancer-prone chronic inflammation and oxyradical overload disease. *Environmental and molecular mutagenesis* **44**:3-9; 2004.
- [202] Bunz, F.; Dutriaux, A.; Lengauer, C.; Waldman, T.; Zhou, S.; Brown, J. P.; Sedivy, J. M.; Kinzler, K. W.; Vogelstein, B. Requirement for p53 and p21 to sustain G2 arrest after DNA damage. *Science* **282**:1497-1501; 1998.
- [203] Agarwal, M. L.; Agarwal, A.; Taylor, W. R.; Stark, G. R. p53 controls both the G2/M and the G1 cell cycle checkpoints and mediates reversible growth arrest in human fibroblasts.

- Proceedings of the National Academy of Sciences of the United States of America* **92**:8493-8497; 1995.
- [204] Chell, S. D.; Witherden, A. R.; Dobson, R. R.; Moorghen, M.; Herman, A. A.; Qualtrough, D.; Williams, A. C.; Paraskeva, C. Increased EP4 receptor expression in colorectal cancer progression promotes cell growth and anchorage independence. *Cancer research* **66**:3106-3113; 2006.
- [205] Shao, J.; Jung, C.; Liu, C.; Sheng, H. Prostaglandin E2 Stimulates the beta-catenin/T cell factor-dependent transcription in colon cancer. *The Journal of biological chemistry* **280**:26565-26572; 2005.
- [206] Cancer drugs: remedy required. *Nat Med* **17**:231; 2011.
- [207] Polyak, K.; Garber, J. Targeting the missing links for cancer therapy. *Nat Med* **17**:283-284; 2011.
- [208] Prensner, J. R.; Chinnaiyan, A. M. Metabolism unhinged: IDH mutations in cancer. *Nat Med* **17**:291-293; 2011.
- [209] Bissell, M. J.; Hines, W. C. Why don't we get more cancer? A proposed role of the microenvironment in restraining cancer progression. *Nat Med* **17**:320-329; 2011.
- [210] Wang, D. Z.; Dubois, R. N. Eicosanoids and cancer. *Nature Reviews Cancer* **10**:181-193; 2010.
- [211] Tuynman, J. B.; Peppelenbosch, M. P.; Richel, D. J. COX-2 inhibition as a tool to treat and prevent colorectal cancer. *Crit Rev Oncol Hemat* **52**:81-101; 2004.
- [212] Blanton, W. P.; Prabakaran, D.; Wang, B.; Yao, M.; Wolfe, M. Cyclooxygenase-2 (COX-2) inhibition attenuates the growth of colorectal cancer associated with the use of immunosuppression following transplantation. *Gastroenterology* **132**:A440-A440; 2007.
- [213] Gravitz, L. CHEMOPREVENTION First line of defence. *Nature* **471**:S5-S7; 2011.
- [214] Obukowicz, M. G.; Raz, A.; Pyla, P. D.; Rico, J. G.; Wendling, J. M.; Needleman, P. Identification and characterization of a novel Delta 6/Delta 5 fatty acid desaturase inhibitor as a potential anti-inflammatory agent. *Biochem Pharmacol* **55**:1045-1058; 1998.
- [215] Fujiyama-Fujiwara, Y.; Umeda, R.; Igarashi, O. Effects of sesamin and curcumin on delta 5-desaturation and chain elongation of polyunsaturated fatty acid metabolism in primary cultured rat hepatocytes. *Journal of nutritional science and vitaminology* **38**:353-363; 1992.
- [216] Kawashima, H.; Akimoto, K.; Jareonkitmongkol, S.; Shirasaka, N.; Shimizu, S. Inhibition of rat liver microsomal desaturases by curcumin and related compounds. *Bioscience, biotechnology, and biochemistry* **60**:108-110; 1996.
- [217] Reti, A.; Barna, G.; Pap, E.; Adleff, V.; V, L. K.; Jeney, A.; Kralovanszky, J.; Budai, B. Enhancement of 5-fluorouracil efficacy on high COX-2 expressing HCA-7 cells by low dose indomethacin and NS-398 but not on low COX-2 expressing HT-29 cells. *Pathology oncology research : POR* **15**:335-344; 2009.
- [218] Reddy, B. S.; Hirose, Y.; Lubet, R.; Steele, V.; Kelloff, G.; Paulson, S.; Seibert, K.; Rao, C. V. Chemoprevention of colon cancer by specific cyclooxygenase-2 inhibitor, celecoxib, administered during different stages of carcinogenesis. *Cancer research* **60**:293-297; 2000.
- [219] Pan, C. X.; Loehrer, P.; Seitz, D.; Helft, P.; Juliar, B.; Ansari, R.; Pletcher, W.; Vinson, J.; Cheng, L.; Sweeney, C. A phase II trial of irinotecan, 5-fluorouracil and leucovorin combined with celecoxib and glutamine as first-line therapy for advanced colorectal cancer. *Oncology-Basel* **69**:63-70; 2005.

- [220] Ashktorab, H.; Dawkins, F. W.; Mohamed, R.; Larbi, D.; Smoot, D. T. Apoptosis induced by aspirin and 5-fluorouracil in human colonic adenocarcinoma cells. *Digestive diseases and sciences* **50**:1025-1032; 2005.
- [221] Sun, Y. J.; Tang, X. M.; Half, E.; Kuo, M. T.; Sinicrope, F. A. Cyclooxygenase-2 overexpression reduces apoptotic susceptibility by inhibiting the cytochrome c-dependent apoptotic pathway in human colon cancer cells. *Cancer research* **62**:6323-6328; 2002.
- [222] Lim, Y. J.; Rhee, J. C.; Bae, Y. M.; Chun, W. J. Celecoxib attenuates 5-fluorouracil-induced apoptosis in HCT-15 and HT-29 human colon cancer cells. *World journal of gastroenterology : WJG* **13**:1947-1952; 2007.
- [223] Li, M.; Zhang, Z.; Hill, D. L.; Wang, H.; Zhang, R. W. Curcumin, a dietary component, has anticancer, chemosensitization, and radiosensitization effects by down-regulating the MDM2 oncogene through the PI3K/mTOR/ETS2 pathway. *Cancer research* **67**:1988-1996; 2007.
- [224] Agrawal, D. K.; Mishra, P. K. Curcumin and Its Analogues: Potential Anticancer Agents. *Med Res Rev* **30**:818-860; 2010.
- [225] Moore, A. E.; Greenhough, A.; Roberts, H. R.; Hicks, D. J.; Patsos, H. A.; Williams, A. C.; Paraskeva, C. HGF/Met signalling promotes PGE(2) biogenesis via regulation of COX-2 and 15-PGDH expression in colorectal cancer cells. *Carcinogenesis* **30**:1796-1804; 2009.
- [226] Tavolari, S.; Bonafe, M.; Marini, M.; Ferreri, C.; Bartolini, G.; Brighenti, E.; Manara, S.; Tomasi, V.; Laufer, S.; Guarnieri, T. Licofelone, a dual COX/5-LOX inhibitor, induces apoptosis in HCA-7 colon cancer cells through the mitochondrial pathway independently from its ability to affect the arachidonic acid cascade. *Carcinogenesis* **29**:371-380; 2008.
- [227] Moonen, H. J. J.; Dommels, Y. E. M.; van Zwam, M.; van Herwijnen, M. H. M.; Kleinjans, J. C. S.; Alink, G. M.; de Kok, T. M. C. M. Effects of polyunsaturated fatty acids on prostaglandin synthesis and cyclooxygenase-mediated DNA adduct formation by heterocyclic aromatic amines in human adenocarcinoma colon cells. *Mol Carcinogen* **40**:180-188; 2004.
- [228] Dommels, Y. E. M.; Haring, M. M. G.; Keestra, N. G. M.; Alink, G. M.; van Bladeren, P. J.; van Ommen, B. The role of cyclooxygenase in n-6 and n-3 polyunsaturated fatty acid mediated effects on cell proliferation, PGE(2) synthesis and cytotoxicity in human colorectal carcinoma cell lines. *Carcinogenesis* **24**:385-392; 2003.
- [229] Fan, Y. Y.; Monk, J. M.; Hou, T. Y.; Callway, E.; Vincent, L.; Weeks, B.; Yang, P. Y.; Chapkin, R. S. Characterization of an arachidonic acid-deficient (Fads1 knockout) mouse model. *Journal of lipid research* **53**:1287-1295; 2012.